Aalto-yliopisto
Insinööritieteiden
korkeakoulu

Vishnu Sreenath

Impact of Building Sway on In-Car Vibration of Ultrahigh-Rise Elevators — Multiphysics Simulation Approach

Thesis submitted in verification of the professional development required for the degree of Master of Science (Technology)

Espoo, 25.11.2018
Supervisor: Assistant Professor Jarkko Niiranen
Advisor: D.Sc. (Tech) Gabriela Roivainen, KONE Corporation

Aalto-yliopisto
Insinööritieteiden
korkeakoulu

Aalto-yliopisto, PL 11000, 00076 AALTO
www.aalto.fi

Abstract of master's thesis

Author Vishnu Sreenath		
Title of thesis Impact of Building Sway on In-Car Vibration of Ultrahigh-Rise Elevators — Multiphysics Simulation Approach		
Degree programme Master of Science (Technology)		
Professorship Programme in Mechanical Engineering		**Code** EN25
Thesis supervisor Assistant Professor Jarkko Niiranen		
Thesis advisor(s) D.Sc. (Tech) Gabriela Roivainen		
Date 25.11.2018	**Number of pages** 83	**Language** English

Abstract

High-rise, high-speed elevators are subjected to both static and dynamic loads. They are transferred into the elevator and perceived as in-car vibrations. Building sway is one of the main contributors to in-car vibration for high-rise elevators. Vibrations transferred into the elevator is greatly influenced by the response of building sway amplitudes.

A finite element model of the elevator was developed using ABAQUS/Standard. Transient dynamic simulation method was utilized to compute the in-car vibrations. Various subroutines were used to include the installation inaccuracies over the travel distance. Aerodynamic loads calculated using computational fluid dynamics were used in the finite element model as pressure loads acting over a specified time interval. Finite difference method was used to study the rope behavior for different building sway amplitudes and elevator speed profiles. The rope forces calculated using this method is extracted and applied in the finite element simulation. The output of each computations is expressed as in-car vibration amplitudes.

This thesis mainly focuses on the prediction of in-car vibration due to building sway for a specific elevator configuration. Human perception of the vibration and the discomfort caused to the passengers because of the in-car vibration is investigated. Finally, the thesis proposes an optimized speed profile approach to mitigate this problem.

51 combinations of various building sway amplitude and speed profiles are computed using finite element method. Multiple regression model function is developed by curve fitting and validated against the test data. The generated function helps to predict the optimized speed profile that needs to be followed in order to maintain the required ride comfort. Also, the benefits of optimized speed profile is demonstrated by using handling capacity assessment calculations.

Keywords High-rise, high-speed, ride comfort, sway, finite element, elevator, Multiphysics, handling capacity, regression analysis

Preface

This thesis marks the end of my student life as a Master of Science in mechanical engineering, which seemed forever and endless. I would like to express my sincere gratitude to my advisor Gabriela Roivainen from KONE Corporation for her practical support, research guidance and help throughout the research work, without which this thesis would not have been possible.

I would also like to thank Anssi Karppinen for giving me the opportunity to make my thesis at KONE Corporation. Also I would like to thank and express my gratitude towards my colleagues and the whole Ride Comfort team, Mikko Vesterinen, Giovanni Hawkins, Jarkko Saloranta and Jaakko Kalliomaki for their constant support and insightful comments.

I also thank my professor Jarkko Niiranen for his support and encouragement throughout the thesis work. Mostly, I am very thankful to my parents for teaching me the value of education and constantly supporting me in every aspect of my life. The motivation of making them proud is what made me get through many sleepless nights.

Espoo 25.11.2018
Vishnu Sreenath

Contents

List of symbols

ρ	Density
d	Deflection of rope
T	Rope tension
τ	Rope wave propagation time
ξ, α, τ	Unit less quantities used to define rope position
A	Area
C	Damping coefficient per unit length
K	Stiffness
V	Velocity
M_c	Mass of elevator car
M_s	Mass of compensating sheave
L_0	Distance between traction and compensating sheave
g	Acceleration due to gravity
a	Wave propagation velocity
t	Time
$\bar{T}_{ij}^{(v)}$	Viscous stress tensor
μ	Molecular viscosity
$\bar{s}_{ij}$	Instantaneous strain rate tensor
u_i	Cartesian component of fluid velocity vector
u	Stream wise fluid velocity component
x_i	Cartesian coordinate vector component
δ_{ij}	Kronecker delta
ν	Kinematic viscosity
~	Subscript used for instantaneous components
$(\overline{\ldots})$	Subscript for ensemble averaged quantities
k	Turbulent kinetic energy
E	Rate of dissipation of turbulence energy
$\boldsymbol{f_S}$	Surface traction force
$\boldsymbol{f_V}$	Body force
V_o	Volume
S	Surface bounding the volume
$\boldsymbol{N}_N$	Finite element interpolation function
u^N	nodal variables
$[T^S]$	Transformation matrix for substructure
$[I]$	Unit matrix
ξ_n	Damping ratio
ω_n	Natural frequency
γ, β	Damping coefficients
Y	Young's modulus

List of acronyms

UEL	User defined elements
DD	Double deck
FEM	Finite Element Method
FDM	Finite Difference Method
FEA	Finite Element Analysis
DOF	Degrees of freedom
SDOF	Single degree of freedom
MDOF	Multiple degrees of freedom
VIBES	Vibrational Excellences
MBS	Multibody Simulation
CFD	Computational Fluid Dynamics
RANS	Reynolds Averaged Navier-Stokes
URANS	Unsteady Reynolds Averaged Navier-Stokes
PDE	Partial Differential Equations
RC	Ride Comfort
DBG	Distance Between Guiderail

1 Introduction

This chapter is divided into five sections. First, background of research is discussed, highlighting the trend of high-rise building and the need for efficient vertical transportation. Second session is a basic introduction to elevator, presenting its structure and main components and their operating mechanism. Third section focuses on factors that affect elevator ride quality and its human perception, mainly focusing on in-car lateral and vertical vibrations.

1.1 Background

The trend of population growth and urbanization has driven people from rural to urban migration. This creates a need to accommodate more people in a limited land area and in turn, exerts a significant demand for high-rise building. Past decade has witnessed an unprecedented boom in the construction of tall/high-rise elevators [1]. In 1950, only 30% of world population used to live in urban areas, while this has climbed to 47% in 2000. It is estimated that by 2030, around 5 billion people (60% world population) will be urban (United Nations, 2001) and by 2050 almost 80% will live in urban areas [2]. Thus, high-rise building is certain to be a part of this problem solution. Also, super high-rise building has become a status of wealth and prestige around some parts of the world. Thus, these iconic buildings enhance global image of a city and each year the tallest buildings in the world are getting taller Figure 1 [1].

The elevator industry has witnessed technological advancements over the past 150 years. The first generation of the elevators powered by steam was introduced in the 1850s. The first breakthrough in the elevator industry was the invention of safety brakes which paved way for the rapid growth of skyscrapers. In 1870s, plungers used in steam-powered elevators were replaced by short hydraulic pistons [3]. Moreover, building industry evolved with the use of concrete and steel frames compared to wood and masonry. These made it possible to build tall structures which used to collapse earlier because of self-weight [4] . Development in elevator industry has also influenced the growth of tall buildings. It is that the tall buildings that we see today could not be possible without elevator and their support structures [5]. There are many engineering challenges that come along with these mega high-rise structures, including structural design, construction methods, and building transportation (elevator) system design. These elevator system design problems mainly address three areas in general: performance efficiency, passenger safety, and comfort [6].

Performance efficiency can be improved by increasing the traveling speed and number of high-rise elevators, which in turn enhances the flow of people in and out of the building and reduces the traveling time. Another important goal of these ultrahigh elevators is to provide a comfortable and safe environment for the users and anyone associated with it. Passenger comfort in elevators is measured or defined using three metrics; in-car vibration levels, noise and ear comfort [7]. This thesis will be mostly discussing the levels of vibration amplitudes in these high-rise high-speed elevators.

The process of elevator design has evolved over the years. Most of the requirements are based on the building architecture, parameters, and customer demands. For low rise elevators, it is usually common to perform some tests on a test tower before the actual installation. In case of

a very tall building, computational methods are essential for design and development of high-rise elevators where testing facilities are limited. This Master's thesis performs dynamic analysis on elevators to investigate the structural vibration inside an elevator car.

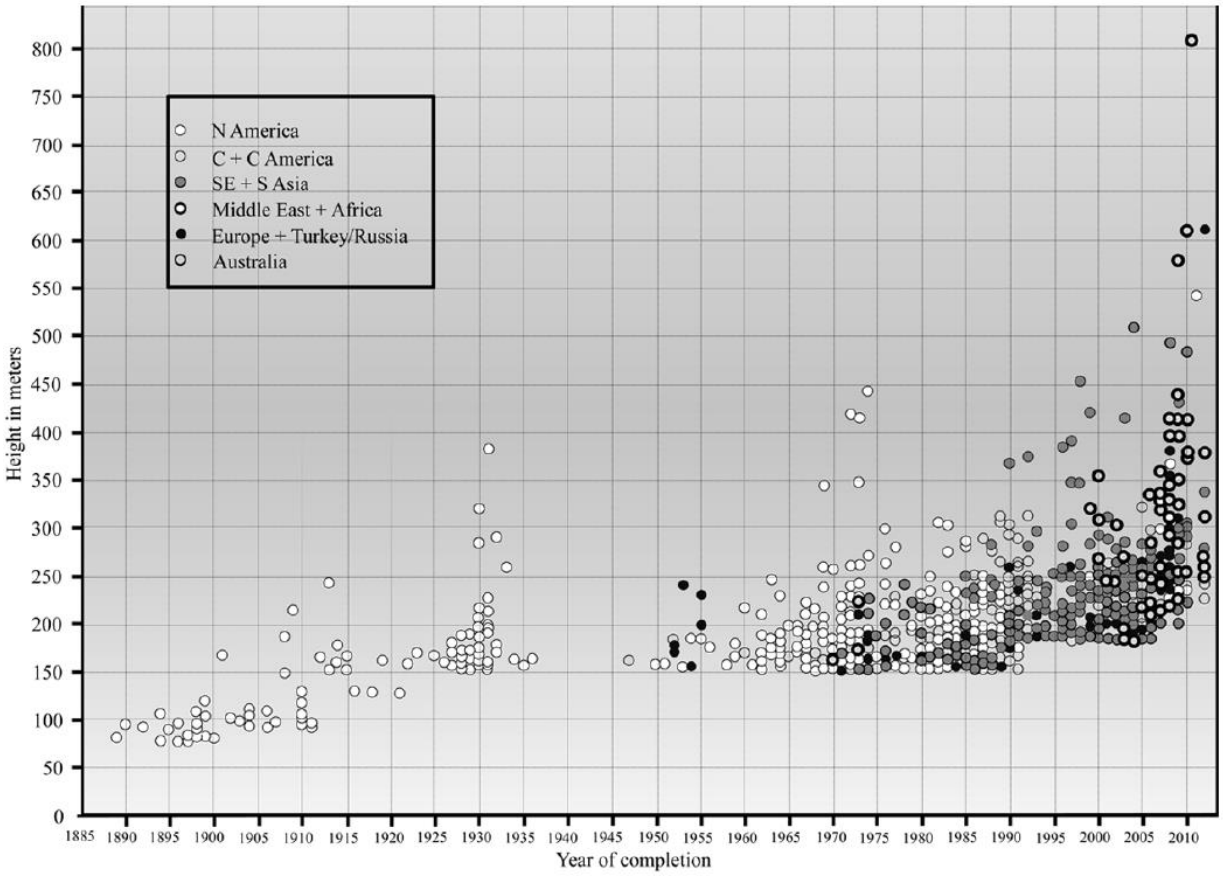

Figure 1. Boom in high-rise building trend over past two decades (Graph by K. Al-Kodmany; adopted from skyscrapercity.com) [1]

1.2 History of Elevators

Hoisting devices are being used since ancient times, most of them driven by winding tackles or drum ropes. Pictures of platforms used for vertical transportation can be found in antique Roman ruins, e.g. to levitate a person in theaters. Between medieval and early modern age, a simple elevating mechanism was used for cargo lifting. Industrial revolution witnessed many advancements in elevator development. They were mainly focused on improving the transport logistics in factories. The first primitive elevator called ''ascending room'' was built in 1823, used to lift tourist to a platform to view London skyline. Next in 1835 came the Teagle-Elevator, which is driven by the transmission shaft of the factory powered by steam, it was installed in an English factory [8].

The major reason for not having a wide operation in human transportation was the lack of adequate safety systems, especially the braking mechanism. Available braking systems had to

be operated by hands at the time of failure. In 1853, Elisha Graves Otis developed the first automatic braking system which uses a clamping device to stop the free fall [8]. Today, with the more sophisticated safety mechanisms, elevators are the safest mode of transportation.

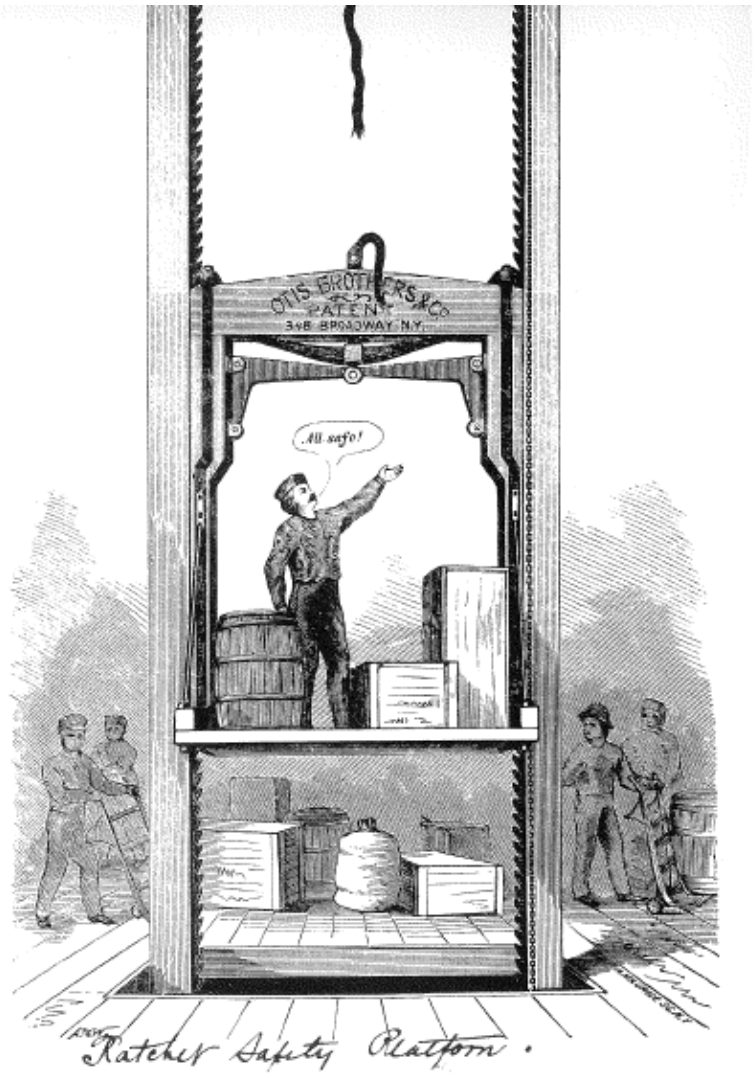

Figure 2. Demonstration of first automatic braking mechanism [8]

Another technological limitation on the widespread application since the late 19th century was the drive mechanism. This problem was solved with the development of electric drives. Electric elevators were fast and required less maintenance. In 1880, electric motors were integrated into the elevator technology by Werner von Siemens and Johann Georg Halske. This design employed an electrically driven gearing scheme, where gear wheel moves along a gear rack attached to the shaft wall.

The invention of elevator technology used in the mining industry is what led to the development of elevators for skyscrapers. Since the load to be transported had to be moved to higher distance with higher speed, rope drums could not be used because of their limitation on having a bigger diameter. Also, they had increased probability of rope breakage failure because of the exposure

to large operational stress. Friedrich Koepe solved this problem in 1877 by creating a drum for driving a pulley machine in a mine shaft of 234 meters depth. The rope was loosely placed over a sheave with a deep recess on the outer edge. This sheave acted as a suspension device and used friction as a drive, hence increasing the safety factor with the possibility to use multiple ropes. This invention led to modern elevator construction [8].

1.3 Elevator and basic components

An elevator can be defined as a device used for vertical transportation of people and goods along a fixed guide rail. Elevators are one of the necessities in a high-rise building. They have evolved over the years from manually hoisted elevators to traction sheave elevators. All the high-rise elevators utilize traction based hoisting mechanics, where suspension ropes pass over a traction sheave, with the car hanging on one end of the rope and a counterweight on the other end. Counterweight balances the weight of the car and the passengers and provides enough traction on the traction sheave that the ropes do not slip.

Guide rails are used to keep the car and counterweight in a straight line while during its travel. They are fixed to the shaft walls firmly using brackets and they are fixed to each other using fishplates. They need to install with great accuracy to ensure smooth and comfortable ride.

Modern elevators have a complex system, but it can be reduced to four basic components:

i. Hoisting equipment includes every part that facilitates in actual physical lifting.
ii. Electrification includes the electrical parts that power the elevator and control its movement.
iii. Signalization components indicate what the elevator is doing and give passengers a means of controlling the elevator.
iv. Doors are crucial part of the system which provides access into the elevator and provide safety and comfort to the users.

Elevator machinery is the power source, often located in a separate machine room. Modern machineries can be so small that they can be installed in the shaft. Suspension ropes transfer the work done by the machinery into moving the car. These ropes pass over the traction sheave and as the machinery rotates the sheave, the friction between the ropes and sheaves moves the ropes. As the travel of elevator increases over 40m, weight of the suspension ropes affects the machinery's workload by creating uneven load. To create a balanced dynamic load on the traction sheave, compensating ropes run from the bottom of the car to the bottom of the counterweight. This provides equal weight on both sides of the traction sheave. For elevators with very high travelling distances, compensating ropes pass under compensator sheaves located at the bottom of the shaft.

Electric drives control the elevator machinery. Drive system runs the machinery at different levels of torque and speed based on the input current and voltage. Travelling cables are used to supply electric power into the elevator car. They connect the control equipment located at top of the shaft to the bottom of the car while allowing the car to move freely.

Signalization includes all the interfaces that provides communication between the passenger and elevator system. Passenger interacts with the elevator through car operating panel. The

push buttons used to send elevators are present on the car operating panel. They receive information about elevator car position and call information from the user. Car operating panel consists of display and control unit located inside the car. Display unit tells the passenger current location of the car and where it is going. Modern elevators provide remote monitoring system which creates a real-time connection between elevator and service center. It makes sure of the smooth elevator operation and provides immediate rescue and maintenance operation.

There are two types of doors in the elevator system. Car doors which are part of the elevator car and move along with the car. Landing doors which are present on each landing levels. Both doors are closed when elevator is running in the shaft to prevent people from falling into the elevator shaft. When elevator has stopped on a landing level, car door opens grabbing the landing door along with it allowing the passengers to get in and out of the elevator car safely.

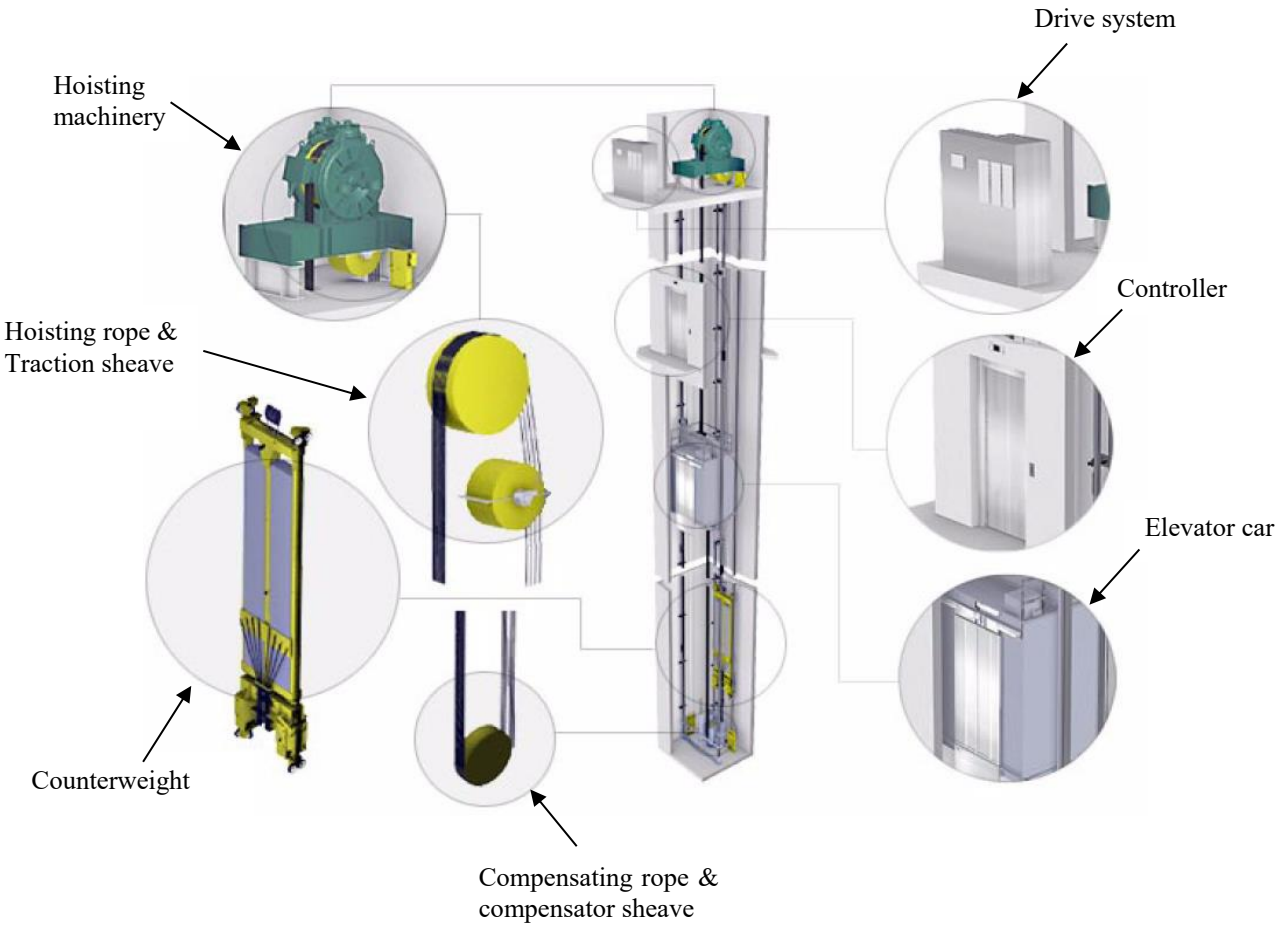

Figure 3. Elevator basic components

Elevator car is attached to a sling rigidly or using springs and dampers. Sling is a beam structure around the elevator car connected to suspension ropes and guide rails. It forms the supporting structure for the car. For high-rise building with long traveling distance, springs and dampers are used for connection to reduce the vibrations from guide rail misalignment and suspension ropes. Slings are loaded with weights at the bottom to achieve static balancing of the car. This helps is providing stable center of gravity, which in turn results in lower roller guide shoe forces and less vibration and noise. Balancing of the sling is a crucial part of ride comfort.

Roller guides are used instead of sliding shoes for high speed elevators. This mainly because of lower friction for rolling contact over sliding contact. Also, at higher speeds, intensity of vibration is higher and roller guide systems prevents the transfer of most of the vibrations into the elevator car. Also use of lubricants is not needed for contact between roller guide and rails. Normal roller guides use springs to absorb most of the vibration, but nowadays due to higher requirements for comfort criterion, active and passive damping systems are used to reduce lateral vibrations of the elevator especially for high- rise building.

Overspeed governors are speed detectors that monitor elevator speed and if the elevator speed rises above the allowable level due to abnormal acceleration, it engages safety devices and brings the elevator to a safe halt. There are electrically operated overspeed governors and mechanically operated safety mechanism, which is triggered by firmly gripping the guide rails and bringing and the car to a stop if the former one fails to stop the car completely. Also, buffers are present at the bottom of the shaft which absorbs and dissipates the kinetic energy from the falling elevators and in turn reducing the intensity of the falling impact.

1.3.1 Double deck elevator

Double deck (DD) elevator is used for the simulations in this thesis. It consists of two elevator cars, so that one is attached on top of the other and connected to a single sling structure. Double deck elevators can serve two consecutive floors simultaneously. This allows passengers to enter the elevator car from two different floors at the same time, in turn increases the handling capacity. It provides efficient people flow which is very critical for high-rise elevators and handling traffic bottlenecks at rush hours [9].

Double deck elevators are more stable compared to single deck for higher travelling speeds. The high mass of cars and sling provides more resistance to external forces that causes vibration from guide rail misalignment and/or rope forces. Also, while traveling at high speeds, the car that is facing the travelling direction acts as a sound buffer to other car and creates a lower sound pressure levels inside the other car. Thus, double deck provides better ride quality compared to single deck elevators [10].

Regarding economical point of view, double deck elevators reduce the overall interior space consumption of the building by reducing the number of running elevators and number of shafts [11]. Volume taken by elevator increases in proportion to building height [6]. For very tall buildings, double deck elevators are most efficient for shuttle applications. They can carry more people and has some effect on the elevator space occupancy. It is crucial for high-rise buildings to save the interior space because area occupied by elevator shafts in lower floors is much more critical. Thus, reducing the number of elevator shafts becomes more important and one way to achieve this is using double deck elevators [12]. In general, an efficient space-saving design is important because elevators demand more space than any other services in high-rises [11].

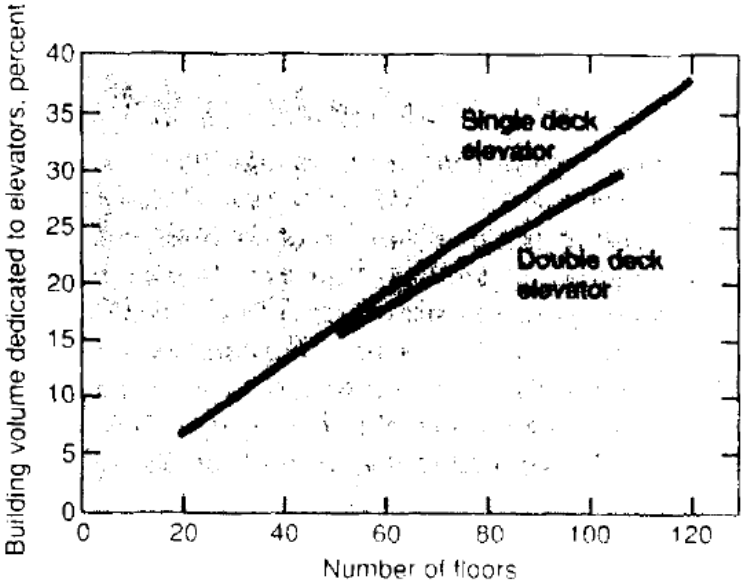

Figure 4. Elevator space occupancy corresponding to building height [6]

1.4 High-rise and high-speed elevators

For almost all city-dwellers, elevators are part of their daily lives. But these awe-inspiring pieces of machinery is overlooked with their technological advancements compared to automobiles, trains or even bicycle [13]. Today, elevators are responsible for moving more than an equivalent of world's population in over 72 hours. That is 7.4 billion people in just 3 days [14]. Today, with the population explosion and more crowded cities, elevators become more important than ever [15].

According to [5], buildings with more than 15 floors are categorized as high-rise buildings. Any building which has 60 or more floors is called mega-high-rise building. Although high-rise and low-rise elevator systems do not differ much with regards to the suspension and guidance system, aspects regarding comfort levels and technology need to be studied with much care. Safety features, intelligent control system, load bearing components and other advanced technology can augment the suspension rope weights and energy consumption proportional to building height [13]. Another challenge that comes along with the building height is the time taken for transportation. Even saving a small amount of time can make a big impact in many ways, so these high-rise elevators need to be fast and efficient in carrying the load to their destination. The aim is to have a fast, efficient and economical elevator [16]. With the latest technological inventions, it is possible to accomplish these goals.

The world as we know today is moving towards ‘‘green’’ focusing on reducing energy loss or/and reusing, in turn, reducing total energy consumption. 40% of world's energy is consumed by buildings and elevators are accountable for 2-10% of building energy. During peak hours, elevators may consume even up to 40% of building energy [17]. Since there are billions of elevator rides taken every day, saving the energy for each ride can help in reducing overall energy consumption significantly. Fortunately, with the current technology involving the use of efficient motor, regenerative converters, better software control systems, it is possible to lower the energy consumption up to 30 percent [18].

Elevator planning is crucial in the development and feasibility of high-rise constructions. They are the backbone of building's structure providing core support. It is important to involve traffic flow analyst, developer, building architect and structural engineer during the initial phase of elevator construction. It helps in determining the number of shafts and elevator requirement with proper space utilization. A good understanding of the latest technology and control systems along with simulation methods are essential for estimating the required elevator configurations for the high-rise, high-speed elevators. ISO 25745-2:2015 standards are used to estimate energy consumption for elevators with speed greater than 0.15 m/s. It can be used to provide values based on measurement and calculation for new, existing and modernized elevators and classify them based on the energy classification system [15].

1.5 Ride Quality

In the mid-19th century for the first generation of elevators, the term ride quality was not thought as of much importance. Back in the 20th century, ride comfort started appearing in some articles and was considered as a measure of performance of an elevator [19]. It mainly focuses on measurable quantities such as vibration, noise, jerk and acceleration. Elevator performance is basically evaluated as a measure of time taken for an elevator to perform normal elevator motion function [20]. In recent years, there has been increase in attention among elevator users related to ride comfort [21].

While an elevator is performing its function of vertical transportation, it generates noise and vibrations. Elevator ride quality is a term that is being used to quantify, measure and analyze these levels of noise and vibration inside an elevator. Lateral and vertical vibrations are the physical factors used to quantify ride quality [21].

$$1gal = 9.8\ mm/s^2 \tag{1}$$

Vibrations that are discussed in this thesis use the unit Galileo (gal) to describe their amplitude.

Vibration amplitude is used to characterize the severity of vibration. Peak to peak value is used to quantify vibration because it is the point of maximum excursion critical for ride comfort. These values are used to define ride comfort classes. They are quantified as a sum of magnitudes of two peaks of opposite sign separated by a single zero crossing [22].

Ride quality is mainly determined based on physical motion. Ride comfort is measured as how human perceive these factors of ride quality, which is discussed in detail under the next chapter 1.6 Ride Comfort.

1.5.1 Lateral and Vertical vibration

Two main elements of an elevator motion are lateral and vertical vibrations. Perceptible levels of each vibrations will affect the ride quality.

Lateral Vibration

Lateral accelerations are mainly caused by the following contributing factors:

a) Roller guide configuration
b) Guide rail misalignment
c) Static and dynamic balance of car frame
d) Aerodynamic load
e) Elevator speed

In elevator world, side to side lateral vibration is also termed as DBG (Distance Between Guiderail) vibration.

a) Roller guide configuration:

Roller guides keep the elevator rollers always in contact with guide rail during the travel. Spring loaded roller guides are always in contact with guide rail and isolate the vibration from traveling inside the elevator. The rubber material used for the rollers and the spring constant has an impact of the ride comfort. Active rollers are used in high speed travel to mitigate the poor ride quality due to considerable changes in the guide rail because of temperature difference, wind forces, building settlement/shrinkage and other sway inducing factors. These active roller guide systems respond in real time functioning as intelligent shock absorbers [11].

b) Guide rail misalignment:

Guide rail misalignment is the main contributor to in-car vibration. Most of the misalignments are caused because of installation inaccuracy and manufacturing intolerance. Manufacturing intolerances causes guiderail curvatures and installation inaccuracies are because of inaccurate joining of rail segments [6]. For high-rise elevators, guide rails can reach over 500 meters and due to the extensive length, installation and manufacturing inaccuracies can add up to hundreds of millimeters for the entire travel length [24]. Through experiments and measurements, it has been shown that the extend of lateral vibration is in proportion to car's travelling speed [6].

c) Static and dynamic balance of car:

Dynamic balance is very important for ride quality and is one of the contributors to lateral vibration. Dynamic imbalance is due to travelling cable that is attached on the frame of the car. The mass of travelling cable vary between a minimum level at the bottom of shaft and a maximum level at the top of shaft. If the rope attachments are not mounted along the centerline of the car, varying unbalanced forces will act on the car resulting in poor ride quality. Guide rails might be deflected if a lateral force of 450N is exerted by the car onto the guiderail [25].

Static balancing mainly means reducing the eccentricity in the center of mass. While designing an elevator, an appropriate design must be selected such that the eccentricity is reduced, and proper weights are added if necessary, to statically balance the whole system. [26]. However, inertia due to building sway and guide rail misalignments cannot be eliminated. The difference in guide shoe forces due to static and dynamic unbalances must fulfill acceptance criteria depending on the ride comfort classification.

d) Aerodynamic load:

Elevator traveling along the guide rails are like trains traveling on the rails, but one of the main differences is that elevators are moving inside an enclosed space. The narrow gap between elevator and shaft can cause various problems such as induced structural vibration, excessive acoustic noise, high air resistance and rapid change of pressure inside the elevator car when it is cruising at high speed in the shaft [27]. The air turbulence can also be caused because the counterweight moving with very high speed in a confined shaft. That is, aerodynamic load created because of the car induced turbulences as it is passes every landing door and counter-weight induced turbulence can cause noise and vibration inside the elevator car [28]. Similar problems can happen when multiple cars pass each other in a common shaft [29].

e) Elevator speed:

Elevator speed has a huge impact of ride quality. As the travelling speed increases, the effect of roller guide, misalignment and air deflection are amplified [25].

Vertical Vibration

A typical elevator velocity curve during its travel is indicated by change from rest to full speed and back to rest again. Vertical acceleration is the change of velocity that happens during the travel and measured as meters per second square (m/s^2). Vertical vibration is caused by motor, the electrical drive and ropes. They are transferred into the elevator car through ropes.

Effects of vertical acceleration on a passenger is both physical and psychological and vary from person to person. Physically, how human body perceives acceleration is mostly determined by the anatomy. Weight, age and other factors influence the physical displacement of body that takes place during acceleration. This physical displacement has a psychological effect. Two people influenced by the same displacement will react differently.

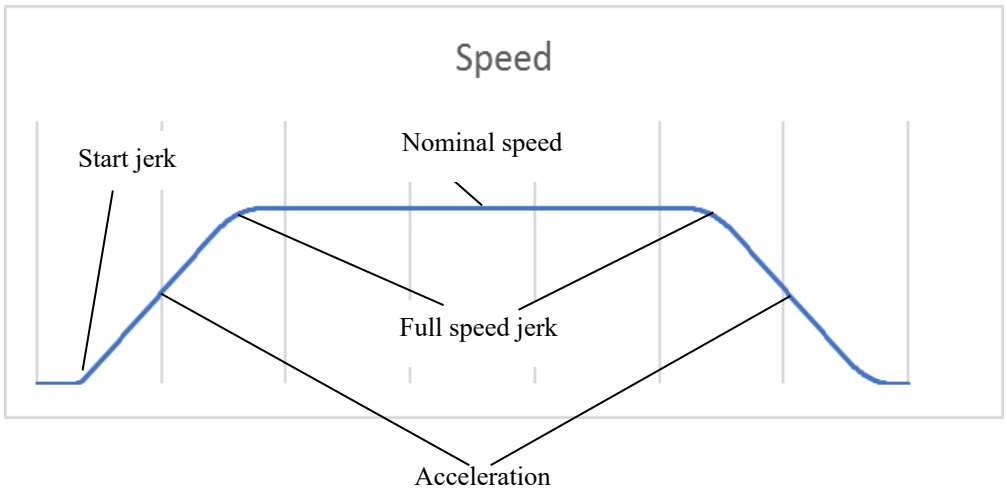

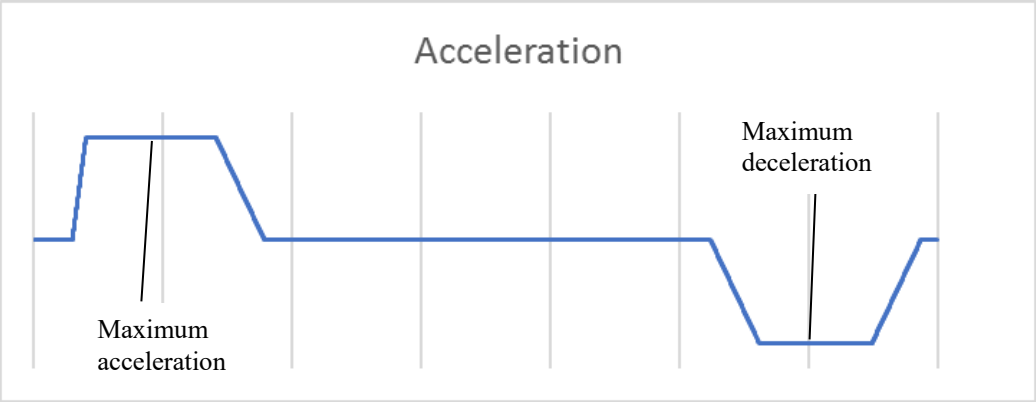

Figure 5. Elevator performance graph showing the velocity and acceleration curve

1.6 Ride Comfort

Ride Comfort is one of the focus of this thesis study because the feeling of comfort and safety that is felt between the moment people step into an elevator until they step out determines the whole elevator experience for a passenger. Until late 1900s, one of the biggest concerns that worried doctors were the nausea-inducing condition known as ‘‘elevator sickness’’, which is caused by the sudden movement of internal organs when elevators came to a sudden halt. Meanwhile, public health advocates have warned the general population regarding the spread of diseases among passengers (neighbors and co-workers) in a shared conveyance. According to Gary, author of books on early history of elevators (2002), one of the biggest debates was about the etiquette people followed back in the days. It raised questions whether a man should keep is hat on in presence of a woman, as he is in a public transport or train, or take them off, when he is at someone’s house or restaurant. These issues reflected the uncertainty regarding the elevator space, as to accept them as a mode of transportation or a tiny moving room. According to German journalist and cultural studies professor Andreas Bernard, in his latest book, Lifted, where he contemplates mankind’s relationship with elevator tracing back to the origin states that, even after a century since the first elevator, the feeling of anxiety and ambiguity never went away, still marking the experience of an elevator ride as awkward and serendipitous [13].

The comfort of an elevator can be evaluated based on the following factors:

a) Waiting time
b) Travel time, and
c) Ride comfort

There are many factors that determine the comfort criterion in an elevator. First two factors are mostly determined by the installation team and traffic flow plan. To achieve improved levels of comfort, high-rise elevators demand additional requirements on acceleration and deceleration enabling smooth vertical movement. Also, there are high recommendations on axial jerk to ensure smooth acceleration and deceleration process [15]. Further, wind-noise energy is in proportion to the sixth power of car velocity. Thus, making it another factor of nuisance when it comes to high-rise elevators. Aerodynamic noise is much higher than mechanical noise for high-rise elevators [23]. At elevator speeds over 8m/s, pressurization and depressurization can also cause discomfort to passenger’s ears.

Ride comfort is also very much influenced by the effect on the passenger resulting from the following factors [30]:

a) Noise
b) Vibration
c) Jerk
d) Acceleration and deceleration
e) Temperature
f) Smell, and
g) Degree of in-car congestion

An elevator is mainly subjected to structure-borne and air-borne noises. Structure-borne noises are generated by the contact between moving components. These noises travel into the elevator car through the car-sling structure. Air-borne noise is generated by turbulence effect because of the high speed of air passing in between the car and shaft. It enters the car through ventilation holes and gaps between seals and doors [29]. Main causes of vertical and horizontal vibrations have already been discussed in previous chapter 1.5.1. While measuring vertical vibrations, frequencies below 80Hz are considered because vertical vibrational frequencies high than 80Hz are damped by our body while it is transmitted to the head. While measuring horizontal vibrations, frequencies below 12Hz are critical because frequencies higher than 12Hz are damped by knees and ankles and thus not perceived by humans [30].

A good ride comfort can conflict with elevator performance (Figure 6). The rate of acceleration and deceleration must be a compromise between passenger comfort and high performance. The challenge is to accelerate fast enough to attain high performance at the same time trying to maintain a constant rate that is not resentful. Ramping up from rest to full speed must be smooth, abrupt change can result in discomfort. Jerk is the rate of change of acceleration or deceleration. Jerk must be constant throughout the ride, changing from one rate to another tends to be objectionable. The ramp of deceleration should also be smooth [25].

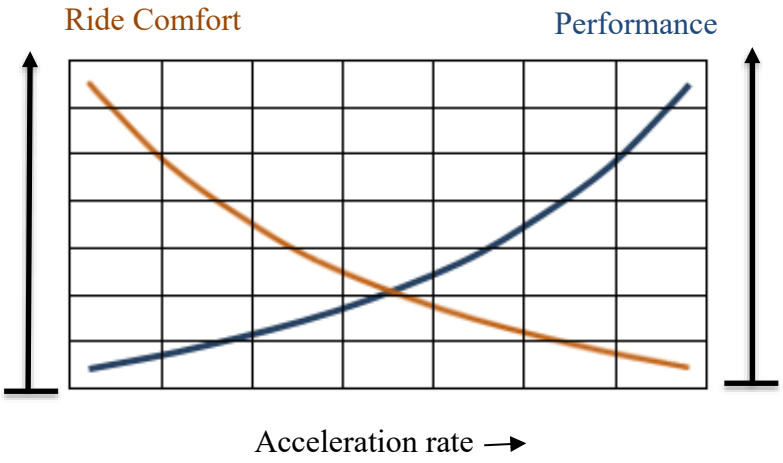

Figure 6. Relation between ride comfort and elevator performance

In addition to these, elevators must have good ventilation, proper lighting and air circulation. Proper air circulation helps to remove bad odors. Also, it must maintain an ambient temperature

that is comfortable for humans, which can be provided by using an air conditioning unit. According to [31], an average person demands $0.28m^2$ of floor space to feel comfortable. But elevators can be crowded, reducing the average floor space for a person to a minimum of $0.19m^2$. However, exceptional cases like in an office building during rush over or if the passengers know each other, densities up to $0.14m^2$ per person have been observed.

Ride comfort goes beyond elevator system, it is important to have a building with high structural integrity such that it can withstand the forces developed by the moving elevator. Also, it is important to consider the building sway on the early phase of building design to ensure good ride quality. Building must have good noise insulation property as well.

While measuring the values of noise and vibrations, it is important to do some post processing such that the results correlate with the human perception. In this thesis, all the vibrational results are filtered using low pass Butterworth Filter of 12Hz.

1.6.1 Elevator standards

Elevator standards are used to set the safety requirements concerning the design, operation, construction and maintenance of the equipment during its life time. In Europe, EN 81-20 'Safety rules for the construction and installation of lifts' defines the safety rules regarding the design and operation of elevators. ISO/TR 25741:2008 provides safety standards related to the protection of the user and vertical transportation equipment during seismic activity. It also provides information for the user to better understand the history behind and the development of latest building and elevator safety standards.

International standards do not classify acceptable and unacceptable levels of ride quality. They just prescribe procedures and set requirements for measuring and reporting elevator ride quality. The main objective of the standards is to have a uniformity in defining, measuring, processing and expressing vibration and noise that defines elevator ride quality. ISO 18738-1:2012 quantifies maximum vibration amplitude as peak-to-peak and as it is particularly relevant for passenger ride comfort. The standard defines peak-to-peak vibration as ''sum of the magnitudes of two peaks of opposite sign separated by a single zero crossing'' [22] .
In this thesis, as mentioned before, 12Hz Butterworth filters are used for later vibrations. ISO 18738-1:2012, does not quantify vibrations based on 12Hz filters.

1.6.2 Human perception of vibration

In this chapter the response of human body to vibration is mainly discussed because this thesis mostly deals with the human perception of vibrations inside an elevator car.

The response of human body to vibration has been studied for over 30 years, compiling data based on the physiological effects. The first attempt to set standards concerned with vibration and human body was published in ISO 2631-1978. This International Standard sets limitation curves based on exposure time ranging from 1 minute to 24 hours for longitudinal and transverse vibration frequency over a range of 1Hz to 80Hz frequency, the most sensitive range to human body [32].

European legislation concerned with human exposure to vibration demands constant tracking of vibration levels at suitable intervals and methods to reduce the risks associated with higher

amplitudes. ISO 2631-1:1997 gives the guidelines on how to measure whole body vibration. It provides whole body vibration frequency curves based on exposure limits and analytical equations to do necessary calculation [33]. Even though the standards do not provide exact time period for minimum and maximum measurement, it states that "the duration of measurement shall be sufficient to ensure reasonable statistical precision and to ensure that the vibration is typical of the exposures which are being assessed." [32].

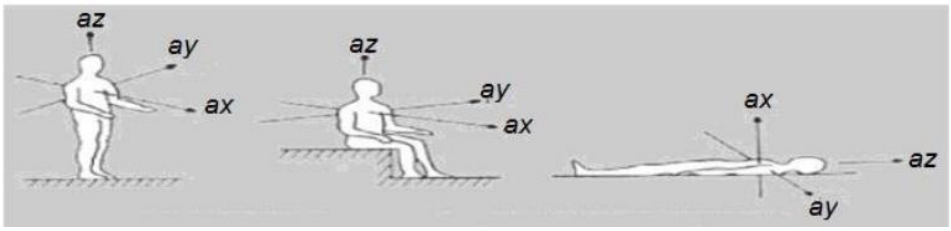

Figure 7. Coordinate system used to evaluate whole-body vibration [33]

ISO 2631-1978 covers a wide range of whole human body vibration considering the direction, magnitude, frequency and duration of vibration. It is subjected to three supporting surfaces, especially feet of a standing person, buttocks of a seated person and supporting area of a lying person. Three criteria for severity assessment are quoted [32] (Figure 8):

i. Comfort criteria, shown by the curve for reduced comfort boundary
ii. Working efficiency relevant for machines and vehicle operators, shown by fatigue-decreased boundary
iii. Threat to health and safety, indicated by exposure limit.

There have been criticisms against ISO 2631: 1978. According to [34], the author claims that the exposure time is independent or not associated with the comfort criteria and frequency weighting method is only relevant for sinusoidal vibrations. Hansson and Wikström criticized the standards for their selection of test subjects for the experiments. According to [35], the subjects for laboratory studies were mostly young males, exposed to sinusoidal vibration along vertical axis.

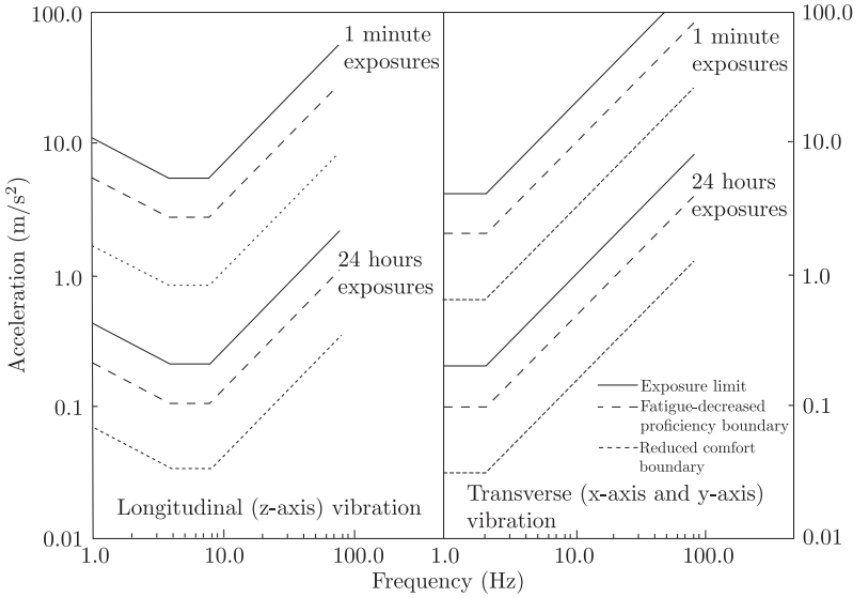

Figure 8. Graph showing the severity criteria for whole body vibrations (Extracted from ISO 2631: 1978) [67]

Human perception to vibration is subjective varying over time and from person to person. Whenever a human body is in contact with a vibration surface (i.e. standing inside an elevator), whole-body vibrations occur [36]. Human body is very sensitive to vibrations and can detect acceleration as small as $0.01 m/s^2$. How humans perceive them is approximately constant for a range of 2Hz to 100Hz frequency and are not dependent on the position of the passenger inside the elevator. ISO code has classified the human body exposure to vibrations into three different kinds depending of frequency:

- Travel sickness (0.1Hz to o.63Hz)
- Whole body (1Hz to 80Hz)
- Hand-arm (6.3Hz to 1250Hz)

Until recently, it was difficult to measure and quantify these vibrations accurately. The challenge is to measure these vibrations in all three axes (X, Y, Z) simultaneously and measure the acceleration, which must be then integrated with human perception [32]. Frequency filter is applied for a vibration measurement of the global value to take into consideration of the human sensitivity varying with frequency [37]. Human body can be considered as a complex system of interconnected elements with viscos-elastic connections. It will exhibit a dynamic response to any external vibration stimulus and the response vary depending on the following factors:

- Nature of applied vibration (amplitude, frequency and point of application)
- Structure and body composition, i.e. the mechanical constants of the constituent elements (weight, tissue distribution and viscous properties, strength and mass of organs)
- Posture of human body: standing, sitting or lying.
- Point of interest (arms, legs, shoulder or whole body)

Figure 9 shows human body as a skeleton bound by elements which can be used as a representation for muscles, ligaments, tendons. It can be seen from the figure below that each element has its own frequency range. Hence at different vibration excitation, each element acts differently and are prone to damage, pain and discomfort different scale [32].

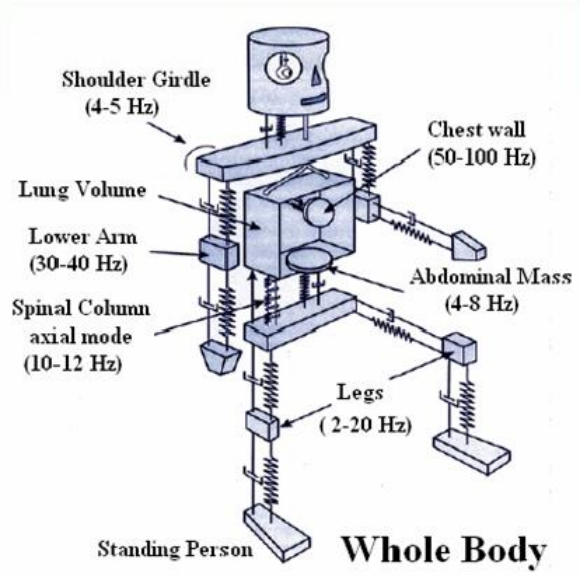

Figure 9. Mechanical model representation of human body with natural frequency range of each elements [28]

Human response to transient vibrations is higher than that of steady state. Human perception of vibration for both steady state and transient are functions of frequency. The frequency range that are perceived by humans corresponds to the natural frequency of most structural systems [20]. To reduce vibration inside an elevator to an acceptable comfort level, it is essential to have a robust elevator guidance system along with meticulously aligned guide rails [15].

2 Scope of Research

This research was borne out of the need to reduce vibration inside an elevator and thereby improve ride comfort. This research aims to study the lateral vibration of elevator while traveling at various speed and various building sway conditions. The biggest challenge for an engineer is to estimate the ride comfort of an elevator during the initial phase of elevator design. Even though architecture provides information related to sway and building properties (2.2.1), these data, while impressive, is still meaningless unless used to generate some understanding related to in-car vibration.

The transient dynamic simulation used for ride comfort computation demands a long computation time. Also, it makes it very difficult for anyone without specific engineering background to use it. Thus, the expected result of this research work is a parametric equation, which is generated by using regression models that predict the peak-to-peak vibration as a function of elevator speed, building height, and sway amplitude. This equation will help engineers to optimize the velocity profile that needs to be followed in order to maintain the required ride comfort for the specific elevator based on the building properties and sway conditions.

Finite element computation is performed using Abaqus [37] for a high-speed high-rise elevator to evaluate in-car vibration for a various elevator and building conditions. Also, the insights and contribution of the thesis can be used to develop competence and knowledge in future ride comfort related studies for high-rise elevators.

2.1 Technical Background

Vibration Excellences (VIBES) was a TEKES (Finnish Funding Agency for Technology and Innovation) research project, from 2012 to 2015, where methods for simulating and improving elevator ride comfort were investigated. The project started with the aim to reduce noise and vibration of an elevator and consequently optimize the ride comfort. The project was executed in three phases: Lateral vibration, in-car noise and building interface noise.

This thesis work is a continuation of VIBES project, in which the target was to develop the model further and include building sway studies. Initially, a multibody simulation (MBS) was developed for a single deck elevator which gave a better understanding on the dynamics of elevator. This was model was further developed to utilize finite element analysis in studying the lateral vibration ride comfort. The MBS model uses flexible structures which helps in optimizing the design parameters. While, finite element study uses rigid components that can help in examining the structural details and material influence.

To compute the lateral vibration, finite element model was defined which consisted of substructures and system level models. Sling and car, guide rails and rollers were reduced to substructures using Guyan reduction (3.1.2) and then imported and used the system level. The model is excited by applying misalignments of the guide rails, vertical travelling speed and aerodynamic load due to counterweight. The aerodynamic load due to counterweight was simulated using Computational Fluid Dynamics (CFD). These loads are quantified by simulating the air flow around the elevator. Fluid dynamics simulations were performed using commercial software Ansys Fluent 14.0/14.5.

2.2 Literature review

There have been many studies concerning the in-car vibration and most of the already published work focuses on a certain specific point related to the origin of vibration and their mitigation strategy. One of the major causes of vibration in a roped elevator is the rope sway forces. Ropes connecting the car and counterweight tend to oscillate because of wind induced building deflection or vibration of the ropes. [38], presents a method to reduce rope forces using a non-stationary optimal controller. [39] focus on the dynamic behavior response of elevator ropes under seismic excitation. Deterministic and stochastic models were used to develop the suspension and compensating ropes equations of motion. It also presents simulated and experimental whirling motion of the rope displacement. Another method to mitigate rope sway is discussed in [40], where dampers with sensors are used to detect the rope movement and dampers position themselves to interrupt the rope sway. [41] shows study on numerical simulation of aerodynamic load variation on a high-speed elevator because of the counterweight. In this study, unsteady turbulent flow of a two-dimensional elevator model is used for the analysis. The numerical results showed higher forces when the counterweight meets the car in the shaft and negative force when counterweight is still located in the elevator car surface vicinity.

One of the main transfer paths of vibration coming from the guiderails are through roller guide systems. Active damping is one of the most researched method to reduce vibration because of guide rail misalignments. [42] Presents a damping method using an active damper which detects instability between car and guide rail to actively damp elevator vibration. [43] also presents an active damping system for reducing lateral vibration in an elevator car. This approach uses an actuator that generates vibration-damping force against the lateral vibration while performing the action of vertical transportation.

Although all these methods focus on reducing in-car vibration generated from a specific source, a holistic approach concerning all the forces that excites the elevator running in a shaft of a high-rise building that sways in either direction has not been researched extensively. Finite element methods are mainly used to optimize the design for stress and weight for different components of elevator. [44] has made a comprehensive analytical and finite element static analysis study to determine the stress and deformations on a car frame component under load conditions. [24] is the only found article that focuses on ride comfort from finite element point of view considering all the important issues that induce vibration in an elevator car. This research is a continuation of this article.

As mentioned in the earlier paragraphs, there are different approaches to tackle the problem of rope sway. An approach for controlling the rope sway of an elevator by varying the travelling speed is discussed in [45]. A similar approach has been used in this thesis work, where I perform finite element analysis to predict the vibration by varying the elevator speed at different shaft height.

2.2.1 Sway

One of the major design considerations particularly related to tall buildings are the concerns of building sway. All buildings irrespective of the height sways during windstorm, but the sway amplitude in skyscrapers or high-rise buildings can be large enough to cause discomfort to

occupants and damage structural integrity. These horizontal wind loads can move the building even hundreds of millimeters in either lateral direction.

Building sway is caused by various factors such as lateral wind loads, strong sunlight and temperature changes and earthquakes. It is important to distinguish forces acting on a building due to wind loads and earthquakes. Earthquake forces are the results of motion of the ground on which the building rests. The foundation of the building structure and its property has an influence on the generated forces. During an earthquake, the ground along with the building foundation moves while the rest of the building which is above the ground resists this motion because of the inertia, and results in structural distortion. This wave travels along with building structure and results in oscillation. Compared to earthquake, behavior of building under wind load is different. Flow of wind can be uniform or turbulent, load due to uniform flow can be considered as static while turbulent flow causes the load to change rapidly and can result in much greater damages than gradually applied load. Under the wind load, building bends slightly in the direction of wind, then moves to a neutral position and then in the direction opposite to that of the wind. Even though along-wind bends the building structure, typical sway problems are related to cross-wind. This back and forth oscillation continue until it eventually stops after some time. Thus, rather than the exposed surface, the impact magnitude of earthquake is a function of mass of the building structure. A building structure comprising of heavy structure tend to sway less in wind, while this does not guarantee safety during an earthquake [46]. These oscillations will adversely affect the performance and safety of elevators operating in the building.

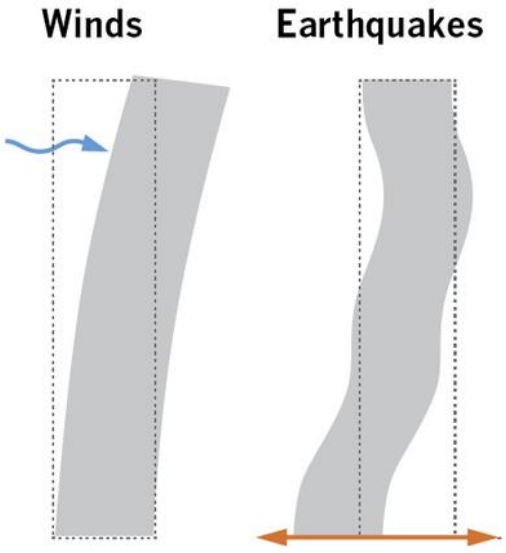

Figure 10. Gradual increase in deflection because of the wind load and structural distortion because of earthquake [83]

2.2.2 Wind load on tall building

The pressures exerted on the building due to the wind loads depend on the wind characteristics and the geometry of the structure. The applied load or pressure keeps on fluctuating as a result of the wind strength, turbulence and vortex shedding towards the edges of the structure. Wind Loading Standards are often referred to while designing a structure, but these standards are not applicable to structures that have unusual shape or location. As mentioned before, even if the loads generate low levels of stress and strain, the crucial sway problem is concerned with the

human perception to resonant motion and vibration [47]. The experience of fear and anxiety as a result of wind-induced building vibration is mainly dependent on the extreme wind condition occurrences and the discomfort mainly results from frequency of such occurrences. Traditionally, such discomforts are measured on 5-years to 10-years interval. But studies have shown that people are more tolerant to discomforts experienced infrequently or for a short period of time. Although such events result in small amount of fear and alarm, it does not necessarily address the overall discomfort experienced by the occupants. Thus, recent trend is to evaluate events on one-year time interval which is more significant in terms of discomfort experienced on shorter regular interval [48].

High-rise buildings tend to have low fundamental frequency, lower than 1Hz, due to its slender shape of the structure. Wind and/or earthquake exerts stochastic load to the high-rise building resulting in the structural vibration in its first natural frequency, also called as the fundamental frequency (f_0) [49]. 'Natural frequency' is the term used for tall building to determine the significance of its dynamic response under severe load conditions. Construction of tall buildings by latest methods using lighter materials leads to wind-induced building sway due to their high flexibility, lower densities, damping properties and lower natural frequencies [50]. ASCE Standard [ASCE 7-05] classification is used to tell between dynamic and rigid behavior of a structure. A structure with natural frequency less than 1 Hz ($f_0 < 1$ Hz) is classified as dynamically sensitive, otherwise considered to be rigid structure. Approximation formula used to determine building frequency is $f_0 = 46/H$, where 'H' is height of the building [51]. In Japan, approximation for building frequency $f_0 = 67/H$ is used based on field measurements [52].

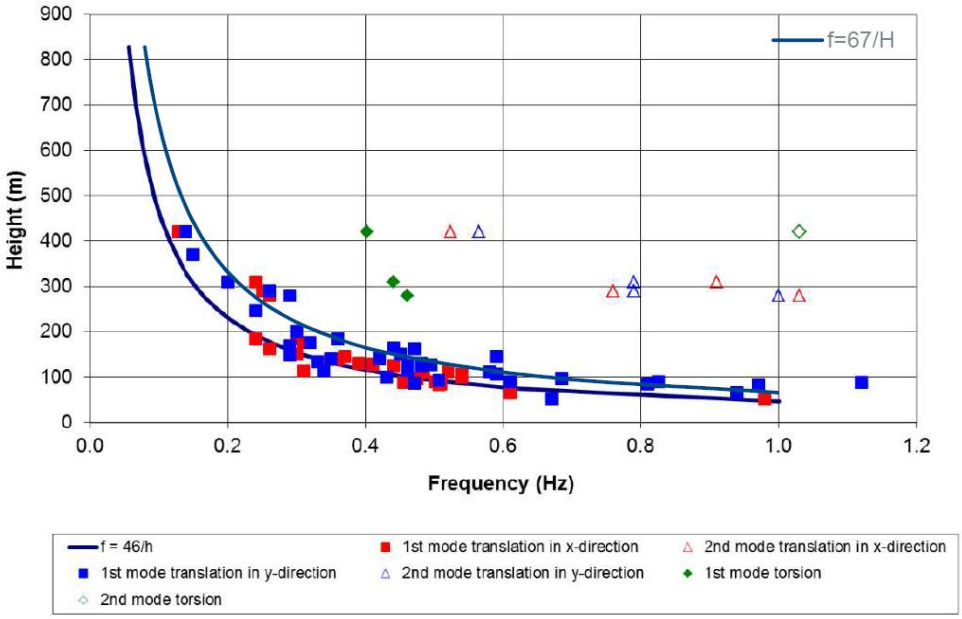

Figure 11. Building frequency measurements showing 46/H and 67/H approximation [51]

Currently there is no internationally accepted levels for maximum allowable building motion. Since the typical vibration frequency range for a wind-excited tall building is in the range of 0.63 – 1 Hz, it was used in the first attempt to set an international standard (ISO 6897: 1984 (International Organization for Standardization 1984)) for acceptable level of building motion

[50]. But studies have been carried out to determine perception limits based on individual response to motion simulators. These testers used sinusoidal excitations producing frequency is the range of 0.125 Hz to 0.500 Hz; and the results were unreliable due to some discrepancies between testing environment and actual structure [53]. Another study carried out in 2006, tried to examine the body movement affected by building motion, and effect of increase in body movement on perception of motion. To observe the acceleration, accelerometers were placed on head and torso of the participants. The study showed an increase of acceleration in the torso within the range of natural body frequency (0.1 – 0.4 Hz). Another important finding observed that postural instability occurred and fall within the existing building frequency effected by wind load [54].

Impact of high wind results in swaying motion of building. This motion will be passed over to the travelling cables and suspension ropes of the elevator in the building. Also, resonance occurs when the amplitudes of the ropes coincide with that of the building under the impact of strong loads. High-rise elevators have at least basic components as shown in the figure below (Figure 12.), when all these components are put together based on the arrangement the system, it will have its own inherent vibration amplitude. This swaying motion with large amplitudes can cause damages to the ropes, cables and other hoisting equipment. Considering the bending and deformation of a high-rise building and analyzing vibration data indicates that when the elevator car is located at the extreme top or bottom of the shaft, rope sway has the maximum amplitude at the middle of the hoist way forming an arc away from its vertical axis. The frequency increases with the load impact. Observed results has shown that the extend of wind related damages can be minimized by reducing the elevator speed or parking the elevator in the non-resonant location [55].

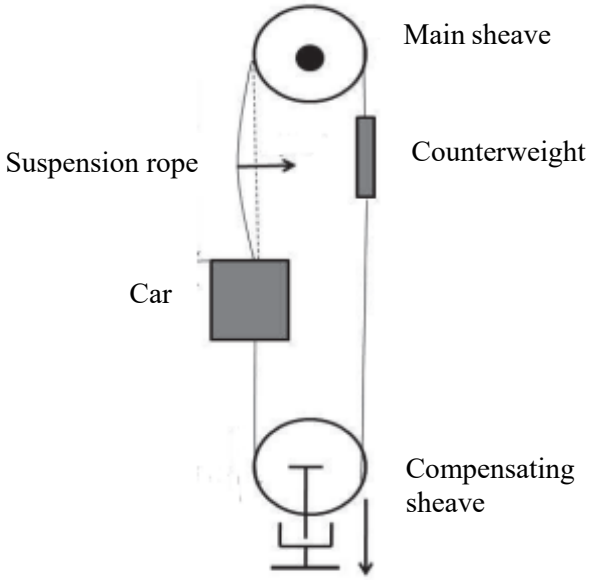

Figure 12. Components of a high-rise elevator and swaying motion [84]

There exist several criteria that evaluate the discomfort recurrence event based on vibration amplitude, vibration frequency and the dependency based on building type (office, hotel and residential). It is challenging for elevator engineers to predict all these criteria prior to the installation in order to provide an estimation of the elevator service that can be provided. However, as discussed before, building motion has considerable impact on the functionality of the

elevator system in a building. Elevator design needs to consider the building response to wind conditions which are generally based on the excitation levels and return period from wind analysis report [52].

For mega high-rise buildings, it could be assumed that the vibrational frequency of the building is linearly inversely proportional to height, so doubling the height would half the frequency. For building sway amplitude, the design criteria is the acceleration level, which can be expressed as,

$$Acceleration = amplitude * frequency^2 \tag{2}$$

That means, if the frequency is halved, the amplitude can be quadrupled for same acceleration level.

2.2.3 Rope dynamics

Natural frequencies of high-rise buildings are lower than that of conventional buildings. Therefore, at certain level the natural frequency of the rope and building will most likely coincide resulting in resonance [56].

For a roped elevator system, the car and counterweight are suspended using suspension rope and rope weight is compensated by compensation sheave and compensating rope. The rope will get excited and starts to vibrate when building is induced by wind forces. [57] presents a solution to the forced vibration of a rope with time varying length. This method approaches the problem with the assumption that rope damping is zero, and car velocity and rope tension is constant.

The model used for vibration analysis is shown in Figure 13. It is assumed that rope is a string and z axis represents the up/down direction of elevator car from sheaves and horizontal rope deflection of rope is represented by‘d’. The differential equation of the rope can be expressed as:

$$\rho A\left(\frac{\partial}{\partial t} - V\frac{\partial}{\partial z}\right)^2 d - \frac{\partial}{\partial z}\left(T\frac{\partial d}{\partial z}\right) + C\left(\frac{\partial}{\partial t} - V\frac{\partial}{\partial z}\right)d = 0 \tag{3}$$

where ρA is the mass density per unit length of the rope, T is the rope tension, C is the damping coefficient per unit length of the rope and V is the velocity of the car [57].

$$T(z) = \begin{cases} T_0 + \rho A g(L_0 - z) & (Suspension\ rope) \\ T_0 + \rho A g z & (Compensating\ rope) \end{cases} \tag{4}$$

$$T_0 = \begin{cases} \left(M_c + \frac{1}{2}M_s\right)g & (Suspension\ rope) \\ \frac{1}{2}M_s g & (Compensating\ rope) \end{cases} \tag{5}$$

M_c is the mass of car, M_s is the mass of compensating sheave, L_0 is the distance between traction and compensating sheave and g acceleration due to gravity.

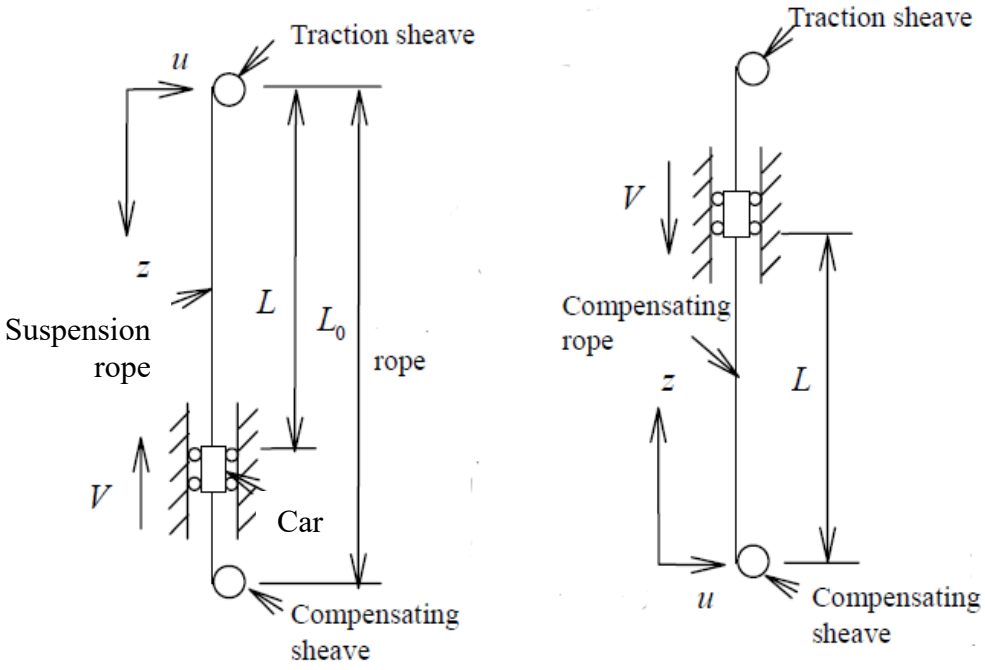

Figure 13. Simulation model with one end fixed and car end moving [57]

According to the assumption, $T = constant$ and $C = 0$, which means equation (3) can be written as follows:

$$\left(\frac{\partial}{\partial t} - V\frac{\partial}{\partial z}\right)^2 d - a^2\frac{\partial^2 d}{\partial z^2} = 0 \tag{6}$$

where the wave propagation velocity is represented by $a = \sqrt{T/\rho A}$

Since traction sheave is in the top of the building, it sways along with the building. Hence, we consider the case where traction sheave is excited, and car is moving.

Figure 13 can be also represented in simple way as shown below (Figure 14), where one end is fixed, and other sheave end moves with time.

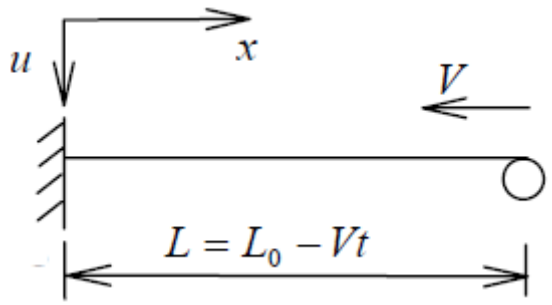

Figure 14. Shows the fixed end and moving sheave end [57]

It is considered that the traction sheave is excited by a sinusoidal function represented by $Sin(2\pi\tau)$. The propagated wave of the rope can be represented as Figure 15.

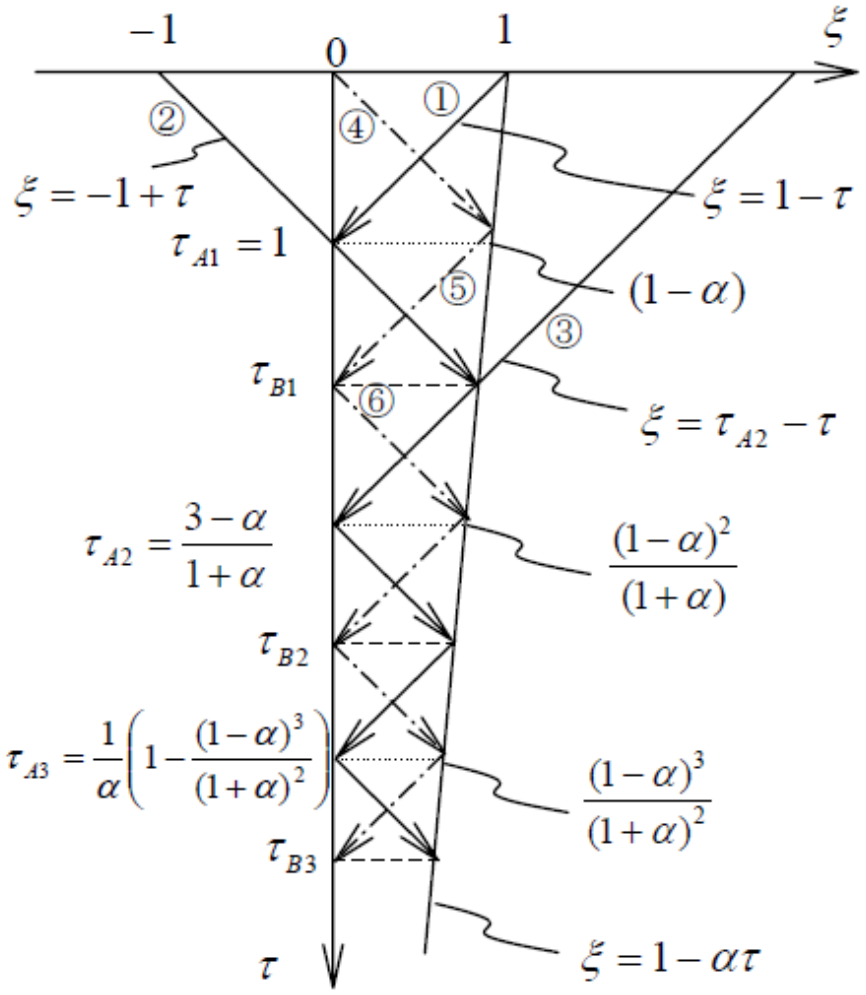

Figure 15. Wave propagation of rope [57]

where $\alpha = V/a,\ \xi = x/L_0$ and $\tau = at/L_0$.

The left end of the rope is represented by τ axis ($\xi = 0$) and right end is given by the line $\xi = 1 - \alpha\tau$. The rope waves reflect at times τ_{An} and τ_{Bn} and corresponding rope length is given by $L(\tau_{An})$

$$\tau_{An} = \frac{1}{\alpha}\left\{1 - \frac{(1-\alpha)^n}{(1+\alpha)^{n-1}}\right\} \tag{7}$$

$$\tau_{Bn} = \frac{1+\tau_{An}}{1+\alpha} \tag{8}$$

$$L(\tau_{An}) = \frac{(1-\alpha)^n}{(1+\alpha)^{n-1}} \tag{9}$$

The rope wave starts from the position $\xi = 1$ and it is expressed as $\xi = 1 - \tau$ and reaches the left end at time $\tau = \tau_{A1} = 1$. The wave happens in the rope when $\xi - 1 + \tau > 0$, and it is expressed as:

$$sin\left(2\pi\frac{\xi+\tau-1}{1-\alpha}\right) * 1(\xi+\tau-1) \tag{10}$$

where $1(\xi - 1 + \tau)$ is a step function. The wave is reflected at left end with same wave length.

$$-sin\left(2\pi\frac{\tau-\xi-1}{1-\alpha}\right) * 1(\tau-\xi-1) \tag{11}$$

The wave then reaches the right end at time τ_{B1} and reflected again. The wave length is reduced to $(1-\alpha)^2/(1+\alpha)$ and it can be expressed as:

$$sin\left(2\pi\frac{1+\alpha}{(1-\alpha)^2}(\xi+\tau-\tau_{A2})\right) * 1(\xi+\tau-\tau_{A2}) \tag{12}$$

Therefore, summing all the waves gives the solution for forced rope vibration when excited by sinusoidal function $Sin(2\pi\tau)$ as:

$$\begin{aligned} d(\xi,\tau) = \sum_{n=1}^{\infty}\Bigg[& sin\left\{2\pi\frac{(1+\alpha)^{n-1}}{(1-\alpha)^n}(\xi+\tau-\tau_{An})\right\} * 1(\tau+\xi-\tau_{An}) \\ & - sin\left\{2\pi\frac{(1+\alpha)^{n-1}}{(1-\alpha)^n}(\xi-\tau-\tau_{An})\right\} * 1(\tau-\xi-\tau_{An})\Bigg] \end{aligned} \tag{13}$$

$$(0 \le \xi \le 1-\alpha\tau)$$

Similarly, if one end of the rope is excited by displacement X_s, exact solution for the vibration is given as:

$$d(\xi,\tau) = \sum_{n=1}^{\infty}\left[X_s\left\{\frac{(1+\alpha)^{n-1}}{(1-\alpha)^n}(\xi+\tau-\tau_{An})\right\} * 1(\tau+\xi-\tau_{An}) - X_s\left\{\frac{(1+\alpha)^{n-1}}{(1-\alpha)^n}(\xi-\tau-\tau_{An})\right\} * 1(\tau-\xi-\tau_{An})\right] \quad (14)$$

$$(0 \le \xi \le 1-\alpha\tau)$$

According to the outcome of set of differential equations described in article [58], it is found that rope displacement in all three (x, y, z) directions appear in each differential equation describing rope motion. This means that rope motion in each direction is coupled to each other and will interact. Thus, displacement in any one direction (e.g. longitudinal) can generate displacement in other direction (e.g. vertical). Consequently, at some point during the travel, the natural frequencies of longitudinal and vertical natural coincide, and this cross coupling will stimulate the elevator vibration.

It is useful to understand the sources of these vibrations, but a practical engineer would try to find ways to minimize the effect of vibrations. Resonance depends on the rope properties such as length and mass, which is specific to elevator configurations and travel parameters. Therefore, it is nearly impossible to avoid resonance completely. Resonant frequency can be lowered by adding additional mass to elevator system, but it simply moves the resonant frequency to higher location. Also, additional mass means higher stress on load bearing components. Rope properties such as damping character has a high contribution to the transfer of vibration. The ability to absorb or dissipate vibrational energy is the key to reducing vibration. Traditional steel ropes provide very little damping, which makes it difficult to dissipate vibrational energy [58]. New hoisting technology such as Ultra-Rope developed by leading elevator company KONE is extremely light and uses carbon fiber core and high-friction coating. The developer states that ‘‘carbon fiber used for ultra-rope resonates at completely different frequency to steel and most other building material,’’ thus able to provide better performance than steel ropes during sway conditions [16].

Several mechanical methods have been patented to restrain the sway amplitude at one or more locations between car hoisting end and car rope attachment [58]. Vibrations due to sway can be minimized by using appropriate vibration dampers between the source and car. Also, rope movement can be minimized using vibration absorbers and use of resonance suppressers can eliminate the interference between control system and vertical vibration [23].

3 Modelling Strategy

It is really important to choose an appropriate modelling strategy that can be applied for dynamic simulation of high-speed elevators. These elevators experience vibration due to many factors of random excitations and parameters that needs to be incorporated in the finite element computation. The theory behind rope vibration during sway has already been explained under section 2.2.3 (Rope Dynamics). The rope model was developed using Finite Difference method. Under this section FEM and CFD simulation strategies utilized for developing the elevator model and the theory behind them are discussed. Also, the nodal analysis approach towards solving a dynamic vibration problem is mentioned under natural frequency and mode shape. The simulation model makes use of Rayleigh damping formulation to determine the damping coefficients, which is explained in the final chapter.

3.1 Finite Element Method (FEM)

Finite element method is one of the most commonly used techniques to perform vibration analysis. It works on the principle that the domain of interest is divided into small subdomains in which the partial differential equations (PDE) are approximately solved. Even though FEM is capable of handling complex loading such as time of frequency dependent loading, it is much restricted by the modelling complexity of structural geometry.

There are three phases of analysis for a typical finite element process, as indicated in Figure 16. The pre-processing phase consists of specifying and checking the input data. This is followed by the solution phase in which the analysis is carried out. The final phase, which is known as the post-processing phase, is concerned with the interpretation and presentation of the results of the analysis [59].

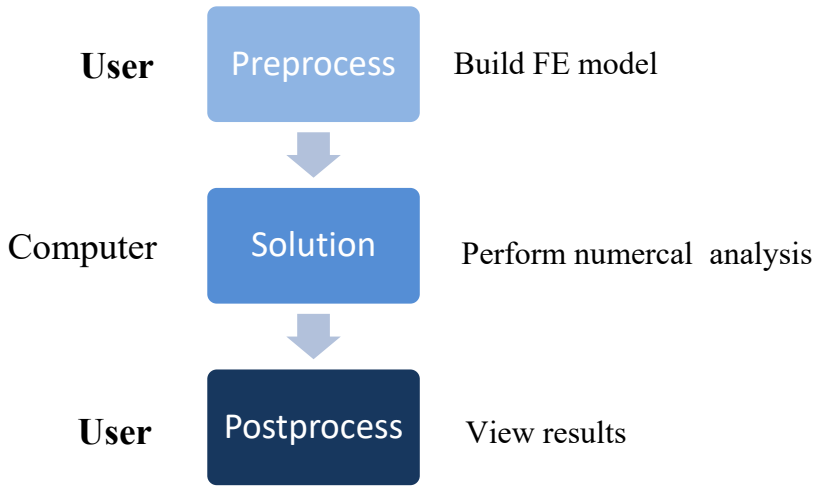

Figure 16. Three phases of FEM analysis

In this research, simulation is performed by using implicit dynamic analysis where nonlinear dynamic responses are studied.

3.1.1 Dynamic Implicit Analysis

Transient dynamic responses of a system are calculated by using dynamic implicit analysis method. This approach was chosen for the simulation because it includes the option for non-linearity and involves interaction of moving body with other components in the model. When using nonlinear dynamic response, system response is obtained by direct integration of all degrees of freedom. This method is expensive because, global equations of motion of the system are integrated across time.

Implicit schemes used in Abaqus/Standard obtain values for the dynamic quantities at time $t + \Delta t$, which means that they are not just solved for the available values at t, but also at increment of small-time step Δt. This approach uses Hilber-Hughes-Taylor operator, which is an extension of trapezoidal rule. Even though implicit schemes are capable of handling nonlinearity, in cases with extreme nonlinearity, it might have difficulties in obtaining a solution. The time step used for implicit integration is determined based on the concept of ‘‘half-step residual’’ introduced by Hibbit and Karlsson (1979). It works in such a way that, when the solution at $t + \Delta t$ is obtained, equilibrium residuals at halfway through time increment is monitored and subsequently accuracy of the solution is assessed and next time step is adjusted accordingly [60].

According to the equilibrium condition, over the volume of material in the body, all the forces and moments acting on a body are always in equilibrium. Equilibrium statement is expressed in the form of virtual work statement so that it can reduced and used in finite element model.

$$\int_{\boldsymbol{S}} \boldsymbol{f_S} dS + \int_{V_o} \boldsymbol{f_V} dV_o = 0 \tag{15}$$

where $\boldsymbol{f_S} = \boldsymbol{t}$ is the surface traction force, $\boldsymbol{f_V} = \boldsymbol{f}$ is body force within the volume, $V_o = V$ denotes the volume occupied by body and S represents the surface bounding the volume.

Surface traction force is defined using Cauchy stress matrix $\boldsymbol{\sigma}$ as;

$$\boldsymbol{f_S} = n\boldsymbol{\sigma} \tag{16}$$

where n is the boundary normal pointing outwards from the structure.

Applying Gauss theorem to the surface integral in the equilibrium equation gives,

$$\int_{\boldsymbol{S}} \boldsymbol{n\sigma} dS = \int_{V_o} \left(\frac{\partial}{\partial x}\right) \boldsymbol{\sigma} dV_o \tag{17}$$

since volume is arbitrary, equation must apply pointwise in the body,

$$\left(\frac{\partial}{\partial x}\right)\boldsymbol{\sigma} + \boldsymbol{f_V} = \mathbf{0} \tag{18}$$

Momentum equilibrium equation can be expressed as,

$$\int_{\boldsymbol{S}} (u \times \boldsymbol{f_S}) dS + \int_{V_o} (u \times \boldsymbol{f_V}) dV_o = 0 \tag{19}$$

equilibrium equation represented by equation (18) is replaced by a ‘‘weak form’’, which is the virtual work principle. Here the pointwise differential equation is multiplied by a ‘‘test-function’’ which is a virtual arbitrary velocity field represented by $\delta \boldsymbol{v}$

$$\int_{V_o} \left[\left(\frac{\partial}{\partial x}\right)\boldsymbol{\sigma} + \boldsymbol{f_V}\right] \delta \boldsymbol{v}\, dV_o = 0 \tag{20}$$

Applying Gauss theorem and using Cauchy stress with the first term, virtual work statement, equation (18) can be written as

$$\int_{\boldsymbol{S}} \boldsymbol{f_S}\, \delta \boldsymbol{v}\, dS + \int_{V_o} \boldsymbol{f_V}\ \delta \boldsymbol{v}\, dV_o = \int \boldsymbol{\sigma} \left(\frac{\partial \delta \boldsymbol{v}}{\partial x}\right) dV_o \tag{21}$$

derived from the basic equations for standard displacement-based finite element analysis, the interpolator that approximates the displacement can be written as;

$$\boldsymbol{u} = \boldsymbol{N_N} u^N \tag{22}$$

where u^N is the nodal variables and $\boldsymbol{N_N}$ interpolation functions that depend on the material coordinate system.

This is used for almost all elements in Abaqus. Beam element (B33) used in this simulation also takes similar form. Using the displacement interpolation assumption, d’Alembert force terms can be expressed as below;

$$\int_{V_o} \boldsymbol{N_N}\, \rho \boldsymbol{N_N}^{\boldsymbol{T}} dV_o \ddot{\boldsymbol{u}}^N + \int_{V_o} \nabla \boldsymbol{N_N} \boldsymbol{D} (\nabla \boldsymbol{N_N})^{\boldsymbol{T}} dV_o d\boldsymbol{u}^N = \int_{\boldsymbol{S}} \boldsymbol{N_N}^{\,T} \boldsymbol{f_S} dS + \int_{V_o} \boldsymbol{N_N}^{\,T} \boldsymbol{f_V} dV_o \tag{23}$$

which is a representation of, mass matrix times the acceleration + internal force vector = external force vector. Where vector and matrix are within the space of u^N nodal variable [60].

3.1.2 Substructures and Guyan reduction

Substructures are used to approximate the motion of a part in dynamic analysis. The basic idea is to eliminate almost all degrees of freedom of a model but the ones that are used to connect the substructure part to rest of model [60]. Substructures are used in the presented simulation

model to save computation time and resources of running very large models. Also using substructures is beneficial for analyses of repeated geometry patterns such as roller guides, where multiple copies of generated substructure can be used, thereby saving time and energy.

In case of dynamic simulation, model transformation is performed to generate substructure. Mass and damping matrices are reduced during transformation, process known as 'Guyan reduction'. Guyan reduction assumes that there is a static relation between the retained nodes and eliminated nodes. Also, since it is a nonlinear analysis, the matrices related to linear relations are only transformed during substructure generation so that it is not calculated for every equilibrium iteration [61].

Guyan reduction can be explained in simple terms as follows [62];
The stiffness equation for a model can be written as given below:

$$[K^n]\{x_n\} = \{F_n\} \tag{24}$$

Stiffness matrix can be represented as a combination of matrices of active and eliminated degrees of freedom.

$$\begin{bmatrix} K^{AA} & K^{AE} \\ K^{EA} & K^{EE} \end{bmatrix} \begin{Bmatrix} x_A \\ x_E \end{Bmatrix} = \begin{Bmatrix} F_A \\ F_E \end{Bmatrix} \tag{25}$$

Superscript A represents active matrices connected to retained degrees of freedom and E represents the eliminated degrees of freedom. But it is obvious that the forces on eliminated degrees of freedom is zero

$$[K^{EA}]\{x^A\} + [K^{EE}]\{x^E\} = \{0\} \tag{26}$$

solving for the displacements at eliminated degrees of freedom gives:

$$\{x^E\} = -[K^{EE}]^{-1}[K^{EA}]\{x^A\} \tag{27}$$

First part of equation (25) can be written as,

$$[K^{AA}]\{x^A\} + [K^{AE}]\{x^E\} = \{F_A\} \tag{28}$$

Now, substituting equation (27) in equation (28) gives

$$[K^{AA}]\{x^A\} - [K^{AE}][K^{EE}]^{-1}[K^{EA}]\{x^A\} = \{F_A\} \tag{29}$$

Manipulating the above equation, transformation matrix for substructure can be written as;

$$[T^S] = \begin{bmatrix} [I] \\ -[K^{EE}]^{-1}[K^{EA}] \end{bmatrix} \tag{30}$$

where $[I]$ is a unit matrix.

Thus, reduced stiffness and mass matrix can be expressed as

$$[K] = [T^S]^T[K^n][T^S] \tag{31}$$

$$[M] = [T^S]^T[M^n][T^S] \tag{32}$$

Finally, generating a substructure involves eigen value problem solving, computation of static modes of substructure stiffness matrix and global system matrix projection onto the space of substructure modal. It demands a lot of computation time and resources.

3.2 Computational Fluid Dynamic (CFD)

Under the section 1.5.1, it is explained that aerodynamic load is one of the major contributors to lateral vibrations in high-speed elevators. The relative motion between elevator car and counterweight were simulated to calculate surface pressure data. The time history of the pressure data was exported and then subsequently used in finite element simulation.

Computational fluid dynamics usually makes use of Navier-Stokes equation for solving numerical simulations. In this research, simulations were performed by solving Unsteady Reynolds Averaged Navier-Stokes (URANS) in a finite volume fluid domain. This approach is mostly used in solving industrial turbulent flows because it enables the users to make use of large computation cells and large time steps. The effect of turbulent vortices is considered by modeling their effect on the momentum transport. Since the effect of discontinuities such as counterweight passing (aerodynamic impact when the counterweight is closest to the elevator travelling at high speed) is to be studies, transient simulation using problem solving is employed.

Governing equations of motion for Reynolds Averaged Navier-Stokes are shown below [63]:

All fluid motions are governed by continuity equation and momentum equation as shown below respectively,

$$\left[\frac{\partial \tilde{\rho}}{\partial t} + \bar{u}_j \frac{\partial \tilde{\rho}}{\partial x_j}\right] + \bar{\rho} \frac{\partial \bar{u}_j}{\partial x_j} = 0 \tag{33}$$

$$\bar{\rho}\left[\frac{\partial \tilde{u}_i}{\partial t} + \bar{u}_j \frac{\partial \tilde{u}_i}{\partial x_j}\right] = -\frac{\partial \tilde{\rho}}{\partial x_i} + \frac{\partial \bar{T}_{ij}{}^{(v)}}{\partial x_j} \tag{34}$$

where $\bar{u}_i = \bar{u}_i(\vec{x}, t)$ is a function of space $\vec{x}$ and time t and $\bar{T}_{ij}{}^{(v)}(\vec{x}, t)$ is the viscous stress tensor.

Viscous stress tensor can be expressed in terms of fluid molecular viscosity (μ) as,

$$\bar{T}_{ij}{}^{(v)}(\vec{x},t) = 2\mu\left(\bar{s}_{ij} - \frac{1}{3}\bar{s}_{kk}\delta_{ij}\right) \tag{35}$$

Instantaneous strain rate tensor $\bar{s}_{ij}$ is given by,

$$\bar{s}_{ij} = \frac{1}{2}\left(\frac{\partial\tilde{u}_i}{\partial x_j} + \frac{\partial\tilde{u}_j}{\partial x_i}\right) \tag{36}$$

Navier-stokes equation can be presented for compressible and incompressible fluids. Incompressible fluids are most commonly used because compressible fluid demands a lot of computation power. Even though the air around the elevator is compressible, incompressible fluid formulation is used in this study.

In case of incompressible fluids, derivative of density across the fluid material is zero. Thus equation (33) and (34) can be simplified to

$$\frac{\partial\tilde{u}_j}{\partial\tilde{x}_j} = 0 \tag{37}$$

$$\left[\frac{\partial\tilde{u}_i}{\partial t} + \bar{u}_j\frac{\partial\tilde{u}_i}{\partial x_j}\right] = -\frac{1}{\rho}\frac{\partial\tilde{\rho}}{\partial x_i} + \nu\frac{\partial^2\bar{u}_i}{\partial x_j\partial x_j} \tag{38}$$

where ν is the kinematic viscosity, ($\nu = \mu/\rho$).

The process of decomposing Navier-Stokes equation into two parts, a mean component (ensemble) and a fluctuating component and inserting them into instantaneous and ensemble averaging results in Reynolds Averaged Navier-Stokes equation.

$$\frac{\partial\bar{U}_j}{\partial x_j} = 0 \tag{39}$$

$$\left[\frac{\partial\bar{U}_i}{\partial t} + \bar{U}_j\frac{\partial\bar{U}_i}{\partial x_j}\right] = -\frac{1}{\rho}\frac{\partial P}{\partial x_i} + \nu\frac{\partial^2\bar{U}_i}{\partial x_j\partial x_j} - \frac{\partial}{\partial x_j}\{\overline{u_iu_j}\} \tag{40}$$

Unsteady Reynolds Averaged Navier-Stokes (URANS) is same as that of Reynolds Averaged Navier-Stokes (RANS) [63].

$k-\varepsilon$ (k-epsilon) turbulence model is used in the simulation to take into account for turbulent fluctuations. For modeling the boundary walls, 'enhanced wall treatment' method is used. In

this approach, solutions close to the boundary walls are independent of the mesh resolutions. In this simulation, large cell-wall distances were used. For lower cell-wall distances, boundary conditions are resolved while for large cell-wall distances, wall functions are recovered.

Mesh is created using approximately 9 million cells. Tetrahedral mesh was used to model complicated parts in order to obtain better quality pressure solution. As the tetrahedral cells are known to be inferior at the surfaces, dynamic mesh which reacts to the motion of object was used in the simulation. The measured pressure values are then exported and used in FEM.

3.3 Natural frequency and mode shape

Modal analysis is the first step to solve a dynamic problem, regardless of what analysis is being performed. Natural frequency and mode shapes are required for any vibration analysis. Modal analysis does accurate lowest natural frequency calculations and evaluates mode shape and higher natural frequencies with less accuracy. Requesting for the number of modes in a modal analysis depends on the natural frequency of the system which is related to the frequency content and loads applied. The loads with frequency close to the natural frequency of the system causes large excitations and the spatial load variation decides which nodes are excited [64]. In systems with multiple degrees of freedom, increase in mode number corresponds to higher natural frequency.

The frequency at which a structure tends to vibrate when excited by external force is called natural frequency. It is only significant when system is having a harmonic behavior. It is observed through various studies that increase in stiffness increases natural frequency and increase of mass decreases natural frequency. The deformed shape of the structure at a specific natural frequency is called mode of vibration. Each mode shape is associated with a natural frequency. Natural frequency and mode shapes are functions of structural properties and boundary condition of a system. If the structural property of a system (for example, the elastic modulus) is changed then the associated natural frequency changes but the mode shape can still be the same. But any change in the boundary condition will change both natural frequency and mode shape.

An elevator car covers a wide range of natural frequencies when moving up and down a hoist way. For high speed travel, not only the mass of the suspended car varies with travel, natural frequency of the suspension rope that acts as a spring also varies. If an external forcing frequency matches with this wide range of tuned natural frequency, undesirable car vibration is expected [23]. These vibrations can be in three different axes: one in the vertical axis of the car (Z) and other two in the horizontal axis from back to front (X) and side to side (Y).

Modal analysis gives complete insight into the system dynamic behavior. Modelling errors in boundary conditions and problems with nodal connectivity can be identified by examining mode shapes [64]. Thus, natural frequency and mode shapes are the most important property of any mechanical system.

3.4 Damping formulations

Equations of motion of a system is formulated using mass inertia, stiffness and damping matrices. Dissipation mechanisms in a system are represented by using damping matrix C [65].

The general understanding on damping matrices is still considerably less compared to inertia and stiffness systems. Therefore, assumptions are made to compensate for the lack of comprehension of damping properties. But it is difficult to predict vibration parameters based on damping characteristics. Damping properties has a huge influence over dynamic response and the strength of vibration. Consequently, to analyze the vibrational response of a system, assumptions on damping properties must be made [66].

There are several damping assumptions available based on single degree of freedom (SDOF) system and multiple degrees of freedom (MDOF) system. There are well established damping theories which includes viscous damping, structural damping and Coulomb damping. Viscous damping is usually represented by a dashpot, where the damping force is proportional to the relative speed of motion between two ends. Coulomb damping force is generated because of the relative motion between surfaces sliding against each other. Structural damping, also known as hysteresis damping is a form of internal damping to model the energy dissipation within the material. This is caused by thermoelectricity and internal friction as the microparticles slide against each other during deformation [66].

In most of the dynamic analysis applications, viscous damping is used because of its simplicity in solving an equation of motion utilizing linearity. Viscous damping is dependent on frequency and independent of the displacement. Equation of motion for a linear MDOF system can be written as

$$[M]\{\ddot{u}(t)\} + [C]\{\dot{u}(t)\} + [K]\{u(t)\} = \{f\} \tag{41}$$

Where $[M]$, $[K]$ and $[C]$ are the mass, stiffness and damping matrices, $u(t)$ is the displacement vector however $\dot{u}(t)$ and $\ddot{u}(t)$ are the first and second order time derivatives and f is the force vector. Damping values need to be assigned to solve the equation, and Rayleigh damping is one of the most used methods to calculate damping ratios [67].

3.4.1 Rayleigh damping

Rayleigh damping is expressed as a linear combination of mass matrix and stiffness matrix, that is,

$$[C] = \gamma[M] + \beta[K] \tag{42}$$

Where γ and β are arbitrary scalar constant coefficients with units s^{-1} and s respectively. Stiffness matrix is constructed using initial tangential stiffness and damping matrix consists of mass and stiffness proportional terms.

To determine the values of γ and β, it is required to choose approximate damping values to the linear system expressed in equation (42). For mode n, damping is quantified by the damping ratio as ξ_n, the ratio of n^{th} mode damping value to the critical damping value.

$$\xi_n = \frac{1}{2}\left(\frac{\gamma}{\omega_n} + \beta\omega_n\right) \tag{43}$$

The coefficient γ and β can be set for any damping ratio to any two modes. The damping coefficients for i^{th} and j^{th} modes can be expressed as,

$$\frac{1}{2}\begin{bmatrix} 1/\omega_i & \omega_i \\ 1/\omega_j & \omega_j \end{bmatrix}\begin{Bmatrix}\gamma \\ \beta\end{Bmatrix} = \begin{Bmatrix}\xi_i \\ \xi_j\end{Bmatrix} \tag{44}$$

Hall (2006) method can be used to determine α and β. Nearly constant damping values for modes within frequency range of $\widehat{\omega}$ and $R\widehat{\omega}$ are developed from this procedure. By selecting a damping value and a frequency range of $\widehat{\omega}$ and $R\widehat{\omega}$ within the desired mode, $R > 1$, Δ can be calculated as,

$$\Delta = \xi\frac{1 + R - 2\sqrt{R}}{1 + R + 2\sqrt{R}} \tag{45}$$

where Δ determines the upper and lower bounds of the damping ratio for the desired modes specified within the frequency range. Thus, this mode within the frequency range with have damping ratio bounded between $\xi + \Delta$ and $\xi - \Delta$.

Damping coefficients can be calculated from:

$$\gamma = 2\xi\widehat{\omega}\frac{2R}{1 + R + 2\sqrt{R}} \qquad \beta = 2\xi\frac{2}{\widehat{\omega}\left(1 + R + 2\sqrt{R}\right)} \tag{46}$$

And the corresponding values can be used to compute actual damping value from equation (32) for nth mode. Figure 17 below shows the damping ratio for different R values with $\xi = 10\%$ and $\widehat{\omega} = 1$:

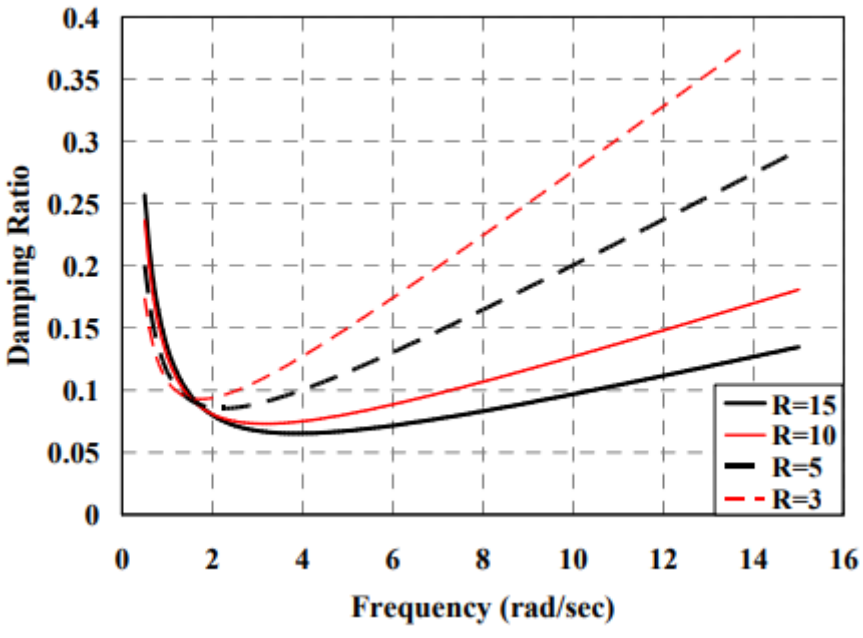

Figure 17. Damping ratio as a function of frequency [65]

3.5 Application of Finite Element Method (FEM) in structural vibration

Vibrations can be explained in simple terms as mechanical oscillations of an object with respect to an equilibrium position. Most of the time, they are undesirable phenomena causing loss of energy, reduction of efficiency, unwanted noise or may even lead to dangerous and harmful working environment. Ride comfort is greatly affected by undesirable structural vibrations of mechanical parts or external excitations [68]. In case of an elevator, some of the main reasons for structural vibrations are due to uneven guide rail profile, movement of suspension ropes, rotational imbalance of motors etc. which can lead to poor ride comfort.

The first crucial step in performing a structural dynamic analysis involves estimation of the natural frequencies and corresponding natural mode shapes of an elastic structure in free unforced vibration without damping [69]. Modal frequency analysis is important for every structure that undergoes external excitation. If the frequency of applied external load gets closer to the structure's natural frequency, then resonance occurs. Resonance can lead to load amplification leading to extreme structural stress and dynamic displacements. Finite Element Method (FEM) is a relevant tool for this type of analysis even for complex structures. It can be used to determine modal frequencies of an element with fast and precision computation [70].

Vibration analysis problem for a finite element structure is usually formulated as an eigensystem, where the eigenproblem consists of stiffness [K] and inertia [M] matrices. Eigenvalues and eigenvectors in a finite element structural model are a representation of natural frequencies and mode shapes, respectively. Solution to the eigenvalue problem gives many eigenvalues and corresponding eigen vectors. Using the finite element tool, step to compute an eigen frequency will generate all or requested natural frequencies of the system. Qualitative displacements can be understood by careful modal analysis of the deformed mode shapes.

Since damping is not considered in modal analysis, the calculated displacement values of a component are meaningless. For example, if a straight beam undergoes modal analysis and generates displacement values of 5cm in one end and 10cm in other end, the theoretical displacement values does not provide any information. That is because the displacement values are normalized, meaning that the largest values is divided to every other displacement value. Thus, the analysis tells much about the relative displacement values of the structure.

After performing the eigenfrequency step to find all the potential modes, then a frequency domain analysis is performed by applying load over a range of frequencies and displacements are measured. It is not necessary to sweep over large range of frequencies, since the resonant modes are already known after eigen frequency analysis, load is applied over the frequency range generated from eigenfrequency analysis step. In the thesis, I am mostly interested in the lowest eigenvalues corresponding to the lowest frequencies of the system because the low frequency vibrations are associated with large displacement amplitude of the structures. This thesis focuses on transient dynamic computation at system level. Several substructures are included in the model for faster computation time and due to limited resources.

4 Architecture of Elevator model

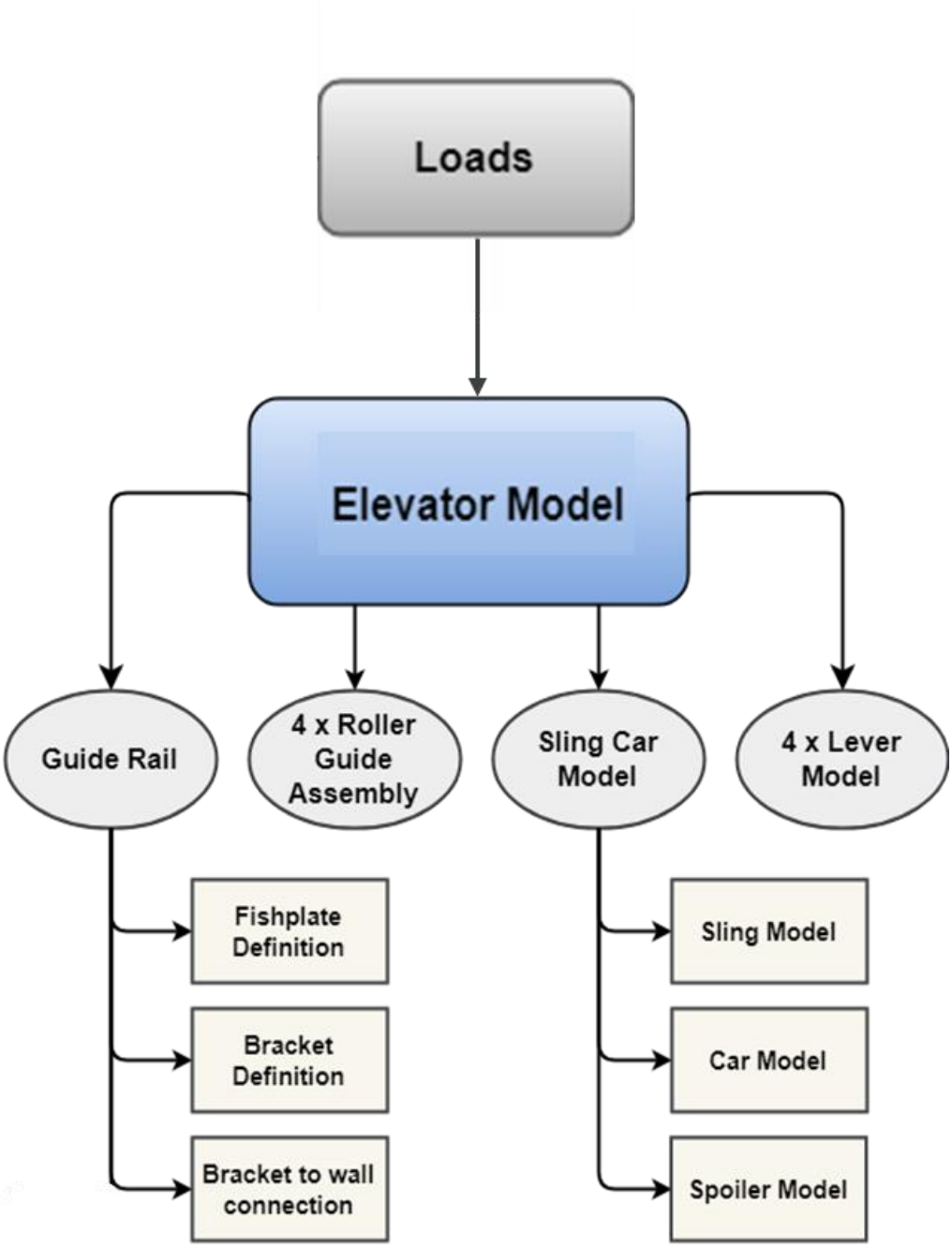

Figure 18. Hierarchical representation of elevator model

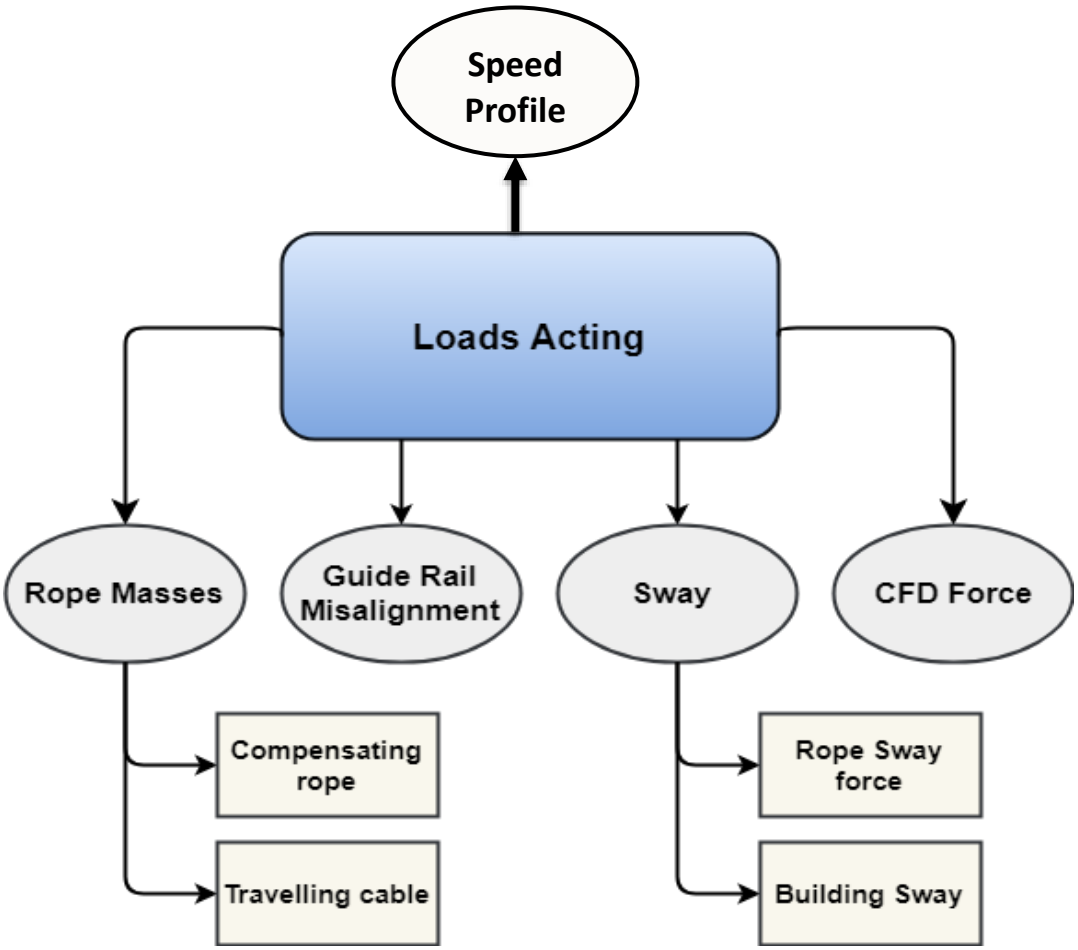

Figure 19. Loads that excite the elvator car

This chapter discusses about the modeling techniques and strategies of each components of the high-rise elevator used in the Finite Element Analysis (FEA). Simulation is performed to predict and improve the ride comfort of high rise and high-speed elevators. ABAQUS/Standard is used for the dynamic analysis of an elevator car traveling more than 500 meters. Structure of the elevator is double deck consisting of two cars. Beam elements and substructures have been used to create the elevator model which contains systems with more than one multiple degrees of freedom. Other factors such as guide rail geometry and guide rail sway movement along with variable rope masses are included using special user-defined elements. This enables the model to consider all the factors that contribute to vibration inside the elevator car such as guide rail misalignment, aerodynamic load from counterweight, roller guide properties, sling and car structure assembly, the impact of suspension ropes, compensating ropes and traveling cables [24] .

In the elevator model, rollers and sling-car are modeled as substructures using Guyan reductions. Guide rails containing brackets and fishplates are modelled using Euler Bernoulli-beam theory. The finite element elevator model consists of 17 substructures in total. For each substructure, frequency analysis is performed for all modes up to 80 Hz and they are defined for both static and dynamic modes.

4.1 Roller Guide Shoes

An elevator has four roller systems in total and each of these is modeled using solid elements and then reduced to four substructures. Rollers are always in contact with the guide rails and to make sure of that, levers are used that pre-tension the roller wheels. Initially, the lever used to be a part of the roller system model substructure, but since levers have rotational degree of freedom they were modeled separately and used as a substructure in roller model. Therefore, each roller model substructure contains three lever substructures. Roller guide system model is used as a substructure in a large system level model. To simplify the analysis, the interaction between roller and guide rail is assumed to be linear and the wheels glide along the rails instead of rolling. User-defined element defines the interaction between rollers and guide rails. The properties of roller rubber material used in the model is based on the behavior of roller and guide rail interaction for various dynamic testing. Neo-Hook incompressible model chosen for rubber for which Prony coefficients defined and modelled using hyper viscoelastic material.

Stoppers are used in the rollers to limit the rotation of levers. This complex connection is defined using connector elements because of their fast-computational abilities. The defined stopping mechanism restricts the range of motion of an otherwise unconstrained relative motion.

When the lever moves beyond expected limit, it meets a rubber and then the steel stopper. Two connector elements are defined, one for the soft rubber contact and other for the hard steel contact. Springs that are used to pretension the wheels are also defined by using connector elements. These elements are defined for stiffness, damping and movement limiters are included. Also, the revolute connector elements are used to define the connection of lever to wheel and roller body, making a total of 20 connector element definition for each roller guide. A total of 41 retained nodes are used to define contact points for connector elements and roller guide fixing to sling and guide rail.

Roller guide model is an assembly of the following parts (Figure 20): body, dust cover, piece of guiderail, wheel rim, rubber wheel, spring rod, lever bush, stopper, stopper rod, stopper rubber. All the parts are modelled as 3D deformable parts using aluminum, steel and rubber.

Lever is modelled separately and used as a substructure in roller model. Retained nodes are created for the connection points (Figure 20) and eigen frequency below 80Hz used for substructure generation.

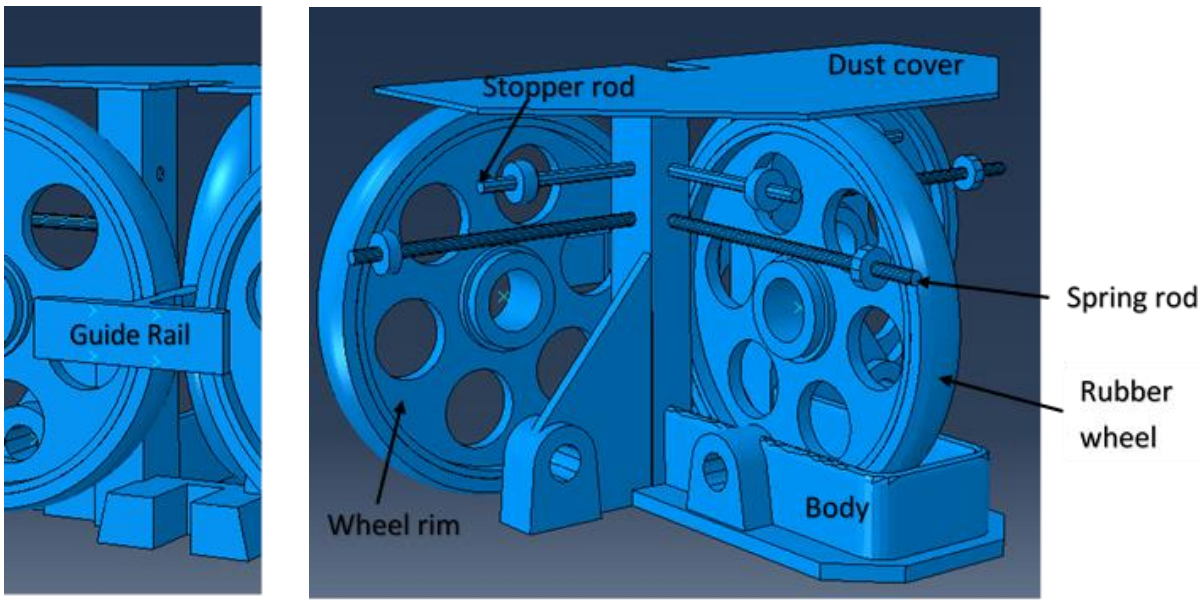

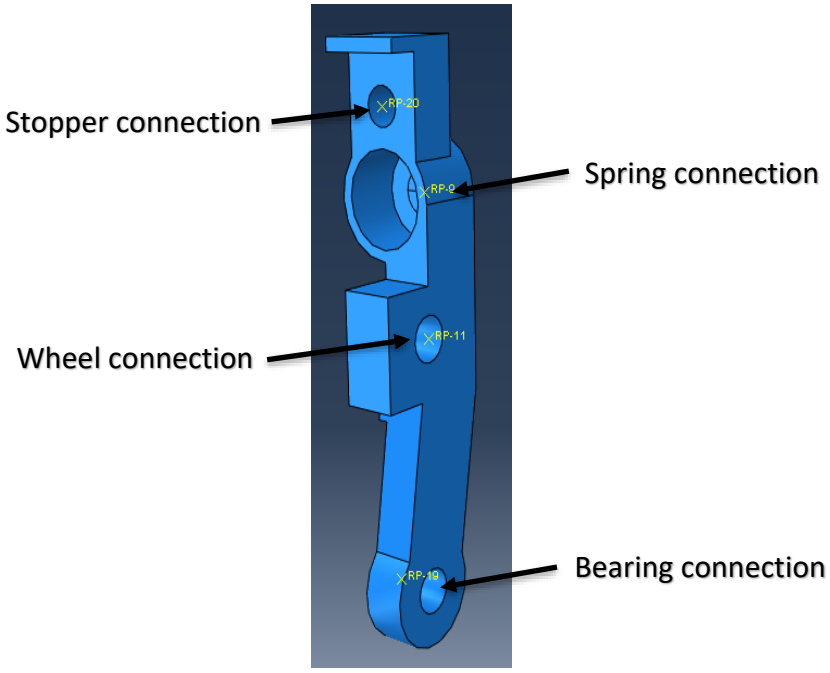

Figure 20. Model of roller guide substructure (on top) and lever substructure with connection points (on bottom)

4.2 Guide Rails

Guide rails function as an internal track that restricts the horizontal movement of elevator car. They are mounted over the two opposite sides of the shaft wall for the entire distance of travel. For high-rise building, length of guide rail can be as high as over 800 meters and it needs to be properly fixed onto the shaft walls. Guide rails are fixed to each other using fishplates and fixed to the walls through brackets.

Guide rails are defined in the elevator model system level. Usually for short travelling distance, guide rails are modelled as solid elements. Guide rails used in this study are modelled for a length of 508 meters and, the solid element approach is too expensive for such long distance. Therefore, at system level, they are modelled as beam elements (B33) with varying I-section profile. Two different profiles, one for continuous guide and one for guide rail with fishplates are used. Brackets are modelled as set of nodal points for which boundary conditions are applied. Instances of left and right guide rails are created and positioned at 2.502 meters apart from each other.

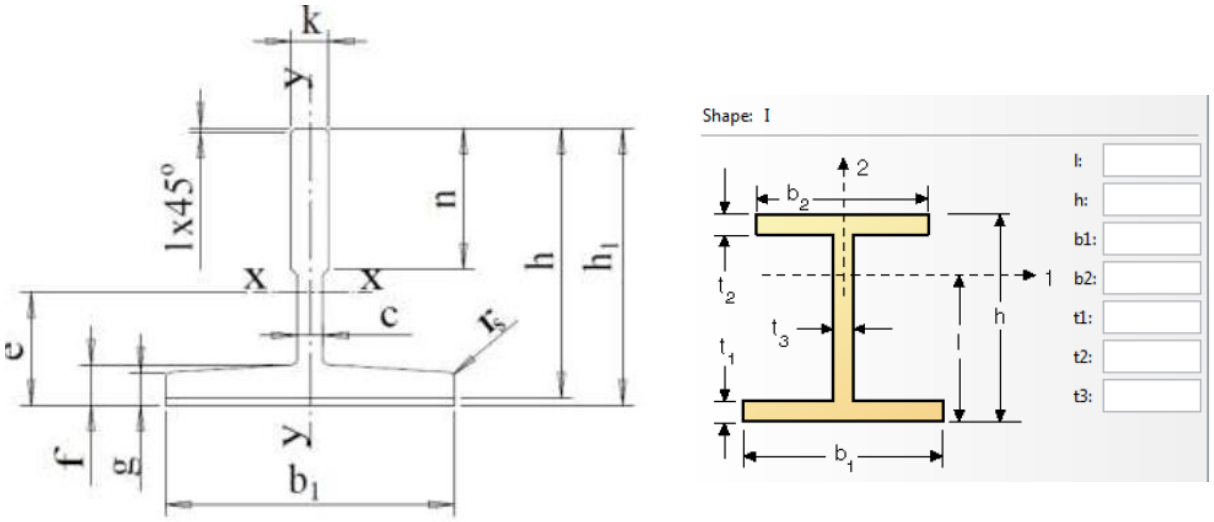

Figure 21. Guide rail profile dimension (left) and simplified I-beam geometry used in simulation (right)

Steel with following properties is used to define guide rail: Y =2.1e11 N/m^2, ν =0.3, ρ =7850 kg/m^3 and damping ratios α =0.005, β =0.45.

The brackets are defined in the system level as spring connections, one node on the guide rail and the other on the shaft. The guide rail misalignment is defined from measurements and implemented as internal variables for the user defined elements. The elevator travels is 508 meters and the total shaft height is 535 meters. Elevator car starts from the first floor which is 7 meters above the compensating sheave level and finishes at last landing floor 515 meters.

4.3 Car and Sling

The elevator used in the model is a double deck. Finite element elevator model is very complex assembly of 121 parts of 9 different materials shown below. For the car roof, wall and floor material the mass was in accordance with the real components. The assembly has a total of 193 instances consisted on 1D, 2D and 3D parts. Shells, solids, beams and springs are used to model the car and sling structure.

The cars are fixed to the sling using flexible connections. The sling and car connection has been done through 28 springs on each side, modelled with longitudinal spring stiffness of 73202 N/m along the line of action and transverse spring stiffness of 38789 N/m along shear direction. 80kg mass is added to the center of both elevator cars to constitute a person standing inside the car. Vibration is perceived by the person due to the contact with the floor and the output is the acceleration of the floor taken from the center of the car in three directions. In the model, only one person is positioned inside the car, this is one of the requirements for classifying the ride comfort class of elevators. In order to consider the human perception, the value of acceleration measured is filtered with a low pass Butterworth filter. Output is taken from a retained node defined at different required positions.

16 retained nodes are defined on the car and sling substructure for roller attachment. Retained nodes are defined on top and bottom of the car for spoiler attachment. They are also defined

behind the car surfaces for aerodynamic CFD load impact and nodes for attaching suspension and compensating ropes are defined. Impact of counterweight is modelled as pressure loads on the walls of the car in the sling-car substructure. The aerodynamic load due to counterweight passing is calculated using a computational fluid dynamic simulation for a specific elevator speed and direction. Since it is not possible to define variable masses in finite element model, rope masses are considered as variable loads function of the sling position in the shaft and building sway computed using finite difference method (FDM). Retained nodes are defined for additional masses at 4 floor corners and 1 node defined at center of top car for output. Also, fairings are used to reduce the air drag.

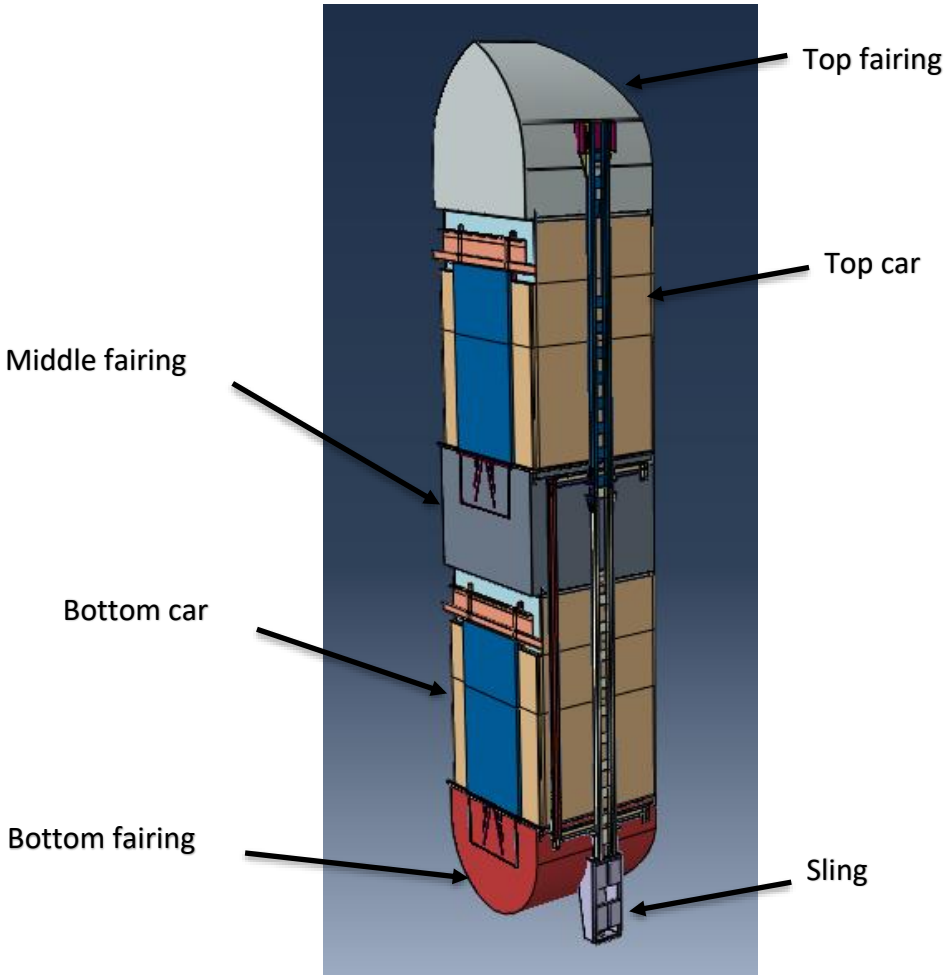

Figure 22. Sling-car substructure

4.4 Global System level

Initially, in the system level, both left and right guide rails are added. Guide rails are defined using script file containing both brackets and fishplates positions as discussed under chapter 4.2. The brackets that are used for connecting guide rails to the wall are defined using spring connections and the spring stiffness in each direction (Kx/Ky/Kz) are defined for brackets node sets.

Then sling-car is imported into the system level. Node sets for roller system, suspension and compensation rope and top and bottom spoiler attachment is defined. Also, node sets are defined for four corner points and one center point inside the elevator car. Roller substructure is imported into the global system level. Four instances of rollers are made and positioned at the bottom of the shaft. Node sets are defined in the part for guide rail and sling-car connections. Also, a reference point is defined, which is used to define MPC beam type constraint for the roller nodes to be connected to corresponding user defined elements (UEL) allowing both translational and rotational misalignment to be defined. Three separate node sets are defined for left, middle and right stopper nodes for each roller. Similarly, three instances of levers for each roller (12 levers in total) are made and positioned accordingly.

All the 20 connector elements are defined in the global system level. Each roller has 5 connector elements (rubber and steel stoppers, spring, wheel and bearing connection to of the body). User defined elements (UEL) are defined for connection between rollers and guide rails. Subroutine UEL is used to include variable rope masses for suspension, compensating and travelling. Also building sway motion is included.

Table 1. Rope Properties

Suspension rope weight per unit length (kg/m)	1.38
Number of suspension ropes	13
Hoisting rope nominal diameter (m)	0.019
Hoisting rope filling factor	0.555
Young modulus of suspension rope (N/m^2)	$75*10^9$
Hoisting rope terminal spring stiffness	600000
Damping ratio of hoisting rope terminal, i.e. rubber bushing friction	0.05
Compensation rope weight per unit length (kg/m)	1.38
Number of compensating ropes	12
Compensating rope nominal diameter (m)	0.019
Compensating rope filling factor	0.555
Young modulus compensating rope (N/m^2)	$75*10^9$
Travelling cable weight per unit length (kg/m)	5.223

Display elements (B31) are used for visualizing the results. These deformable elements are just used to visualization purposes, they require no meshing and often ignored during the analysis. It gives a rough idea on how the links behave during analysis (Figure 23)

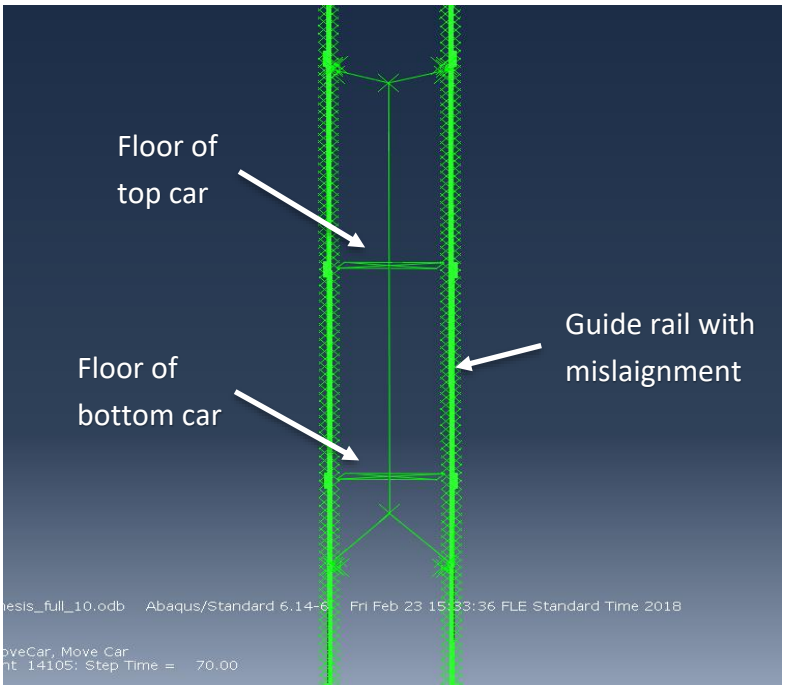

Figure 23. Guide rail with misalignment

4.4.1 Load Definition

In the system level, there are four main loads that are defined which excite the elevator car during its travel. These are some of the main parameters that contribute to in-car vibration and needs to be applied with great precision. This session explains these loads inducing factors and how they are defined in the global system level:

a) Misalignment of guide rails
b) Aerodynamic load impact
c) Variable rope mass
d) Sway load
    i. Rope sway force
    ii. Building sway

a) Misalignment of guide rails:

As discussed earlier, guide rails tend to have misalignment because of installation and manufacturing inaccuracies and building settlements. These needs to be considered in the model with great precision. These misalignments are one of the biggest contributors to in-car vibrations. They are implemented in the model as amplitudes through a user defined element. Misalignments are implemented as excitation based on measurements taking from existing site for a specific elevator and extrapolated for the required longer travel distance (Figure 24).

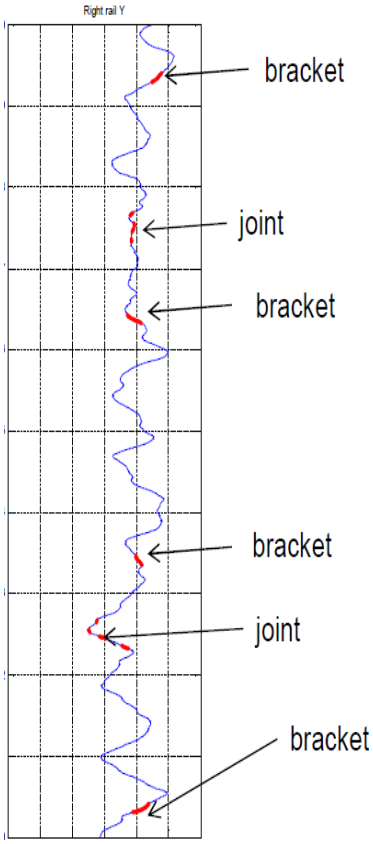

Figure 24. Guide rail misalignment measured on existing site

The user-defined element (UEL) for guide rail to roller guide connection contain three nodes: two nodes define the beam element and third one is a master node for roller and guide rail attachment point (Figure 23, Points A, B and C respectively). This means that for every user-defined element there is a corresponding guide rail element, i.e. number of roller guide UEL are equal to the number of elements of guide rail. During the car travel, the misalignment of the corresponding element is calculated by linear interpolation between the current position and the position of the closest measurement value. This calculated misalignment is then added to the guide rail definition within the user-defined subroutine used by user defined elements (UEL).

The mathematical formula used for the user defined element (Figure 24) is described as follows:

F – represents force acting at each nodal point

k – stiffness vale used for spring connection

According the equilibrium condition, force equation can be written as:

$$F_A + F_B + F_C = 0 \tag{47}$$

$$F_B * L + F_C * X = 0 \tag{48}$$

The roller guide attachment position is defined as *R=X/L*.
For misalignment value 'α', force acting at the roller guide attachment point is:

$$F_C = k * (U_c - (U_A + U_B * R + \alpha)) \tag{49}$$

From equation (3), (4) and (5),

$$\begin{Bmatrix} F_A + \alpha * k * (R-1) \\ F_B - \alpha * k * R \\ F_C + \alpha * k \end{Bmatrix} = k * \begin{pmatrix} (R-1)^2 & -R*(R-1) & (R-1) \\ -R*(R-1) & R^2 & -R \\ (R-1) & -R & 1 \end{pmatrix} \begin{Bmatrix} U_A \\ U_B \\ U_C \end{Bmatrix} \tag{50}$$

Based on equilibrium condition, equation for torsional moments can be written as:
M – represents torsional moment at each node
Δφ – rotational misalignment
And $M_A = M_B$

$$M_A + M_B + M_C = 0 \tag{51}$$

$$M_C = k_\varphi * (\varphi_c - (\varphi_A + (\varphi_A + \varphi_B) * R + \Delta\varphi)) \tag{52}$$

$$\begin{Bmatrix} M_A - 0.5 * k_\varphi * \Delta\varphi \\ M_B - 0.5 * k_\varphi * \Delta\varphi \\ M_C + k_\varphi * \Delta\varphi \end{Bmatrix} = k * \begin{pmatrix} -0.5*(R-1) & 0.5*R & 0.5 \\ -0.5*(R-1) & 0.5*R & 0.5 \\ (R-1)*\varphi_A & -R & 1 \end{pmatrix} \begin{Bmatrix} U_A \\ U_B \\ U_C \end{Bmatrix} \tag{53}$$

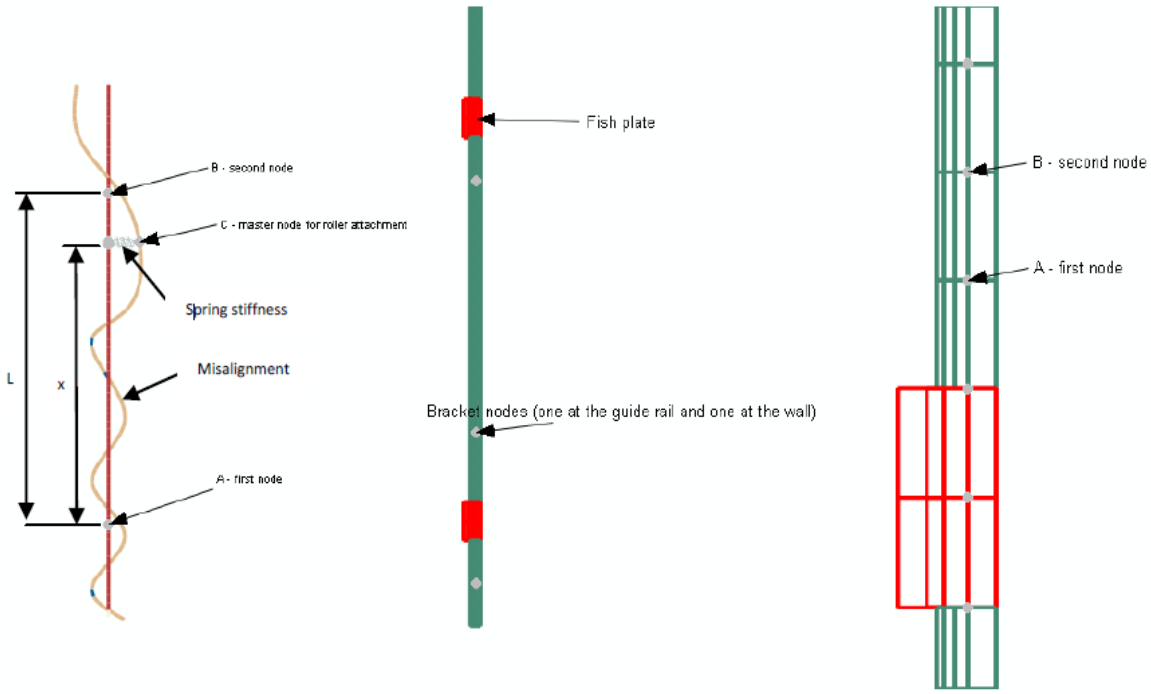

Figure 25. User defined element representation.

b) Aerodynamic load impact:

For speeds higher than 4m/s the “wind effect” starts to have an important contribution both in vibrations and in noise. Even a single high peak of acceleration magnitude can destroy the ride comfort. This contribution is perceived more aggressively because of irregularities in the shaft wall due to obstacles such as landing doors or counterweight. Based on the experience, it has been seen that counterweight has the high impact, especially in high-rise elevators and cannot be neglected from the model.

The aerodynamic impact of counterweight passing at high speed is computed using Computational Fluid Dynamics (CFD) for 10m/s speed elevator speed and upwards traveling direction. Transient 3D models with sliding meshes are used to predict the effect of relative motion between elevator car, counterweight and shaft. The simulation results are transient rigid body forces and moments exerted on elevator. Surface pressure values are extracted from CFD simulation and used in Finite Element Simulation as the impact loads. Since the impact of counterweight is only relevant when is it passing the car and sling, they are applied only for the time window close to when counterweight is passing the elevator (Figure 26). Hence the impact time of the aerodynamic load amplitude needs to be changed based on the elevator travelling speed or distance.

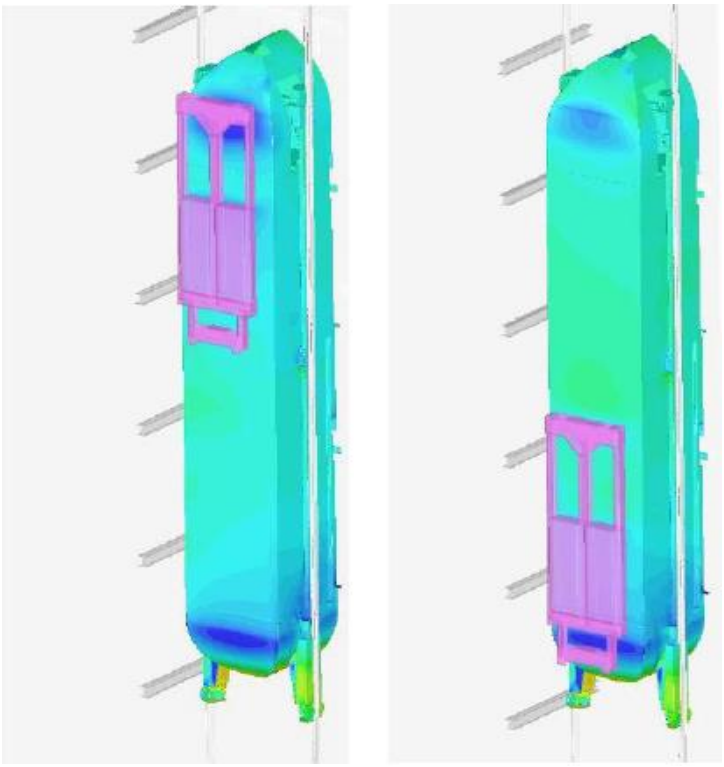

Figure 26. Transient CFD computation of aerodynamic load impact on elevator car due to counterweight (pink) [23]

c) Variable rope mass:

High-rise elevators have considerable load influence because of changing mass of compensating rope and travelling cable attached at the bottom of car sling. In case of high-rise elevators, the mass of the ropes and cables are significant. As the elevator car travels higher, the rope and cable masses at the bottom of the car increases resulting in mass imbalance. This is mainly compensated by adding balancing mass to the car sling. In the elevator FEM model, variable rope masses are defined using element B31. Unit mass of the element is defined as UEL, which varies with the position of elevator in the shaft.

d) Sway load:

Another factor that needs to be considered is the movement of guide rails because of building sway. Since the sway properties are specific to building types and location, building movement due to sway is computed and provided by architecture based on building height, shapes and weather conditions. Excitation because of sway is mainly perceived as building movement and rope movement, which are applied to the model by two approaches:

i. Rope sway is applied as a variable force on car-sling substructure modelling the impact of suspension rope, compensating rope and traveling cable:

   All the ropes are modelled as variable force function of elevator car position in the shaft and building sway properties such as sway amplitude and frequency. They are computed using finite difference method and applied to retained node on the car-sling substructure used for rope attachments. User defined element (UEL) subroutine is included that defines the variable mass of suspension rope, compensating rope and traveling cables. Masses are applied as variable gravity loads on the corresponding user defined element (UEL).

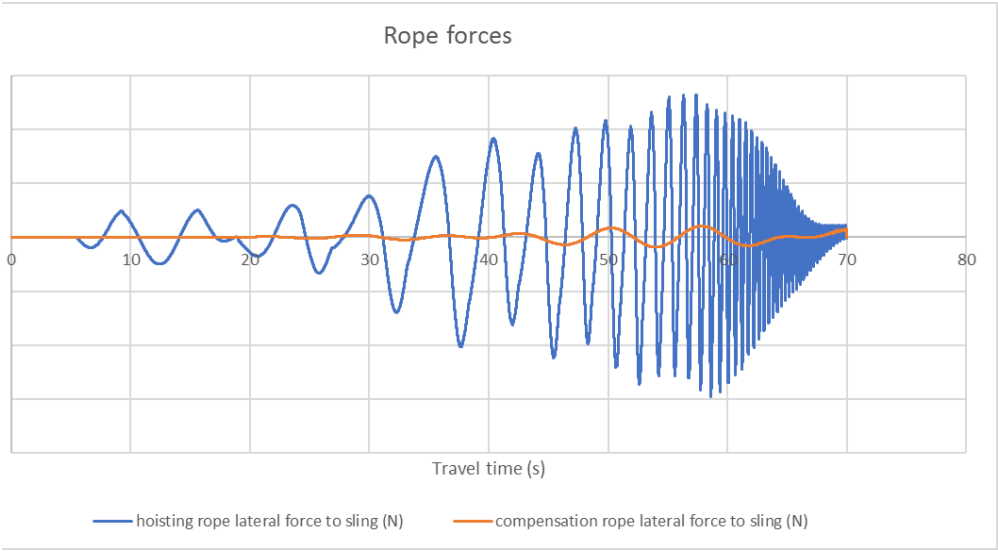

Figure 27. Suspension (hoisting) and compensating rope impact loads because of the sway of the building

ii. Building sway is applied as a displacement on guide rail connections to building:

Sway motion is applied in the model by describing the motion of the bracket nodes based on modes shape excitation in specific direction. The building specification used in the study has a total shaft length of 535 meters and according to the coordinate system 'z' represents the vertical direction of the shaft in meters.

Rough model of the elevator system used for finite element modelling is shown below (Figure 28). Total height of the building is H_b and the building top is swaying with an amplitude A_b and frequency f_b. It is assumed that $A_b/H_b << 1$, so that the sway deflection can be considered purely horizontal.

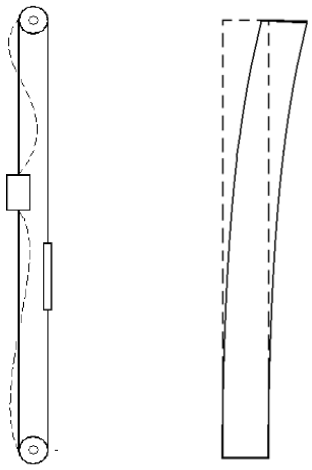

Figure 28. Rope sway (left) and building sway (right) deflection

The shaft deflection at height z at given time t seconds is defined in the model as follows:

$$A(z,t) = A(Z,t) * \sin(2\pi * f * t) * (z/Z)\text{^}1.5 \quad (54)$$

where $A(Z,t)$ is the maximum displacement at the top of shaft (Z =top level) at time t seconds, f is the sway frequency and z =0 level is assumed to be at compensating sheave level. The term " $(z/Z)^{1.5}$ " is the modal shape approximation used.

Table 2. Sway parameters

	Frequency (Hz)	**Max building amplitude (1-year return period)**	**Sway direction**
Y-Sway	F1	A1	Guide-rail to guide-rail
X-Sway	F2	A2	Front to back

X-sway i.e. back to front sway direction frequency and amplitudes are used in the system level model for vibration analysis.

5 Simulation Results and Regression Analysis

The results are presented under two separate chapters. The simulation results are presented in first chapter and regression analysis under the second chapter. All the computation results are measured for ride comfort expressed as a quantitative measure of peak-to-peak in-car acceleration. The spatial acceleration of the node at the center of the car is exported using a custom filed output python script and compared for each case. One of the advantages of this approach is that the node acceleration can be analyzed for a time interval down to one hundredth of a second.

5.1 System level simulation results

Several combinations of design parameter variables such as building sway amplitude, travel distance and speed were simulated to evaluated ride comfort. A hypothetical elevator with following parameters is used for computation. Target is to evaluate the performance in sway conditions.

Table 3. Elevator parameters

Travel [m]	508
Acceleration [m/s2]	0.8
Jerk [m/s3]	1.2
Nominal speed [m/s]	10
Sway amplitude [mm]	88
Rated load [passengers]	21
Building frequency [Hz]	0.1394
Rated load for top car (kg)	1600

5.1.1 Study of speed profile

Study of simulation results showed that it is possible to use variable drive curves with acceptable level of in-car vibration and flight time. The challenge is to find a speed curve with an acceptable ride comfort both in terms of in-car vibration and flight time. When using 10m/s profile, peak to peak car vibration is 28.5 gals and flight time is 64s (Figure 29), which does not meet the acceptance criteria. By using the usual approach of reducing the speed to half (5 m/s), the peak to peak car vibration is 18.1 gals and the flight time is 109 s (Figure 30). Even though the vibrations are within the limits, the increased flight time reduces the lift efficiency.

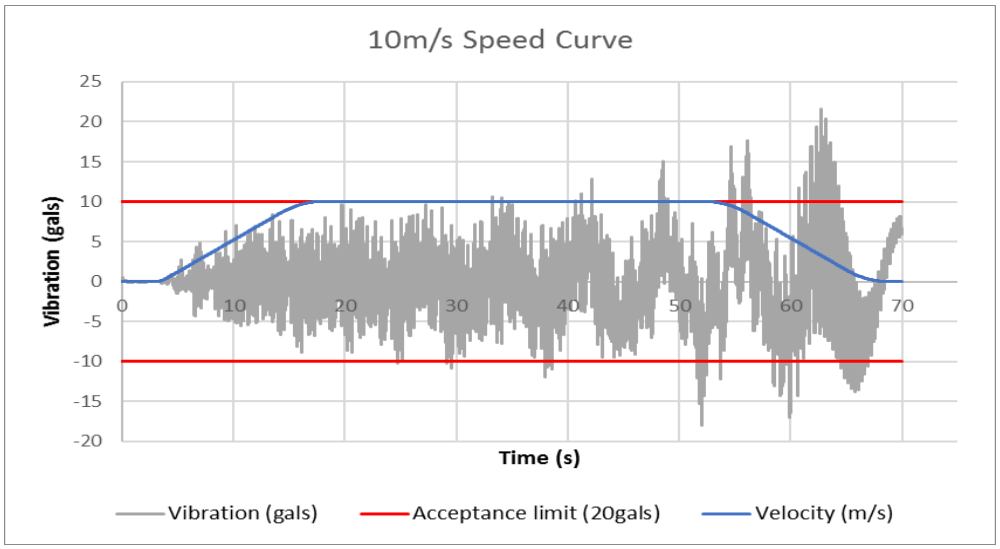

Figure 29. In car vibration for nominal speed (10m/s)

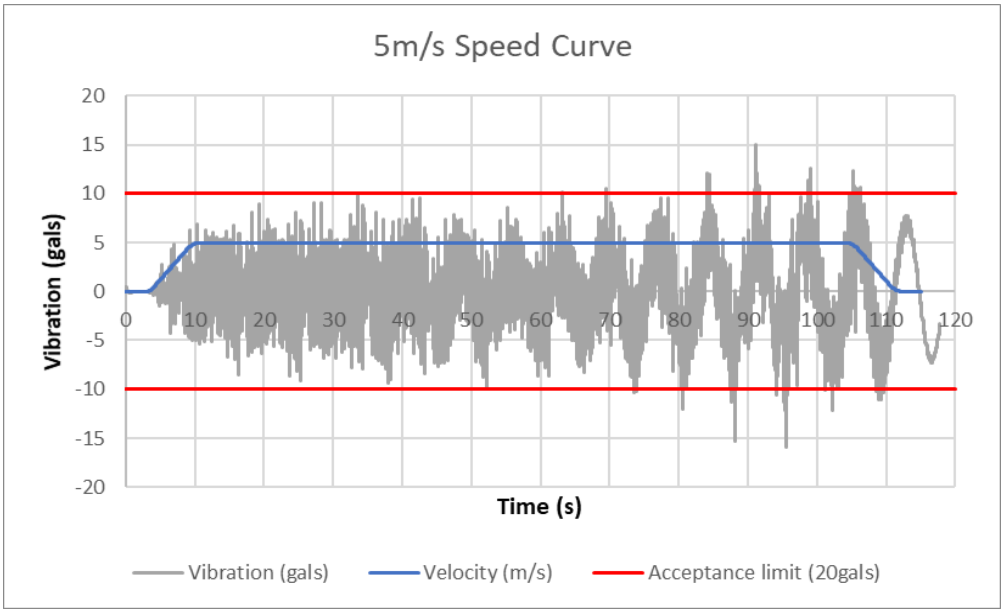

Figure 30. In car vibration for half speed (5m/s)

The threshold travel height is calculated above which building sway has considerable impact over ride comfort. For this case, computed in car vibrations throughout the travel distance were compared against acceptable range. The criteria are that the peak to peak vibration amplitudes are under the 20gals acceptable limit. Analyzing the graph (Figure 29) shows that sway is critical only after 35 seconds, which is equivalent to a travel height of 290 meters.

To study the impact of speed on ride comfort, 18 different profiles were analyzed (Figure 31). For each case, in car vibrations and travelling time were computed and compared. Since the impact of sway is found to be higher only when car pass the level of 250m height, the curves are constructed by running at lower speeds over the regions of higher sway impact. These regions of travel height are chosen at 252m, 302m, 352m and 402m. Speed is lowered from nominal value (10m/s) to 8m/s, 6m/s, 4m/s and 2m/s at these different travel lengths. Constant acceleration/deceleration of 0.8m/s^2 is used for all the cases. From all the cases studied, an optimized solution is chosen.

Based on the simulation study of all the velocity profiles shown in Figure 31, the optimal curve is found to be the one where car can travel with 10m/s until 402m and then it decelerates to 4m/s. Elevator performance while using optimal curve is analyzed against the nominal speed curve (10m/s) and usual practice of 5m/s speed profile. Optimal speed profile delivers better ride comfort with 19.7 peak to peak in car vibrations and flight time of 71s. To get much deeper understanding of the elevator performance, handling capacity of these profiles are evaluated based on traffic simulations.

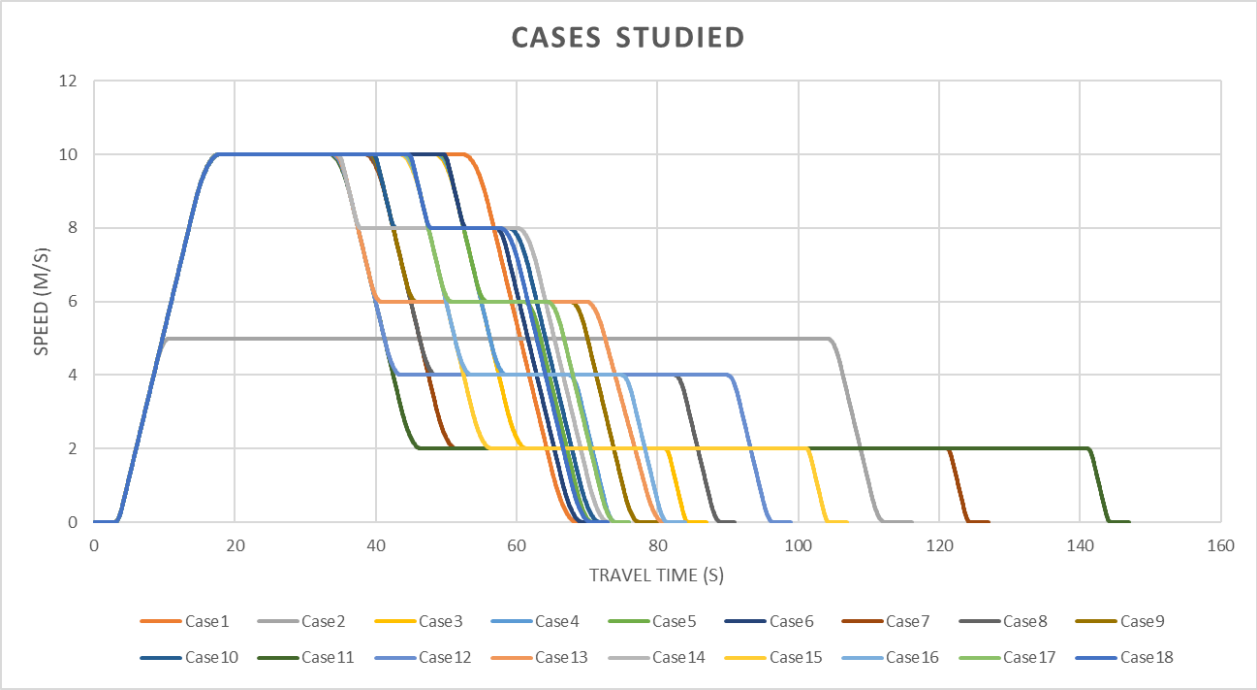

Figure 31. Speed profiles studied

The table below (Table 4) shows the total travel time and maximum vibration amplitude for each studied case. The optimal speed profile is mainly used when sway mode is triggered, hence the results shown in the table are for maximum sway amplitude conditions.

Table 4. Simulation results for studied case

Cases	Starting Speed (m/s)	Reduced Speed (m/s)	Height at speed change (m)	Building Sway (m)	Total travel time (s)	Max. Pk-Pk vibration (gals)
1	10	10	Whole run	0.088	63.3	28.528
2	5	5	Whole run	0.088	109	18.100
3	10	2	402	0.088	80.5	19.134
4	10	4	402	0.088	69.75	19.780
5	10	6	402	0.088	66.166	24.070
6	10	8	402	0.088	64.375	27.741
7	10	2	302	0.088	120.5	18.225
8	10	4	302	0.088	84.75	20.642
9	10	6	302	0.088	72.833	20.864
10	10	8	302	0.088	66.875	25.136
11	10	2	252	0.088	140.5	18.286
12	10	4	252	0.088	92.25	18.616
13	10	6	252	0.088	76.166	18.699
14	10	8	252	0.088	68.125	22.409
15	10	2	352	0.088	100.5	18.433
16	10	4	352	0.088	77.25	20.483
17	10	6	352	0.088	69.5	20.738
18	10	8	352	0.088	65.625	25.202

The following conclusions can be drawn instantly by looking at the table. The simulation results presented in the table shows that (Table 4)

- case 1 has vibration result much higher than the acceptable ride comfort limit (20gals) but the lowest travel time.
- case 2 has the highest travel time but lowest in car vibration results which is within the acceptable range.
- case 4 has lower vibration amplitude than that of case 2 with lower travel time.
- It is possible to choose a curve that allows the car to travel within the acceptable comfort limit and still able to save travel time.

Based on the analysis, optimal curve is chosen as case 4. In this case, it is possible for the car can to run at 10m/s until 402m and then decelerate to 4m/s. The peak to peak car vibration is 19.78gals and the flight time is 71s.

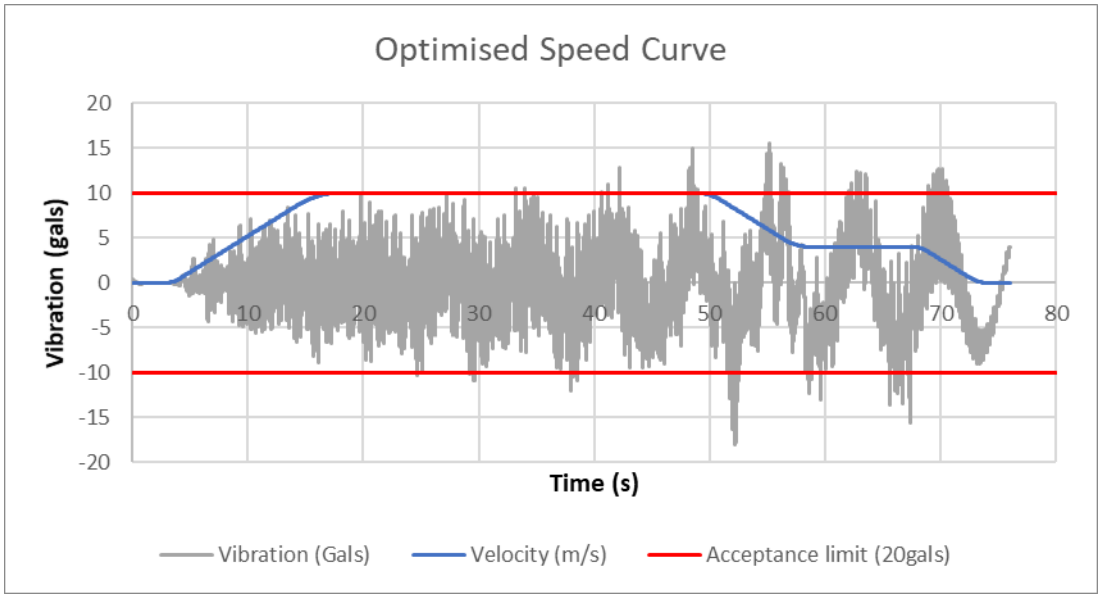

Figure 32. In car vibration for optimized speed curve

5.1.2 Handling Capacity assessment

Handling capacity is a criterion used in elevator planning to evaluate how well an elevator system can handle up/peak traffic. Traffic simulation can be used to calculate handling capacity where the rate of car load is 80%. Handling Capacity (HC) is defined as the number of passengers an elevator system can transport from the lobby or entrance floor to destination floor during up-peak within a defined time, usually in five minutes (HC5). Usually Handling Capacity is given in relative units, percent of population in 5 minutes. Relative value of Handling Capacity is obtained by dividing the absolute value (persons/5 minutes) by the total population at the served floors (%HC5).

$$Handling\ Capacity = \frac{0.8 * \text{rated load} * 300}{interval}\ [\frac{persons}{5\ minutes}] \tag{55}$$

Interval (INT) shows the average frequency how often an elevator leaves the lobby during up-peak. It is measured as the average time between elevators leaving from the main entrance floor. It is obtained by dividing the round-trip time (RTT) by the number of elevators in group. Round time is calculated as the time measured from the moment the car starts up to the next time it starts after two reversals [71]. Rated load is the number of passengers that can be carried.

$$RTT = 2(trvael\ time) + \text{stop time} + \text{passenger transfer time} \tag{56}$$

For simplicity, it can be assumed that elevator parameters such as stop time and passenger transfer time as zero. Here the travel time is the time used in simulation which is the total running time that elevator takes to reach top floor. Estimate number of passengers for 1600kg load is 21 persons.

The 5-minute handling (HC5) capacity is assessed for all three cases. Based on the assumption and simulation procedure, elevator is a shuttle lift serving only the lobby/entrance floor and top observation deck which is 508 m high. Also, it is assumed that there is only one elevator in the group which means round-trip time (RTT) is same as interval (INT).

We assume that all the discussed cases are shuttle lifts where the dominant traffic is assumed to be two-way traffic. The handling capacity for the nominal speed curve of 10m/s (Case 1), half speed curve 5m/s (Case 2) and optimized speed curve (Case 12) are calculated as follows:

i. Case 1:

   INT = RTT = 2*63.3 = 126.6s
   HC5 = (0.8*21*300) /126.6 = 40 persons/5 minutes

ii. Case 2:

   INT = RTT = 2*109 = 218s
   HC5 = (0.8*21*300) /218 = 23 persons/5 minutes

iii. Case 4:

   INT = RTT = 2*69.75 = 139.5s
   HC5 = (0.8*21*300) /139.5 = 36 persons/5 minutes

From the calculated results, setting the curve to half speed reduces the handling capacity by approximately 42.5% while using optimized curves results in only ca. 10% handling capacity reduction.

It is worth noting that, the best possible solution chosen here considers only the simulated cases. To get the global optimal solution, it requires that simulation needs to be performed for all the possible existing cases, which is impractical. Since there are only 3 design parameters that needs to be varied for each case, a regression analysis can be performed. It can be used to predict the behavior of elevator speed and building sway amplitude on the in-car vibration. Also generating an equation for the fitting curve can be utilized to predict the necessary speed change to maintain the required in-car ride comfort.

5.1.3 Sway Amplitude study

At first, the threshold sway magnitude is calculated over which the ride comfort is no longer in the acceptable range. To study this case, peak to peak acceleration is measured for nominal elevator speed for 5 cases: 88mm sway amplitude, 66mm sway amplitude, 52.8mm sway amplitude, 44mm sway amplitude and no sway condition. Car vibration for each case are then compared against the acceptable criteria, which is agreed to be 20gals. 12Hz Butterworth low pass filter is applied to the acceleration results to consider the human perception. Measured values are saved in Gals (cm/s^2).

Table 5. Impact of Sway on ride comfort

Percentage	Amplitude (m)	Pk-Pk Vib (Gals)
Full Sway	0.088	28.53
75% Sway	0.066	21.75
60% Sway	0.0528	19.06
50% Sway	0.044	18.48
No Sway	0	18.399

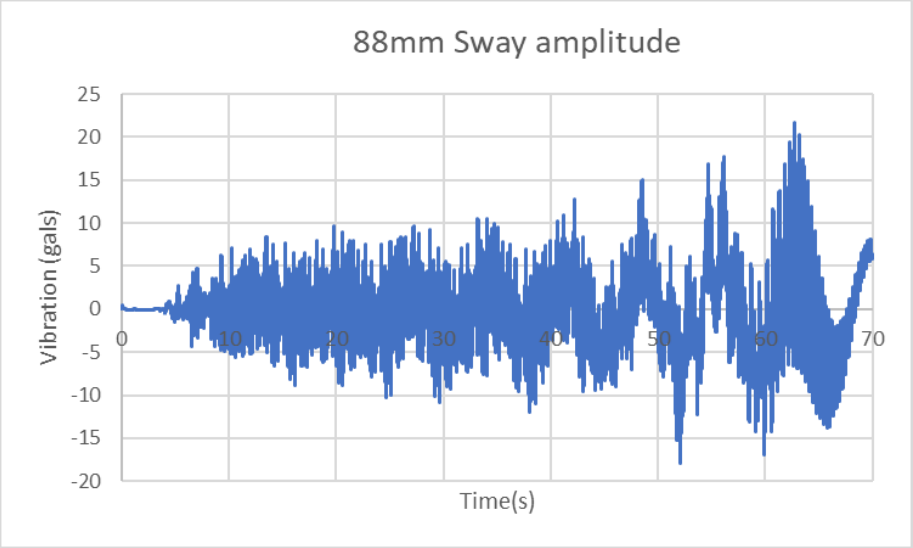

Figure 33. In-car vibration plot for 88mm sway amplitude

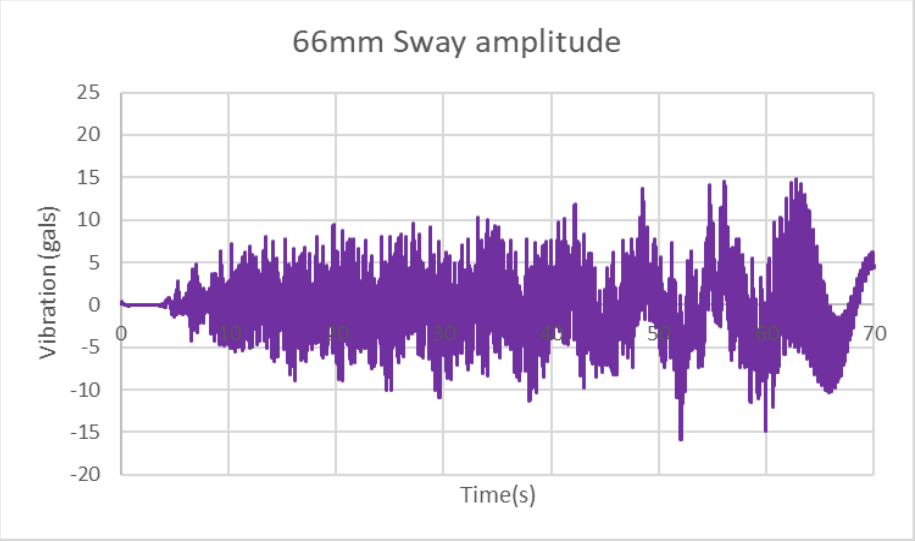

Figure 34. In-car vibration plot for 66mm sway amplitude

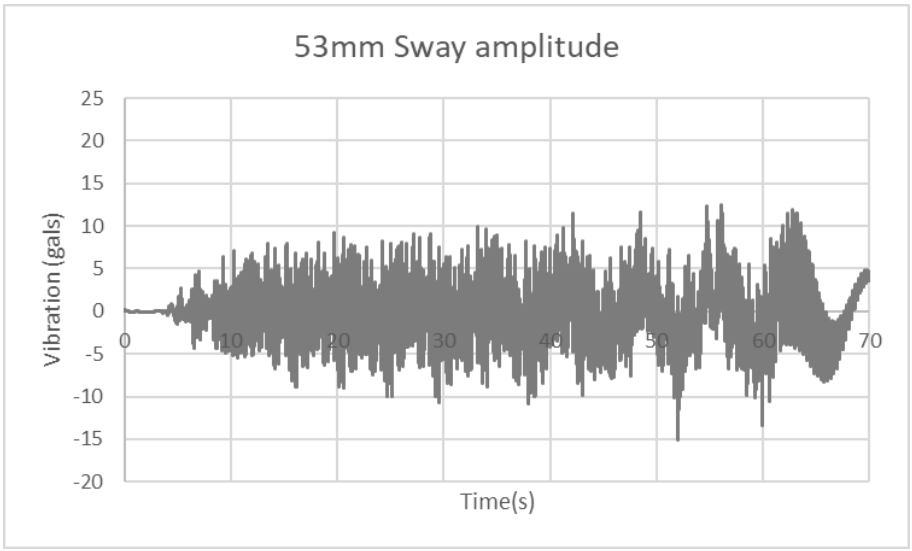

Figure 35. In-car vibration plot for 53mm sway amplitude

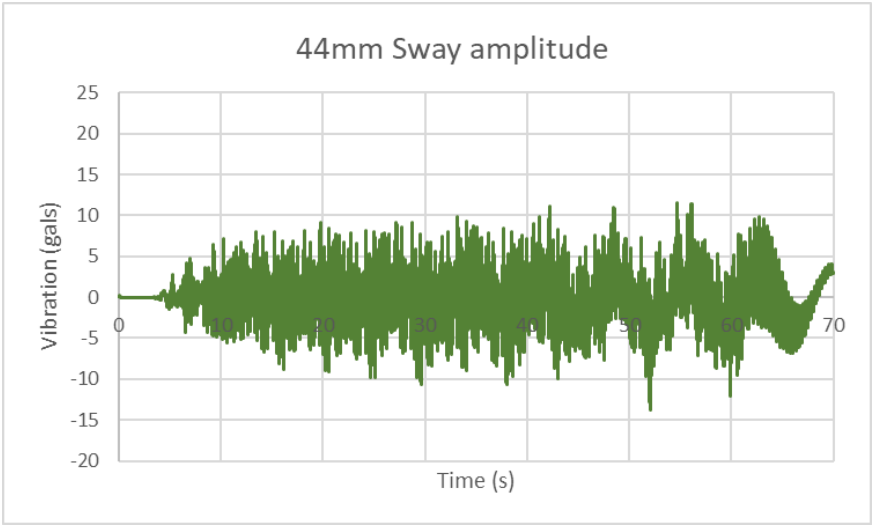

Figure 36. In-car vibration plot for 44mm sway amplitude

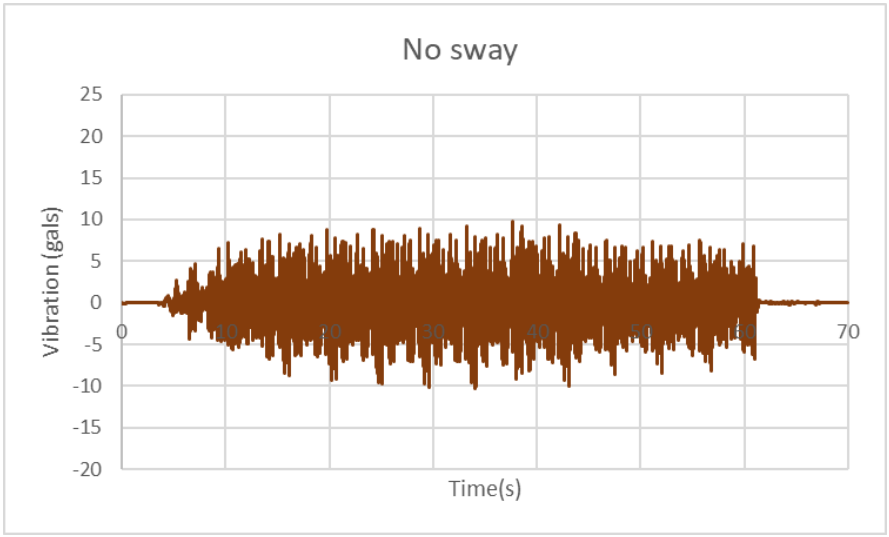

Figure 37. In-car vibration plot for no sway condition

The graphs show that the in-car vibration amplitudes are lower for lower building sway amplitudes. For cases with building sway, even after the car has stopped moving, there is high value of vibration at the top of the building because of the swaying motion of the building is perceived as vibrations inside the elevator car (Figure 37).

Analyzing the results show that sway amplitude below 0.044m does not have any significant effect over the in-car vibration. The in-car vibration values are almost constant until 0.044m building sway amplitude. When the building sway amplitude increases beyond 0.044m, in-car vibration increases linearly with building sway amplitude. Figure 38 shows that ride comfort is always within the acceptable range when the building sway is less than 61.6mm amplitude. This means that the nominal speed of 10m/s can be used for the whole run when the observed sway is less than 61.6 millimeters.

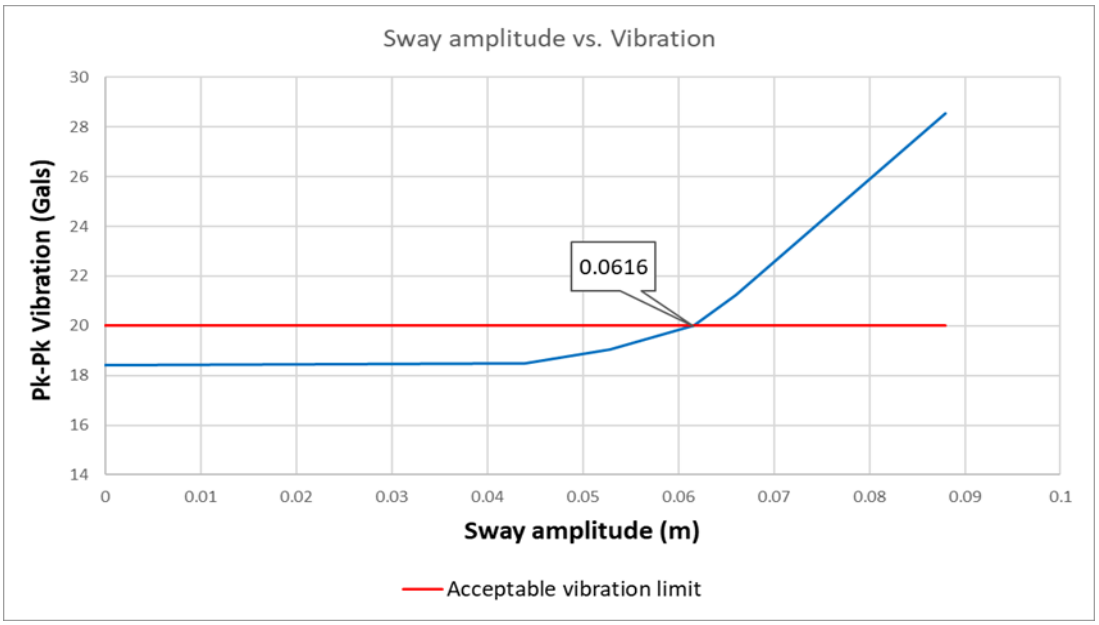

Figure 38. Impact of sway amplitude on in-car vibration

Therefore, it can be assumed that speed needs to be reduced when maximum sway amplitude is beyond the threshold value of 61.6 millimeters. That is, for any sway amplitudes greater than the threshold value, variable drive curve should be used to attain good level of ride comfort. The usual practice is to run at half speed 5m/s. This practice helps in maintaining the in-car vibration within the acceptable range at the expense of flight time.

Based on this results, in-car vibration is computed for all the speed profile cases discussed in the previous chapter when wind mode is triggered. Each curve is simulated for 0.0616m and 0.0748m sway amplitudes. These vibration values combined with the full sway amplitude values (Table 6) is used as inputs for regression analysis.

Table 6. Ride comfort analysis for high wind mode conditions

Cases	Starting Speed (m/s)	Reduced Speed (m/s)	Height at speed change (m)	Building Sway (m)	Max. Pk-Pk vibration (Gals)
1	10	2	252	0.0616	18.47124122
2	10	2	252	0.0748	18.52734014
3	10	4	252	0.0616	17.2221117
4	10	4	252	0.0748	17.46032078
5	10	6	252	0.0616	18.38944769
6	10	6	252	0.0748	18.4452982
7	10	8	252	0.0616	21.1046443
8	10	8	252	0.0748	21.39655495
9	10	2	302	0.0616	16.05482027
10	10	2	302	0.0748	15.93858921
11	10	4	302	0.0616	18.18327983
12	10	4	302	0.0748	18.0516395
13	10	6	302	0.0616	18.37878132
14	10	6	302	0.0748	18.24572563
15	10	8	302	0.0616	22.14259839
16	10	8	302	0.0748	21.98229403
17	10	2	352	0.0616	15.66003193
18	10	2	352	0.0748	16.50873773
19	10	4	352	0.0616	17.40187121
20	10	4	352	0.0748	18.34497715
21	10	6	352	0.0616	17.61800205
22	10	6	352	0.0748	18.57282134
23	10	8	352	0.0616	21.60489368
24	10	8	352	0.0748	22.57108526
25	10	2	402	0.0616	15.69697199
26	10	2	402	0.0748	17.55967191
27	10	4	402	0.0616	16.22750327
28	10	4	402	0.0748	18.15315931
29	10	6	402	0.0616	19.74661541
30	10	6	402	0.0748	22.0898711
31	10	8	402	0.0616	23.16040468
32	10	8	402	0.0748	25.45904445

5.2 Regression Analysis

This chapter presents the background and specific analysis to construct a regression model and explain the specific logic behind the approach that is used for model fitting. The multiple regression modelling technique and procedures followed for process output prediction is also presented in this thesis. Finally, the efficiency of the regression model is validated using test data.

The most time-consuming process in a model analysis is the data collection. The collected data can be characterized into dependent and independent variables. Independent variables are the ones that are varied during each simulation, in this study, they are change of elevator speed, height at which the velocity is changed and building sway amplitude. Dependent variables are the measure or observed output of the simulation, which is a function of the dependent variable and in this study, they are the maximum peak to peak in-car vibration amplitude. Since there are 3 independent variables, for every combination of independent variable, we get a dependent variable output using computation. Finally, regression analysis is performed to define a mathematical relationship between the set of independent and dependent variables. Fundamentals of regression analysis aims at representing a relationship between an independent and dependent variable. This relationship is represented by using a regression equation, which can be also termed as fitting function [72].

5.2.1 Model selection

Curve fitting is used in almost all engineering applications. One of the most commonly used method is fitting by using simple linear function, but data with non-linear functionality can be a bit challenging. Selection of the regression model is an iterative process. There are many commercial software's that are dedicated to solving regression analysis, but this thesis study uses solver add-in function of the most widely used software; Microsoft Excel. It utilizes multiple regression technique to generate a function that fits the data accurately.

Curve fitting is used to standardize data such that it can be easily recognized. It describes data in the form of mathematical equation$y = f(x)$, where y is the dependent is variable, x is the independent variable and f is the fitting function. The experimental data used in this thesis includes three functional variables. One of the easiest methods is to use Microsoft Excel to fit the non-linear curve. The advantage of using excel is that it is easily available and can be found in almost every computer as an included part of Microsoft Office. It doesn't have any additional expenses and is among the most commonly used tool by engineers even at rudimentary scale [73]. SOLVER function of Excel contains multiple regression tool that is also suitable for fitting non-linear experimental data. Curve fitting follows the principle that deviation of measured data from actual data is as minimum as possible. The regression method achieves this by minimizing the sum of the squares of difference between observed value and predicted value. This approach of minimizing squared errors is known as least-squares method.

5.2.2 Multiple regression

In multiple regression model, if we consider an example of multiple independent variables of the type

$$y = a_0 + a_1x_1 + a_2x_2 + a_3x_3 + \cdots + a_kx_k + e$$

where x_1, x_2, x_3. . . are the independent variables, a_0, a_1, a_2 . . . are the coefficients used for estimation and e is the random error. When using multiple regression, we assume that the dependent variable can be expressed as a combination of independent variables.

If we consider that there are n number of observations, then ith observation can be represented as

$$y_i = a_0 + a_1x_{i1} + a_2x_{i2} + a_3x_{i3} + \cdots + a_kx_{ik} + e_i$$

where y_i is the actual data for ith observation. If y is the predicted value using regression mode for the same data sample, it can be expressed as

$$y = a_0 + a_1x_{i1} + a_2x_{i2} + a_3x_{i3} + \cdots + a_kx_{ik}$$

That means, the aim of the prediction model is to estimate the unknown coefficients a_0, a_1, a_2 . . . a_k. Multiple regression utilizes least square method for the coefficient estimation.

It can be noted that the error in the model is the difference between predicted and actual data, given by

$$e_i = y_i - y = y_i - (a_0 + a_1x_{i1} + a_2x_{i2} + a_3x_{i3} + \cdots + a_kx_{ik})$$

Least square regression method follows the approach of minimizing square of error $\sum_{i=1}^{n} {e_i}^2$.

Next chapter lays out a fitting strategy and explains the application of least-squares regression method to a nonlinear problem encountered in ride comfort prediction of high-rise elevators.

5.2.3 Data fitting strategy and validation

Model fitting is done using least square regression that estimates regression coefficients. This requires a data analysis tool with multiple regression capabilities.

Since the aim is to find the required speed reduction to maintain a good ride comfort, speed change is used as one of the independent variables for simulation. The other two being height at which speed is changed and building sway. 51 different combination of these three independent variables are simulated for ride comfort. Following cases are used for the simulation combination:

- Travelling speed reduction from 10m/s to 2m/s, 4m/s, 6m/s and 8m/s
- Building sway amplitude of 0.088m, 0.0748m and 0.0616m
- Speed change at height of 252m, 302m and 402m

In the regression equation, independent variables are represented as a ratio of elevator parameter, i.e. lowering the speed from 10m/s to 2m/s is represented as 0.2, building sway of 0.0616m is represented as 0.70 (0.0595/0.088) and height at which speed is reduced is represented as a percentage of total building height (e.g. 252 = 49.61% of 508m). Two cases of least square regression are performed to fit the curve using linear and quadratic function. Each case is then analyzed for accuracy.

For the analysis, data is randomly shuffled and exported to excel. The regression model is then applied to the data set. During which the model learns the impact of each variable on the output. Finally, the coefficients of the independent features that contribute to in-car vibration is generated.

Following steps are carried out in excel to perform multiple regression analysis:

1. Activate the Analysis ToolPak from Add-ins

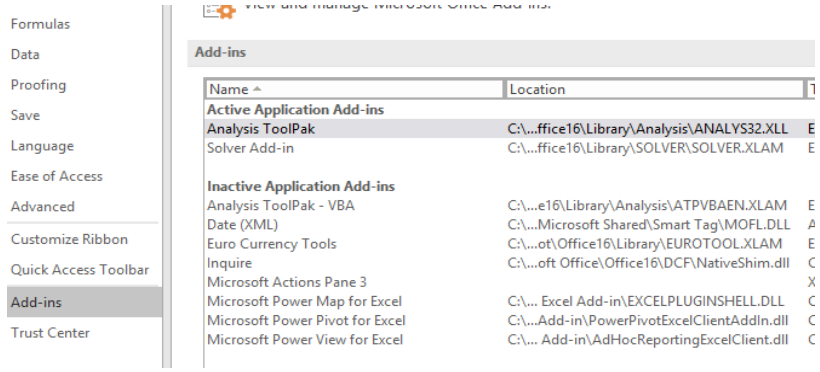

Figure 39. Activate Analysis ToolPak

2. Using Data Analysis tab, open regression window and enter data into the window such that Y-input contains dependent variable and X-input contains all independent variables. It should be noted that independent variables need to be in continuous columns.

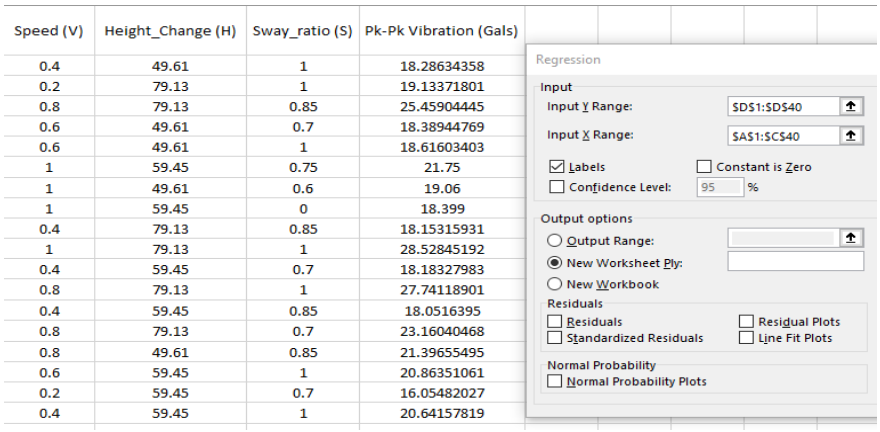

Speed (V)	Height_Change (H)	Sway_ratio (S)	Pk-Pk Vibration (Gals)
0.4	49.61	1	18.28634358
0.2	79.13	1	19.13371801
0.8	79.13	0.85	25.45904445
0.6	49.61	0.7	18.38944769
0.6	49.61	1	18.61603403
1	59.45	0.75	21.75
1	49.61	0.6	19.06
1	59.45	0	18.399
0.4	79.13	0.85	18.15315931
1	79.13	1	28.52845192
0.4	59.45	0.7	18.18327983
0.8	79.13	1	27.74118901
0.4	59.45	0.85	18.0516395
0.8	79.13	0.7	23.16040468
0.8	49.61	0.85	21.39655495
0.6	59.45	1	20.86351061
0.2	59.45	0.7	16.05482027
0.4	59.45	1	20.64157819

Figure 40. Entering data into regression tool

In case of linear function, variables used are speed ratio (V), percentage of total travel height at which speed is changed (H) and building sway ratio (S). Ride comfort (RC) equation will be represented as

$$RC = a_0 + a_1V + a_2H + a_3S$$

In case of quadratic function, apart from V, H and S, additional variables such as V*H, V*S, H*S, V*H*S, V^2, H^2 and S^2 are used.

$$RC = a_0 + a_1V + a_2H + a_3S + a_4VH + a_5VS + a_6HS + a_7VHS + a_8V^2 + a_9H^2 + a_{10}S^2$$

Output of regression has three components:

1. Regression statistics table

Table 7. Regression Statistics table

Regression Statistics		
	Linear function	*Quadratic function*
Multiple R	0.851035825	0.937197135
R Square	0.724261975	0.878338469
Adjusted R Square	0.700627288	0.834887923
Standard Error	1.786615381	1.326827252
Observations	39	39

The most significant values of interest are R Square and Adjusted R Square value.
Multiple R represents the correlation between y_i and y, which when squared gives R Square.
R Square and Adjusted R Square is a measure of how good the function fit to data. Adjusted R Square is used when there is more than one independent variable because it is R Square modified based on degrees of freedom.

Adjusted R Square = R Square – [(1 – R Square) *(k – 1)/ (n – k)]
where k = number of coefficients and n = number of observations

Adjusted R Square = 0.701means that 70.1% of the variation in Ride Comfort can be expressed as a combination of independent variables. The closer R Square is to 1, the better regression curve fits to the data. Standard Error also referred to as standard error of regression because it is a measure of standard deviation of the error e.

Analyzing the regression table for both linear and quadratic function shows that quadratic regression function has higher Adjusted R Square value and lower Standard Error, which mean quadratic function has a better fit to data.

2. Analysis of variance (ANOVA) table

Table 8. Analysis of variance table for linear function

ANOVA				
	Linear function			
	df	*SS*	*F*	*Significance F*
Regression	3	293.4467	30.64403	6.70116E-10
Residual	35	111.7198		
Total	38	405.1665		

Table 9. Analysis of variance for quadratic function

ANOVA				
Quadratic function				
	df	*SS*	*F*	*Significance F*
Regression	*10*	*355.8733*	*20.21467*	*2.94222E-10*
Residual	*28*	*49.29318*		
Total	*38*	*405.1665*		

There are three rows regression, residual and total and df represents the degrees of freedom for each row. In case of linear regression function, there are 3 degrees of freedom (k = 3) and 35 residual degrees of freedom (n – k – 1) where n is the number of observations.

The total variability in predicted value is represented as sum of squares total SS Total (SST). Note that SST is same for both linear and quadratic function because the both functions are trying to predict the same RC value. Some of this variability is captured by the sum of squares regression (SSR) and the rest by the residual or sum of squares error (SSE). Thus, better fit function means most of variation is captured by regression, i.e. higher SSR value.

F values gives the significance of the regression function by testing the null hypothesis, i.e. the model fit is tested when all regression coefficients are simultaneously zero. High F value means that the model does not well support the null hypothesis. Significance F shows the probability that results occur randomly.

Analyzing the variance table shows that quadratic function provides a better data fit due to higher SST value meaning that the variability in X (independent variable) does a better job in explaining the variability in RC (dependent variable). Also, lower Significance F value shows that the results are not very random and more significant.

3. Regression Coefficient table

The coefficients or the numbers that needs to be multiplied with each independent variable is described in the coefficient table shown below (Table. 10). Using this the regression equation is made for both linear and quadratic function.

Table 10. Regression Coefficient Table

	Linear Function Coefficients	*Quadratic Function Coefficients*
Intercept	3.378	34.8050
Speed Change(V)	9.56	-22.4870
Height Change (H)	0.056	-0.0279
Sway Ratio (S)	9.16	-44.9120
V*H	0	0.2355
V*S	0	27.6130
H*S	0	0.3190
V*H*S	0	-0.1376
V^2	0	0.8030
H^2	0	-0.0019
S^2	0	15.0728

Regression equation for linear function:

$$RC = 3.378 + 9.56V + 0.056H + 9.16S$$

Regression equation for quadratic function:

$$RC = 34.8050 - 22.487V - 0.0279H - 44.912S + 0.2355VH + 27.613VS + 0.3190HS - 0.1376VHS + 0.8030V^2 - 0.0019H^2 + 15.0728S^2$$

5.3 Validation

Data set contains 51 observations. As discussed previously, 25% of the data, which is equivalent to 12 observations, are discarded for later model validation and only 75% of the data, equivalent to 39 observations are used for model fitting.

First the output of the predicted values using quadratic and linear functions are plotted against the observed ride comfort values from simulation.

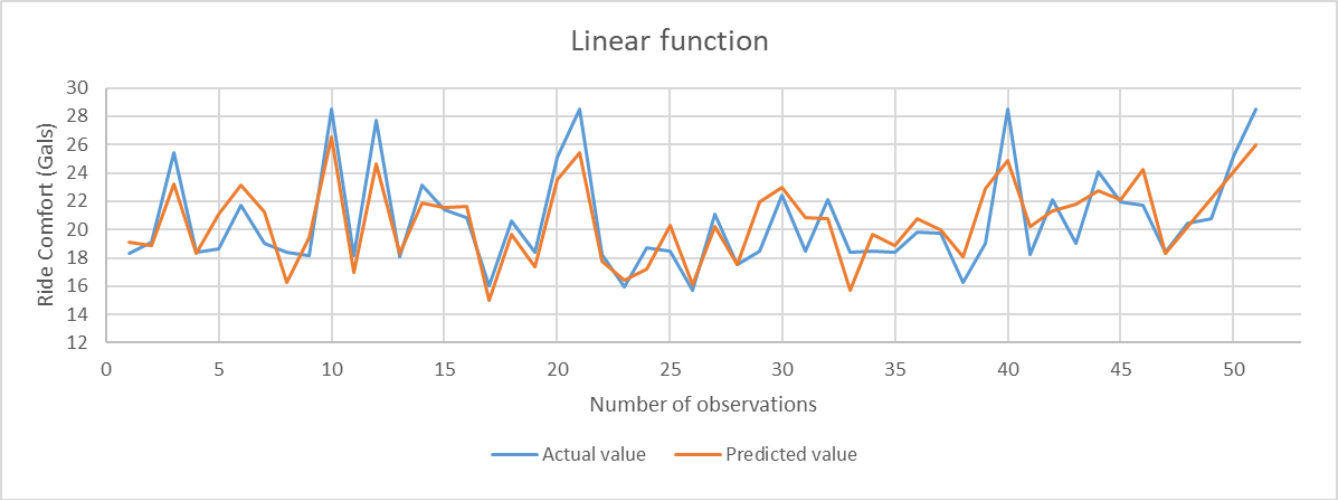

Figure 41. Linear regression function fit

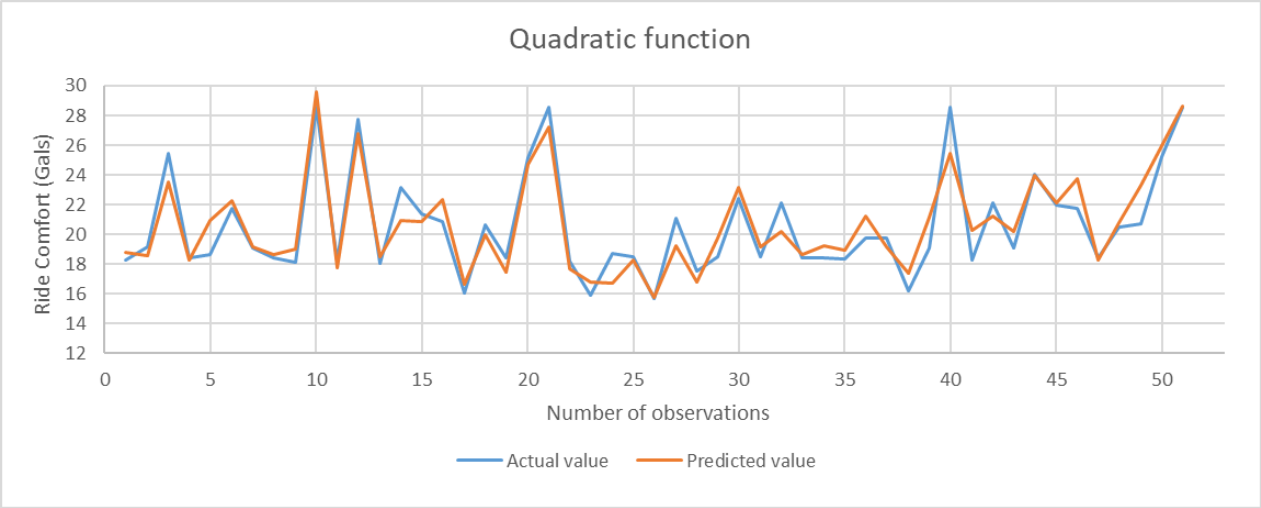

Figure 42. Quadratic regression function fit

Analyzing these plots shows that the curve of quadratic function provides a better fit against the true value. Linear function also follows the trend of actual value curve but with less accuracy.

Another term of interest in least square regression analysis are the residuals. Residuals are the difference between observed and predicted values. Residual plots give a better understanding on whether the observed errors (residuals) are consistent with random or unpredictable error. It means that residuals should not be predictable, i.e. when plotted they should not be systematically above or below the axis line. Rather a good regression will have residuals constantly spread over the axis.

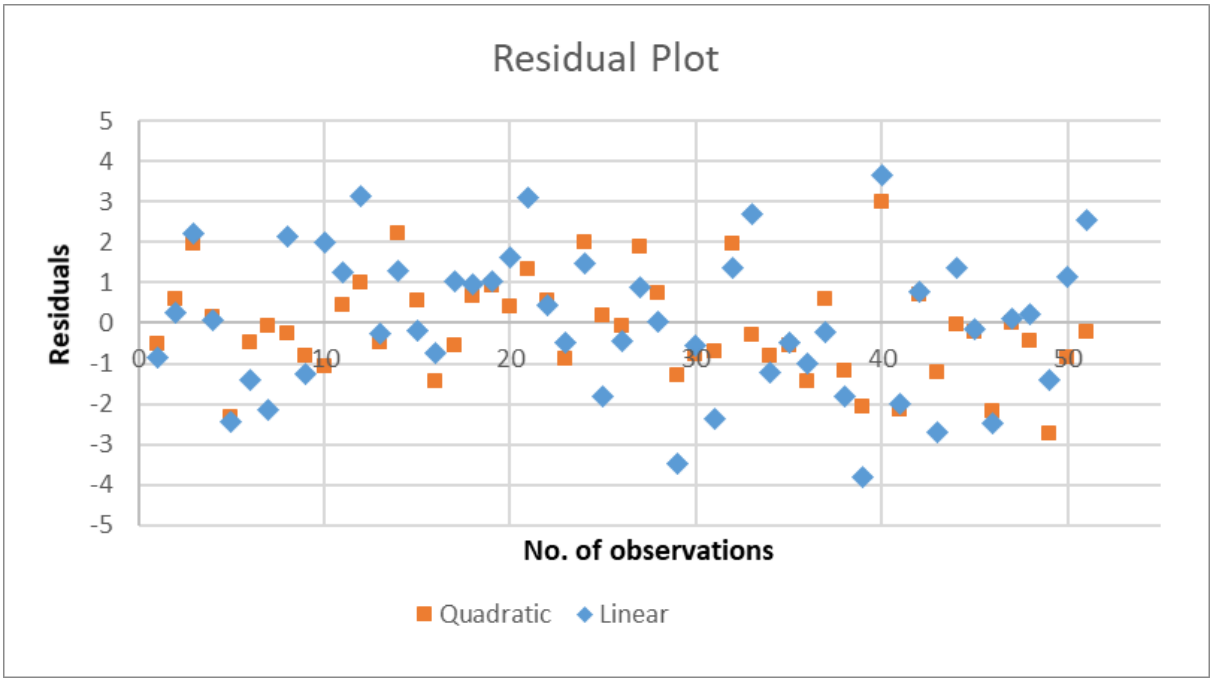

Figure 43. Residual plot

The plots show that the adjacent residuals are not correlated with each other for both linear and quadratic regression function and it follows a random pattern. This means that the predictors are reliable for both functions.

Thus, in order to maintain the optimized speed curve, the required speed reduction is predicted by solving the regression function. Quadratic regression function is chosen as the predictor function because of its better fit model.

$$RC = 34.8050 - 22.487V - 0.0279H - 44.912S + 0.2355VH + 27.613VS + 0.3190HS - 0.1376VHS + 0.8030V^2 - 0.0019H^2 + 15.0728S^2$$

Based on the data samples that are used for developing the regression function, there are some limitations that needs to be considered when choosing the variables. One of the most common limitation is that the multiple regression is sensitive to outliers, i.e. if a variable is chosen further from the data range could swing the regression estimation. Therefore, it is essential to set the range for which the regression function is valid as given below;

$16\ Gals \leq RC \leq 30\ Gals$
$50\% \leq H \leq 79\%$ (percentage of total travel distance 508m)
$0.7 \leq S \leq 1$ (ratio of maximum building sway amplitude 0.088m)
$0.2 \leq V \leq 1$ (ratio of maximum travel speed 10m/s)

For example, if we try to find the required speed reduction to maintain, RC = 18 Gals when the building is sway amplitude is 0.066m (sway ratio, S = 0.75) and speed is lowered at 401m (H = 79% of total travel height), the quadratic regression function reduces to;

$$0.803V^2 + 8.67445V - 3.5618 = 0$$

Solving gives $V = 0.396$, which is the ratio of speed reduction. That is when multiplied by 10 gives approximately 4m/s as the required speed that needs to be maintained after travelling 401m for ride comfort of 18Gals.

6 Conclusion and Future Work

In this research work, multiphysics approach has been used to compute vibrations inside an elevator for various speed curve and building sway conditions. First, the components that influence the elevator ride comfort has been listed down and how they contribute to the in-car vibrations has been explained. Secondly, impact of various speed profiles and building sway conditions were studied. Based on the simulation results, optimized speed profile and threshold building sway amplitude was chosen. Finally, the studied cases are used to generate the regression function.

Transient dynamic simulation method used in this research work can be implemented in high-rise elevators because this approach considers almost all variables that cause in-car vibrations. Multiphysics simulation approach, the first of its kind, is presented in this research, where factors such as installation variables, component dimensional parameters, rope forces, change of rope masses, aerodynamic force due to counterweight passing, building sway amplitude and frequency are well accommodated in the study. The in-car vibration results are then combined with ride comfort and handling capacity to get a wider perspective and better understanding of the elevator system performance. Analyzing the simulation results have proved that, optimization of the velocity profile during building sway conditions can reduce the degradation of ride comfort. Also, variable drive curve can be utilized to meet the required ride comfort with only moderate increase in travel time. This technique allows to maintain good elevator handling capacity and provides better service to the passengers by avoiding unnecessary slowdowns from normal operating speed of elevators.

In the elevator model, there are many factors that contribute to in-car vibrations. The variables that are chosen for the regression model are not significant enough on its own to predict the in-car vibration precisely. Thus, the possibility to include more variables to get a better regression function could be considered in the further studies. Also using higher observations number than 51 helps to improve the model prediction. The regression function is invalid for null hypothesis, i.e. the variables are only sensitive within the specified outliers. One of the biggest limitations of the model is the mechanical validation, mainly because of the challenges to find a test tower 508 meters high and replicate the building sway and rope forces. As a further study, validation without the building sway can provide at least some understanding of the simulation model and areas to improve.

7 References

[1] K. Al-Kodmany, "5. The Logic of Vertical Density: Tall Buildings in the 21st Century City," *International Journal of HighRise Buildings,* vol. 1, 2012.

[2] M. M. Ali and P. J. Armstrong, "Overview of sustainable design factors in high-rise buildings," in *Proc. of the CTBUH 8th World Congress*, 2008.

[3] K. Al-Kodmany, Eco-towers: Sustainable cities in the sky, WIT Press, 2015.

[4] E. Hallebrand and W. Jakobsson, "Structural design of high-rise buildings," *TVSM-5000,* 2016.

[5] J. M. S. D. Valente, "Tall Buildings and Elevators: Historical Evolution of Vertical Communication System," *Universidade Tecnica de Lisboa, MS Thesis,* pp. 34-382, 2012.

[6] T. Ishii, "Elevators for skyscrapers," *IEEE Spectrum,* vol. 31, pp. 42-46, 1994.

[7] R. Roberts, "Control of high-rise/high-speed elevators," in *American Control Conference, 1998. Proceedings of the 1998*, 1998.

[8] R. Appunn and K. Hameyer, "Modern high speed elevator systems for skyscrapers," in *Maglev*, 2014.

[9] M. L. Siikonen, "Double-Deck Elevators: Savings in time and space," pp. 65--69, 1998.

[10] T. Ojanen, ”Aero-vibro Acoustic Simulation of an Ultrahigh-Speed Elevator,” 2016.

[11] K. Al-Kodmany, "Tall Buildings and Elevators: A Review of Recent Technological Advances," *Buildings,* vol. 5, pp. 1070-1104, 2015.

[12] T. Lau, "Power, Elevator and Customer-Oriented Sustainability Strategies," *CTBUH: Chicago, IL, USA,* 2014.

[13] L. Neyfakh, *How the elevator transformed America,* 2014.

[14] H. Bijl, *9 Elevator Facts You Didn’t Know,* 2016.

[15] W. Jochem, *Elevator planning for high-rose buildings,* 2007.

[16] S. Mohaney and M. Shah, "Emerging Trends in Vertical Elevating System," *International Journal of Engineering and Management Research,* vol. 5, pp. 51-56, 2015.

[17] B. Nemeth, "Energy-Efficient Elevator Machines," *ThyssenKrupp Elevator: Frisco, TX, USA,* 2011.

[18] S. Kwatra and C. Essig, "The promise and potential of comprehensive commercial building retrofit programs," 2014.

[19] G. Simbierowicz and J. Kortelainen, "Assessment of different computational methods used for estimating the lateral quaking in a high-rise elevator," in *Proceedings of the 20th International Congress on Sound and Vibration*, 2013.

[20] R. A. Crist, "Measurement of noise and vibration," *Ride quality, vibration & noise,* 1984.

[21] K. K. Li, M. T. Suen and W. K. Wu, "A general survey on lift ride quality at public building of the hong kong special administrative region," in *Proc. of the CTBUH 2004 Seoul Conference*, 2004.

[22] ISO 18738-1:2012, "Measurement of ride quality — Part 1: Lifts (elevators)," Internation Organisation of Standardization, October 2012. [Online]. Available: https://www.iso.org/standard/54395.html. [Accessed 4th April 2018].

[23] N. Anzaiana and E. Watanabe, "The challenges of super high-speed lifts," *Ride quality, vibration & noise,* 1982.

[24] J. Hernelind and G. Roivainen, "High Rise Elevators--Challenges and Solutions in Ride Comfort Simulations," 2017.

[25] E. Abraham, "Car Ride Quality," *Ride quality, vibration \& noise,* vol. I, pp. I-19--I-22, 1984.

[26] D. F. Rogers, "Elevator Balance," *NAR-associates Report,* 2005.

[27] H.-l. Bai, G. Shen and A. So, "Experimental-based study of the aerodynamics of super-high-speed elevators," *Building Services Engineering Research and Technology,* vol. 26, pp. 129-143, 2005.

[28] J. K. Salmon and Y. S. Yoo, "Reduction of noise and vibration in an elevator car by selectively reducing air turbulence". United States of America Patent US5018602A, 28 May 1991.

[29] N. Singh, S. Kaczmarczyk and T. Ehrl, "An analysis of airflow effects in lift systems," in *Lift and Escalator Symposium*, 2017.

[30] T. Kiivanen and S. Starck, "Ride Comfort for high-rise elevators," KONE Corporation, Hyvinkää, 2010.

[31] G. R. Strakosch, The Vertical Transportation Handbook, John Wiley & Sons, 1998.

[32] C. Druga, D. Barbu and S. Lache, "Vibration and the human body," *Fascicle of Management and Technological Engineering,* vol. 6, pp. 168-173, 2007.

[33] ISO 2631-1:1997, "Mechanical vibration and shock-Evaluation of human exposure to whole-body vibration-Part 1: General requirements," May 1997. [Online]. Available: https://www.iso.org/standard/7612.html. [Accessed 4th April 2018].

[34] D. J. Oborne, "Whole-body vibration and International Standard ISO 2631: a critique," *Human factors,* vol. 25, pp. 55-69, 1983.

[35] J. HANSSON and B. WIKSTRÖM, "Comparison of some technical methods for the evaluation of whole-body vibration," *Ergonomics,* vol. 24, pp. 953-963, 1981.

[36] M. A. Bellmann, Perception of whole body vibrations: From basic experiments to effects of seat and steering wheel vibrations on the passenger's comfort inside vehicles, Shaker, 2002.

[37] V. Raillard and P. Rebilard, "Study of passenger comfort and vibrations of an elevator)," *Ride quality, vibration & noise,* 1995.

[38] M. Otsuki, K. Yoshida, K. Nagata, S. Fujimoto and T. Nakagawa, "Experimental study on vibration control for rope-sway of elevator of high-rise building," in *American Control Conference, 2002. Proceedings of the 2002*, 2002.

[39] S. Kaczmarczyk, "The dynamic behaviour of lift ropes and components under seismic excitation," 2017.

[40] R. J. Mangini and R. K. Roberts, "Elevator rope sway detection and damping". United States of America Patent US9359172B2, 7 June 2016.

[41] S. Li-qun, L. Ying-zheng, J. Si-yu and C. Zhao-min, "Numerical simulation of unsteady turbulent flow induced by two-dimensional elevator car and counter weight system," *Journal of Hydrodynamics, Ser. B,* vol. 19, no. 6 SHI, Li-qun; LIU, Ying-zheng; JIN, Si-yu; CAO, Zhao-min;, pp. 720--725, 2007.

[42] J. Husmann and E. Cortona , "Elevator vibration damping apparatus and method". United States of America Patent US Patent 7,401,683, 22 July 2008.

[43] K. Utsunomiya, "Elevator apparatus having vibration damping control". Japan Patent US8141685B2, 27 March 2012.

[44] Y. A. Onur and C. E. Ímrak, "Reliability analysis of elevator car frame using analytical and finite element methods," *Building Services Engineering Research and Technology,* vol. 33, pp. 293--305, 2012.

[45] T. Hakala, S. Saarela, J. Kalliomäki and J. Saloranta, "Method for controlling an elevator, and an elevator using starting position data of the elevator and sway data of the building". Finland Patent US8579089B2, 12 November 2013.

[46] B. S. Taranath, Wind and earthquake resistant buildings: Structural analysis and design, CRC press, 2004.

[47] P. Mendis, T. D. Ngo, N. Haritos, A. Hira, B. Samali and J. Cheung, "Wind loading on tall buildings," *Electronic Journal of Structural Engineering,* 2007.

[48] B. M. Melissa Burton, "Wind-Induced Motion of Tall Buildings: Designing for Occupant Comfort," *International Journal of High-Rise Buildings,* 2015.

[49] P. Persson, P. H. Kirkegaard, L. V. Andersen and F. Steffen, "Analysis of wind-induced vibrations in high-rise buildings," in *INTER-NOISE and NOISE-CON Congress and Conference Proceedings*, 2016.

[50] D. Walton, S. Lamb and K. C. S. Kwok, "A review of two theories of motion sickness and their implications for tall building motion sway," *Wind and Structures,* vol. 14, p. 499, 2011.

[51] D. Boggs and J. Dragovich, "The nature of wind loads and dynamic response," *Special Publication,* pp. 15--44, 2006.

[52] J. Kalliomäki and J. Saloranta, "Megacities," 2014.

[53] A. Kareem, T. Kijewski and Y. Tamura, "Mitigation of motions of tall buildings with specific examples of recent applications," *Wind and structures,* vol. 2, pp. 201-251, 1999.

[54] M. D. Burton, K. C. S. Kwok and P. A. Hitchcock, "Wind climate and duration of a wind event: effects on occupant comfort," in *7th UK Conference on Wind Engineering, Glasgow, UK*, 2006.

[55] P. Jie and D. Yonggang, "The Impact of wind on a high-rise tower," *Ride quality, vibration & noise,* 1999.

[56] O. Flodén, K. Persson and G. Sandberg, "Reduction methods for the dynamic analysis of substructure models of lightweight building structures," *Computers & Structures,* vol. 138, pp. 49--61, 2014.

[57] H. Kimura, H. Ito and T. Nakagawa, "Vibration analysis of elevator rope: forced vibration of rope with time-varying length," *Transactions of the Japan Society of Mechanical Engineers. Series C.,* vol. 71 , no. 706, pp. 1871--1876, 2005.

[58] P. Andrew and S. Kaczmarczyk, "Rope dynamics," *Elevator World,* vol. 263, pp. 45-56, 2011.

[59] M. Petyt, Introduction to finite element vibration analysis, Cambridge university press, 2010.

[60] Dassault Systemes, "Abaqus V2016, Software documentation," 2016. [Online]. Available: http://h0cml82:2080/v2016/. [Accessed 27 May 2018].

[61] M. Belyi, V. Belsky, A. Bajer, K. M and I. C, "Advanced linear dynamics and substructuring capabilities in Abaqus with applications in noise and vibration analysis," in *Proceedings of ISMA*, 2012.

[62] P. Avitabile, ”Model reduction and model expansion and their applications–part 1 theory,” tekijä: *Proceedings of the Twenty-Third International Modal Analysis Conference*, Orlando, FL, 2005.

[63] V. D. Narasimhamurthy, Unsteady-RANS simulation of turbulent trailing-edge flow, Citeseer, 2004.

[64] C. C. Spyrakos, Finite Element Modeling, WVU press, West Virginia, 1994.

[65] A. Preumont, Twelve lectures on structural dynamics, Springer, 2013.

[66] M. Liu and D. G. Gorman, "Formulation of Rayleigh damping and its extensions," *Computers & structures,* vol. 57, pp. 277-285, 1995.

[67] A. Alipour and F. Zareian, "Study rayleigh damping in structures; uncertainties and treatments," in *Proceedings of 14th World Conference on Earthquake Engineering, Beijing, China*, 2008.

[68] G. Takacs and others, "Basics of Vibration Dynamics," in *Model Predictive Vibration Control*, Springer, 2012, pp. 25-64.

[69] P. R. Heyliger and J. N. Reddy, "A higher order beam finite element for bending and vibration problems," *Journal of sound and vibration,* vol. 126, pp. 309-326, 1988.

[70] R. C. Russell, "Computer Finite Element Simulation in Mechanical Design," 2013.

[71] D. G. Barney, Elevator Traffic Handbook: Theory and Practice, New York: Spon Press, 2003.

[72] D. C. Harris, "Nonlinear least/squares curve fitting with Microsoft Excel Solver," *Journal of chemical education,* vol. 75, no. 1, p. 119, 1998.

[73] A. Brown, "A step-by-step guide to non-linear regression analysis of experimental data using a Microsoft Excel spreadsheet," *Computer methods and programs in biomedicine,* vol. 65, no. 3, pp. 191-200, 2001.

[74] K. Nguyen, A. Camara, O. Rio and L. Sparowitz, "Dynamic Effects of Turbulent Cross-wind on the Serviceability State of Vibrations of a Slender Arch Bridge Including Wind--Vehicle--Bridge Interaction," *Journal of Bridge Engineering,* vol. 22, p. 06017005, 2017.

[75] T. Curwen, "Los Angeles Times," New Wilshire Grand, 2 November 2014. [Online]. Available: http://graphics.latimes.com/wilshire-grand-earthquakes/. [Accessed 17 April 2018].

[76] M. Benosman, "Lyapunov-based control of the sway dynamics for elevator ropes," *IEEE Transactions on Control Systems Technology,* vol. 22, no. 5, pp. 1855--1863, 2014.

8 Appendices

Appendix 1. Python Script to read peak to peak vibration

APPENDIX 1: PYTHON SCRIPT TO READ PEAK TO PEAK VIBRATION

```
 #!/usr/bin/python
#import os
import pandas as pd
#import matplotlib.pyplot as plt
#from decimal import *
import sys #sys.exit()

def calculate_difference(new_valley_vib,new_peak_vib):
    abs_diff = abs(new_valley_vib-new_peak_vib)

    return abs_diff

def update_max_difference_info(new_peak_index,new_valley_index,new_peak_time,new_valley_time,new_valley_vib,new_peak_vib,current_max_peak_index,current_max_valley_index,current_max_peak_time,current_max_valley_time,current_max_difference_peak_vib,current_max_difference_valley_vib,current_max_difference_vib):
    new_diff = calculate_difference(new_valley_vib,new_peak_vib)
    #print 'new_diff: ',new_diff

    if (new_diff > current_max_difference_vib):
        return new_peak_index,new_valley_index,new_peak_time,new_valley_time,new_peak_vib,new_valley_vib,new_diff
    else:
        return current_max_peak_index,current_max_valley_index,current_max_peak_time,current_max_valley_time,current_max_difference_peak_vib,current_max_difference_valley_vib,current_max_difference_vib

def main():
    headers = ['Time','Vibration']
                # EDIT FILE NAME
    df = pd.read_csv('Vibration_Thesis_45s_8ms.csv', delimiter = ";", names =  headers)
    #print df.head()

    look_for_peak = False
    look_for_valley = False
    peak_found = False
    valley_found = False

    temp_peak_index = 0
    temp_peak_time = 0
    temp_peak_vib = 0
```

```
    temp_valley_index = 0
    temp_valley_time = 0
    temp_valley_vib = 0

    max_difference_peak_time = 0
    max_difference_valley_time = 0
    max_difference_peak_index = 0
    max_difference_valley_index = 0
    max_difference_peak_vib = 0
    max_difference_valley_vib = 0
    max_difference_vib = 0

    for index,row in df.iterrows():
        #print index,(row['Time']),(row['Vibration'])

        if (index == 0):
            if (row['Vibration'] > 0):
                look_for_peak = True
                #print ('Finding Peak first!')
            elif (row['Vibration'] < 0):
                look_for_valley = True
                #print ('Finding Valley first!')

        if (look_for_peak == True):
            if (row['Vibration'] > 0):
                if (row['Vibration'] > temp_peak_vib):
                    temp_peak_index = index + 1
                    temp_peak_time = row['Time']
                    temp_peak_vib = row['Vibration']
            elif (row['Vibration'] < 0):
                peak_found = True
                #print ('Peak found!')
                look_for_peak = False
                if (valley_found == True):
                    #TODO: find difference
                    #print('Finding difference...')
                    max_difference_peak_index,max_difference_valley_index,max_difference_peak_time,max_difference_valley_time,max_difference_peak_vib,max_difference_valley_vib,max_difference_vib = update_max_difference_info(temp_peak_index,temp_valley_index,temp_peak_time,temp_valley_time,temp_valley_vib,temp_peak_vib, max_difference_peak_index,max_difference_valley_index,max_difference_peak_time,max_difference_valley_time,max_difference_peak_vib,max_difference_valley_vib,max_difference_vib)
```

```
                #print 'max_difference: ',max_difference_vib

                #keep present peak and look for next valley again
                valley_found = False
                look_for_valley = True

                temp_valley_index = index + 1
                temp_valley_time = row['Time']
                temp_valley_vib = row['Vibration']
            else:
                look_for_valley = True

                temp_valley_index = index + 1
                temp_valley_time = row['Time']
                temp_valley_vib = row['Vibration']
        elif (look_for_valley == True):
            if (row['Vibration'] < 0):
                if (row['Vibration'] < temp_valley_vib):
                    temp_valley_index = index + 1
                    temp_valley_time = row['Time']
                    temp_valley_vib = row['Vibration']
            elif (row['Vibration'] > 0):
                valley_found = True
                #print ('Valley found!')
                look_for_valley = False
                if (peak_found == True):
                    #TODO: find difference
                    #print ('Finding Difference')
                    max_difference_peak_index,max_difference_valley_index,max_difference_peak_time,max_difference_valley_time,max_difference_peak_vib,max_difference_valley_vib,max_difference_vib = update_max_difference_info(temp_peak_index,temp_valley_index,temp_peak_time,temp_valley_time,temp_valley_vib,temp_peak_vib, max_difference_peak_index,max_difference_valley_index,max_difference_peak_time,max_difference_valley_time,max_difference_peak_vib,max_difference_valley_vib,max_difference_vib)
                    #print 'max_difference: ',max_difference_vib

                    #keep present valley and look for next peak again
                    peak_found == False
                    look_for_peak = True

                    temp_peak_index = index + 1
                    temp_peak_time = row['Time']
                    temp_peak_vib = row['Vibration']
                else:
```

```
                look_for_peak = True

                temp_peak_index = index + 1
                temp_peak_time = row['Time']
                temp_peak_vib = row['Vibration']

    # final result prints
    #print '\n\n'
    print 'max_peak_index: ',max_difference_peak_index
    print 'max_valley_index: ',max_difference_valley_index
    print 'max_peak_time: ',max_difference_peak_time
    print 'max_valley_time: ',max_difference_valley_time
    print 'max_difference_peak_vib: ',max_difference_peak_vib
    print 'max_difference_valley_vib: ',max_difference_valley_vib
    print 'max_difference_vibration: ',max_difference_vib

if __name__ == "__main__":
    main()
```